

# **PERFORMANCE OF LIME/CEMENT LIGHTLY TREATED CLAYEY SOILS**

**September 2013**

**Department of Science and Advanced Technology  
Graduate School of Science and Engineering  
Saga University, Japan**

**NGUYEN DUY QUANG**

# **PERFORMANCE OF LIME/CEMENT LIGHTLY TREATED CLAYEY SOILS**

**BY**

**NGUYEN DUY QUANG**

*A dissertation submitted in partial fulfillment of the requirement for the degree of Doctor  
of Philosophy in Geotechnical Engineering.*

Examination Committee	Prof. Jinchun Chai (Supervisor)  Prof. Koji Ishibashi Prof. Takenori Hino Associate Prof. Daisuke Suetsugu  Prof. Norihiko Miura (External Examiner)
Nationality:	Vietnamese
Previous Degrees:	Bachelor of Civil Engineering Ho Chi Minh City University of Technology Ho Chi Minh City, Viet Nam  Master of Geotechnical Engineering Ho Chi Minh City University of Technology Ho Chi Minh City, Viet Nam  Master of Geotechnical Engineering (Professional) Asian Institute of Technology (AIT) Bangkok, Thailand
Scholarship Donor:	Strategic International Postgraduate Program (SIPOP)

Department of Science and Advanced Technology  
Graduate School of Science and Engineering  
Saga University, Japan  
September 2013

## ACKNOWLEDGMENT

The work presented in this dissertation deals with physico-chemical and mechanical behavior of lime/cement lightly treated clayey soils. The study was sponsored by Strategic International Postgraduate Program (SIPOP's scholarship) and Prof. Chai's laboratory, Department of Civil Engineering and Architecture, Saga University. My supervisor was Professor Jinchun Chai. I would like to express my deep gratitude for his consult and advice throughout my studies. I am also grateful to my former professor, Prof. Dennes T. Bergado; to my former supervisors, Dr. Seah Tian Ho and especially, Associate Professor Pham Huy Giao at Asian Institute of Technology (AIT), Bangkok, Thailand, who appreciated my intentions in the studies and supported me in applying this scholarship.

The author is also grateful to all the examination committee, Prof. Kouji Ishibashi, Prof. Takenori Hino and Associate Prof. Daisuke Suetsugu for their valuable suggestions and comments on my dissertation. Sincere thank and appreciation are due to Prof. Norihiko Miura for his advice and suggestions as well as serving as external examiner. I also thank to Assistant Prof. Takehito Negami and Mr Akinori Saito for their help and earnest assistance on laboratory testings.

I am also grateful to my boss, Mr Tran Tan Phuc and all the members of Board of Directors who give me financial support and honest encouragements.

I would like to express my thanks to my seniors, Dr. Ong Chin Yee, Dr. Putera Agung, Dr. Pongsivasathit Supasit; to my colleagues, Ms. Katrika Sari, PhD student, Mr Md. Julfikar Hossain, PhD student, Mr Xu Fang, PhD student, Mr. Kimikazu Sugita and Mr Kidera, former Master students for kind helping me in various ways during the course of these studies. Thanks are also extended to secretary in the research team, Mrs Kanada Yasuko for her kindness help about administrative applications and documents.

Finally, I would like to thank my wife, Mrs Huynh Thi Thanh Truc and all the members of my family for their endless support and encouragements, also in my studies.

## ABSTRACT

In this study, behavior of lime-/cement-treated, especially lime/cement lightly treated clayey soils has been investigated. The main items investigated are: (1) physico-chemical properties, (2) permeability (3) undrained shear strength ( $s_u$ ) and (4) consolidation behaviour also. A hybrid method has been proposed by using waste clayey soil as embankment backfill, which combines light cement/lime treatment and using dual function (drainage and reinforcement) geocomposite. A key point of the method is predicting  $s_u$  value of the clayey backfill during and after an embankment construction. A prediction method has been proposed and validated by analyzing two case histories in Japan.

(1) *Physico-chemical properties*. To understand the fundamental effect of cementation process of lime/cement treatment on the change of micropore network in soil structure, series of physico-chemical property tests, e.g. pH measurement, Atterberg limit, particle size distribution, electrical conductivity, ion concentration tests, mercury intrusion porosimetry (MIP) test and the images of scanning electron microscope (SEM) were carried out. The results indicate that the plastic limit increases with an increase of cement/lime content, and the rate of increase is higher at lower cement/lime content. When the cement content is less than 4% or for the lime 2% by dry weight, there were obvious changes in particle size distributions but insignificant change in shear strength. For adding 2 and 4% of the cement or the lime into the Ariake clay cases, the values of thickness of diffusive double layer ( $1/K$ ) were estimated. It can be seen that the cement-treated cases have relative smaller  $1/K$  value, and it implies that under the same microstructure condition, the cement-treated soils tend to have a thinner DDL and a higher permeability than the lime-treated soils.

(2) *Undrained shear strength ( $s_u$ )*. To investigate the effect of cement/lime on shear strength and compression behavior of clayey soils, unconfined compression test and oedometer consolidation test were conducted. Unconfined compression strength ( $q_u$ ) of the lime treated soils was higher than that of the cement-treated soils. For less than 16% of lime/cement content, the relationship between  $q_u$  and apparent yield stress ( $p_y$ ) with the amount of additive is non-linear.

(3) *Compression and secondary compression indexes ( $C_c$ ,  $C_\alpha$ ) and coefficient of vertical consolidation ( $c_v$ )*. With the increase of the amount of lime or cement content, compression index ( $C_c$ ) increased whereas secondary compression index ( $C_\alpha$ ) decreased. And about the coefficient of consolidation results, in the overconsolidated range, the data are scattered, but in the virgin consolidation range, for both treated soils there is a clear trend increase in  $c_v$  with the increase of lime/cement content.

(4) *Permeability ( $k$ )*. Several researches investigated the influence of lime or cement treatment on the hydraulic conductivity ( $k$ ) of the treated soils. However, there are still no unified understanding. Some researchers reported that the treated soil has a higher  $k$  value than the untreated soil, while some

results indicated that the treated soil has a lower  $k$  value or the same as the untreated soil. So, to fundamentally understand the factors influencing on  $k$  value of lime-/cement-treated clayey soils, the flexible-wall permeameter was developed and used in this study. The test results are compared with the values deduced from the oedometer consolidation test results. The test results indicate that: (a) For cement treatment (up to 8% of cement content by dry weight), under the same void ratio ( $e$ ) condition, permeability ( $k$ ) is almost the same as that of untreated soils and decreases significantly when cement content is higher than 8%. But for lime-treated soils, when the lime content is more than 4%,  $k$  value reduces with the increase of lime content. (b) Investigation on microstructures of the soils by mercury intrusion porosimetry test (MIP) and scanning electron microscope (SEM) images indicates that when the cementation products formed by pozzolanic reaction mainly fill the intra-aggregate pores,  $k$  value does not change much, and when the cementation products start to fill the inter-aggregate pores,  $k$  value reduces, and the strength of the treated soils increases. (c) Further the test results indicate that the chemical properties of pore water influence  $k$  value by altering the thickness of the diffuse double layer (DDL), and the cement-treated soils had thinner DDLs and higher  $k$  values than the lime-treated soils with similar microstructures. (d) The  $k$  values from the permeability test and oedometer test are similar and comparable, but the results from the oedometer test seems more scatter than these of the flexible-wall permeability test.

(5) *A hybrid method for using waste clayey soil as embankment fill material.* A effective and economic way of using waste clayey soil as backfill material has been proposed. Firstly, treating the waste clayey soil with high water content by small amount of cement or lime to make it transportable. Then, use it as backfill material with dual function (drainage and reinforcement) geocomposite to accelerate its self-weight induced consolidation and increase its strength and stiffness. In design, one of the basic requirements is to predict the geocomposite induced consolidation, and the undrained shear strength ( $s_u$ ) increase during the construction process. In case of combining lime/cement treatment and using dual function geocomposite, both the effects of cementation and consolidation on  $s_u$  value have to be considered. In this study, laboratory large scale model tests were conducted to investigate the behavior of geocomposite induced consolidation of clayey soils with and without lime/cement additives. Then, using the laboratory measured  $s_u$  values, a method for predicting  $s_u$  value of the lime/cement lightly treated clayey soil during an embankment construction has been proposed. Finally, validity of the proposed method has been demonstrated by analyzing two case histories in Japan.

## TABLE OF CONTENTS

<b>ACKNOWLEDGMENT</b>	i
<b>ABSTRACT</b>	ii
<b>TABLES OF CONTENTS</b>	iii
<b>LIST OF TABLES</b>	vi
<b>LIST OF FIGURES</b>	vii
<b>LIST OF SYMBOLS</b>	ix
<b>CHAPTER 1 INTRODUCTION</b>	<b>1</b>
1.1 General background	1
1.2 Objective and scopes	1
1.3 Organization of thesis	2
<b>CHAPTER 2 LITERATURE REVIEW</b>	<b>4</b>
2.1 Introduction	4
2.2 Physico-chemical analysis	7
2.3 Consolidation and permeability	11
2.4 Consolidation induced by geocomposite	13
2.5 Predicting method of undrained shear strength	14
2.6 Summaries	15
2.6.1. About permeability	15
2.6.2. Method for predicting undrained shear strength ( $s_u$ )	15
<b>CHAPTER 3 PHYSICO-CHEMICAL PROPERTIES OF TREATED CLAYEY SOILS</b>	<b>17</b>
3.1 Introduction	17
3.2 Test methods	17
3.3 Materials used and specimen preparations	17
3.3.1. Materials used	17
3.3.2. Specimen preparation	18
3.4 Cases tested	19
3.5 Atterberg limit and pH measurement	19
3.6 Ion concentration and electrical conductivity	21
3.7 Particle size distribution	22
3.8 Pore size distribution from mercury intrusion porosimetry (MIP) tests	23
3.8.1. Testing method and procedure	23
3.8.2. Results	24
3.9 Scanning electron microscope (SEM)	27
3.9.1. Testing method and procedure	27
3.9.2. Results	28

3.10 Mechanism of the effect of cement and lime additive on particle size distribution .....	30
3.11 Summaries.....	30
<b>CHAPTER 4 LABORATORY CONSOLIDATION AND PERMEABILITY TESTS.....</b>	<b>32</b>
4.1 Introduction.....	32
4.2 Permeability and oedometer tests .....	32
4.2.1. Flexible-wall permeameter and consolidometer .....	32
4.2.2. Procedure for flexible-wall permeability test.....	35
4.2.3. Procedure for oedometer consolidation test.....	36
4.2.4. Cases tested .....	37
4.3 Oedometer consolidation test results .....	37
4.3.1. Apparent consolidation yield stress ( $p_y$ ) .....	37
4.3.2. Compression and secondary compression indexes ( $C_c$ and $C_\alpha$ ) .....	39
4.3.3. Coefficient of vertical consolidation ( $c_v$ ).....	39
4.4 Permeability test results .....	41
4.4.1. Permeability .....	41
4.4.2. Factors affecting permeability .....	43
4.5 Summaries.....	49
<b>CHAPTER 5 LARGE SCALE CONSOLIDATION TESTS USING GEOCOMPOSITE.....</b>	<b>50</b>
5.1 Introduction.....	50
5.2 Laboratory model test .....	50
5.2.1. Equipment .....	50
5.2.2. Test procedure.....	52
5.2.3. Materials used .....	53
5.2.4. Cases tested.....	53
5.3 Laboratory vane shear test for model grounds.....	54
5.3.1. Equipment and specimen preparation .....	54
5.3.2. Test results of the model grounds .....	55
5.4 Large scale model test results .....	56
5.4.1. Settlement.....	56
5.4.2. Variation of excess pore water pressure ( $u$ ).....	58
5.4.3. Undrained shear strength ( $s_u$ ).....	61
5.5 Summaries.....	63
<b>CHAPTER 6 UNDRAINED SHEAR STRENGTH.....</b>	<b>64</b>
6.1 Introduction.....	64
6.2 Unconfined compression test for cement/lime treated samples.....	64
6.2.1. Equipment and specimen preparation .....	64
6.2.2. Test results .....	65
6.2.3. Correlation between $q_u$ and admixture water-lime ratio .....	68

6.3	Predicting undrained shear strength ( $s_u$ ) .....	71
6.3.1.	Method for predicting excess pore pressure ( $u$ ).....	71
6.3.2.	Method for predicting $s_u$ value.....	73
6.3.3.	Application of proposed method on laboratory large scale model test 74	
6.4	Analyzing case histories.....	78
6.4.1.	Brief description of case histories.....	78
6.4.2.	Prediction of undrained shear strength increment ( $\Delta s_u$ ) .....	81
6.4.3.	Evaluation of factor safety (FS).....	85
6.5	Summaries.....	86
<b>CHAPTER 7 CONCLUSIONS AND RECOMMENDATIONS.....</b>		<b>88</b>
7.1	Conclusions.....	88
7.2	Recommendations.....	90



## LIST OF TABLES

<b>Table No.</b>	<b>Title</b>	<b>Page</b>
Table 2-1	Consistency parameters determined on samples from SEDCON cells after a curing period of more than 100 days (Locat et al., 1996) .....	7
Table 2-2	Basic properties of the cemented samples in the active zones.....	8
Table 2-3	Empirical equations related to $S_u$ and effective stress ( $p'$ ) (data from Das M., Advanced Soil Mechanics, 2008).....	15
Table 3-1	Soil properties of clayey soils tested.....	18
Table 3-2	Chemical composition of cement and quicklime used.....	18
Table 3-3	List of the physico-chemical tests.....	19
Table 3-4	Effect of lime/cement on ion concentration in pore water.....	22
Table 3-6	Effect of lime/cement on particle size distribution.....	22
Table 4-1	Summary of the tests conducted .....	37
Table 4-2	Estimated thickness of DDL.....	49
Table 5-1	Soil properties of natural, cement- and lime-treated Ariake clay and dredged mud.....	52
Table 5-2	Structure and index properties of geocomposite.....	54
Table 5-3	List of tested cases .....	54
Table 5-4	Reduction of void ratio for tested cases.....	58
Table 6-1	Summary of fitted values in Eq. 6-1.....	68
Table 6-2	Geocomposite and soil parameters used for predicting the behavior of the model tests .....	74
Table 6-3	Basic properties of backfill soil (data from Nagahara et al., 2000 and Tatta, N. et al., 2003)...	81
Table 6-4	Parameters for predicting $\Delta s_u$ values of the case histories.....	82
Table 6-5	Parameters for stability analysis .....	85

## LIST OF FIGURES

Figure No.	Title	Page
Fig. 2-1	Liquefied soil stabilizing method (LSS method, Miki et al., 2005) .....	4
Fig. 2-2	Production system for foam mixed lightweight soil .....	5
Fig. 2-3	Light-weight banking method using in-situ surface soils (Miki et al., 2005).....	5
Fig. 2-4	Cement treated soil using as slope protection (Tang et al., 2001) .....	6
Fig. 2-5	Placement of cement treated soil along slope (Tang et al., 2001) .....	6
Fig. 2-6	Two stages construction method using lightly lime/cement treated clayey soils (Hino et al., 2008) .....	6
Fig. 2-7	Effect of cement content and curing time on Atterberg limit for treated clays ( $w_i = 120\%$ ).....	7
	(Chew et al., 2004).....	7
Fig. 2-8	The derivative of pore volume intrusion of mercury as a function of pore radius (Locat et al., 1996) .....	9
Fig. 2-9	Effect of cement content and curing time on particle size distribution of treated clays .....	9
	(Chew et al., 2004).....	9
Fig. 2-10	Scanning electron microscope images: samples prepared in rings after 80 days of curing a) natural clay, b) treated with 2 % lime, c) and d) treated with 10 % lime (Locat et al., 1996) .....	10
Fig. 2-11	SEM images: cement treated Ariake clay after 28 days of curing (Yamadera, 1999).....	11
Fig. 2-12	Permeability curves vs. void ratio of lime treatment after 30 days of curing (Locat et al., 1996) .....	12
Fig. 2-13	$e - \log \sigma'_v$ , and $e - \log k$ relations in remolded and cement stabilized Ariake clay (Yamadera, 1999) .....	12
Fig. 2-14	Void ratio and permeability ( $e - \log k$ ) relationship of treated.....	12
Fig. 2-15	Sandwich reinforcement (Yasuhara et al., 2001) .....	13
Fig. 2-16	Proposed model of geocomposite induced consolidation of clayey soils under stepwise load ..	14
Fig. 3-1	Casagrande liquid limit device and pH measurement device .....	20
Fig. 3-2	Atterberg's limit of cement/lime treated Ariake clay .....	20
Fig. 3-3	Atterberg's limit of cement/lime treated dredged mud.....	20
Fig. 3-4	pH measurement of cement/lime treatment .....	21
Fig. 3-5	Electrical conductivity of cement/lime treatment.....	21
Fig. 3-6	Particle size test using sieves analysis and hydrometer .....	22
Fig. 3-7	Particle size distribution curves.....	23
Fig. 3-8	MIP apparatus (Micromeritric instrument).....	24
Fig. 3-9	Effect of cement treatment on pore size distribution curves of treated Ariake clay.....	25
Fig. 3-10	Effect of lime treatment on pore size distribution curves of treated Ariake clay .....	25
Fig. 3-11	Effect of cement treatment on pore size distribution curves of treated dredged mud .....	26
Fig. 3-12	Effect of lime treatment on pore size distribution curves of treated dredged mud.....	26
Fig. 3-13	Comparison between measured and MIP derived water content.....	27
Fig. 3-14	SEM apparatus (JEOL-5800 machine) and freezing drying equipment.....	27
Fig. 3-15	SEM images of treated and untreated Ariake clay .....	28
Fig. 3-16	SEM images of treated and untreated dredged mud.....	29
Fig. 3-17	Cementing process.....	30
Fig. 4-1	Schematic illustration of flexible-wall permeameter .....	33
Fig. 4-2	Detail of flexible-wall permeameter .....	34
Fig. 4-3	Load frame and consolidometer .....	34

Fig. 4-4 Oedometer compression curves of untreated and treated soils with curing time of 28 days.....	38
Fig. 4-5 Yield stress and water content vs. cement or lime content with curing time of 28 days.....	38
Fig. 4-6 Compression index vs. cement and lime content with curing time of 28 days.....	39
Fig. 4-7 Secondary compression index vs. cement and lime content with curing time of 28 days.....	40
Fig. 4-8 $c_v - \sigma'_v$ relation of lime-/cement-treated dredged mud with curing time of 28 days.....	40
Fig. 4-9 $c_v - \sigma'_v$ relation of lime-/cement-treated Ariake clay with curing time of 28 days.....	41
Fig. 4-10 Permeability of cement treated Ariake clay.....	42
Fig. 4-11 Permeability of lime treated Ariake clay.....	42
Fig. 4-12 Permeability of cement treated dredged mud.....	43
Fig. 4-13 Permeability of lime treated dredged mud.....	43
Fig. 4-14 Pore size distributions of cement-/lime-treated and untreated Ariake clay.....	45
Fig. 4-15 SEM images of lime/cement treated Ariake clay after permeability test.....	46
Fig. 4-16 Comparison of variations of pore size distributions and permeability.....	47
Fig. 4-17 Strain – stress curves of unconfined compressive test.....	47
Fig. 5-1 Illustration of geocomposite reinforced plain strain “unit cell”.....	51
Fig. 5-2 Large scale model test set-up.....	51
Fig. 5-3 Laboratory mini vane shear device.....	55
Fig. 5-4 Surface vertical settlement of Cases 1, 2 and 3.....	57
Fig. 5-5 Surface vertical settlement of Cases 4, 5 and 6.....	58
Fig. 5-6 Comparison between measured and predicted excess pore pressure of Cases 1, 2 and 3.....	59
Fig. 5-7 Comparison between measured and predicted excess pore pressure of Cases 4, 5 and 6.....	60
Fig. 5-8 Excess pore water pressure without consolidation during 50 days of curing time.....	61
Fig. 5-9 Increase of undrained shear strength ( $s_u$ ) of Cases 1, 2 and 3.....	62
Fig. 5-10 Increase of undrained shear strength ( $s_u$ ) of Cases 4, 5 and 6.....	62
Fig. 6-1 Unconfined compression apparatus.....	64
Fig. 6-2 Unconfined compressive strength curves of the dredged mud with curing time of 28 days.....	65
Fig. 6-3 Unconfined compressive strength curves of the Ariake clay with curing time of 28 days.....	65
Fig. 6-4 Non-linear relationship between unconfined compression strengths vs. lime content.....	66
Fig. 6-5 Non-linear relationship between unconfined compression strengths vs. cement content.....	67
Fig. 6-6 Unconfined compression strengths vs. curing time of lime treated soils.....	67
Fig. 6-7 Unconfined compression strengths vs. curing time of cement treated soils.....	68
Fig. 6-8 $q_u - w_c/c$ relationship of lime treated dredged mud.....	69
Fig. 6-9 $q_u - w_c/c$ relationship of cement treated dredged mud.....	69
Fig. 6-10 $q_u - w_c/c$ relationship of lime treated Ariake clay.....	70
Fig. 6-11 $q_u - w_c/c$ relationship of cement treated Ariake clay.....	70
Fig. 6-12 Unit cell model (Chai et. al., 2011).....	72
Fig. 6-13 Stepwise loading (Chai and Miura, 2002).....	73
Fig. 6-14 Comparison between measured and predicted excess pore pressure of Cases 1, 2 and 3.....	75
Fig. 6-15 Comparison between measured and predicted excess pore pressure of Cases 4, 5 and 6.....	76
Fig. 6-16 Increase of undrained shear strength ( $s_u$ ) of Cases 1, 2 and 3.....	77
Fig. 6-17 Increase of undrained shear strength ( $s_u$ ) of Cases 4, 5 and 6.....	77
Fig. 6-18 Cross section of embankment of Case A.....	79
Fig. 6-19 Layout of geocomposite of Case A.....	79
Fig. 6-20 Cross section of embankment of Case B.....	80
Fig. 6-21 Arrangement of geocomposite of Case B.....	80

Fig. 6-22 Comparison between measured and predicted average excess pore water pressure of Case A .	83
Fig. 6-23 Comparison between measured and predicted average excess pore water pressure of Case B..	83
Fig. 6-24 Prediction of $\Delta s_u$ values of Case A .....	84
Fig. 6-25 Prediction of $\Delta s_u$ values of Case B .....	84
Fig. 6-26 Effect of $s_u$ increment and $T_a$ on $FS$ of embankment in Case A .....	86
Fig. 6-27 Effect of $s_u$ increment and $T_a$ on $FS$ of embankment in Case B .....	86

## LIST OF SYMBOLS

$B$	Half of space between two plane strain geocomposite sheets
$c$	Lime content
$c_v$	Vertical coefficient of consolidation
$C_c$	Compression index
$C_r$	Recompression index
$C_\alpha$	Secondary compression index
$D$	Entrance pore diameter
$D_e$	Diameter of unit cell
$D_w$	Dielectric constant
$d$	Diameter of vane
$d_w$	Equivalent diameter of geocomposite strip
$e$	Void ratio
$e_o$	Initial void ratio
$e_f$	Final void ratio
$EC$	Electrical conductivity
$G_s$	Specific gravity
$H$	Initial height of model ground
$h$	Height of vane
$i$	Hydraulic gradient
$I_L$	Liquidity index
$IC$	Ion concentration
$k$	Coefficient of permeability
$k_v$	Vertical permeability of model ground
$1/K$	Thickness of diffuse double layer
$l$	Length of geocomposite
$M_B$	Resisting moment at the bottom of the soil cylinder
$M_S$	Resisting moment at the side of the soil cylinder
$M_T$	Resisting moment at the top of the soil cylinder
$m$	Constant value in Ladd equation
$m_v$	Coefficient of volume compressibility
$N$	Avogadro's number
$n$	Fitted value in $q_u$ equation
$n_o$	Electrolyte concentration
$OCR$	Overconsolidation ratio
$PI$ or $I_p$	Plasticity index
$p'$ or $\sigma_v$	Effective vertical stress

$p'_c$ or $\sigma_p$	Pre-consolidation stress
$P_{cell}$	Cell pressure
$P_L$	Vertical consolidation pressure
$p_y$	Yield stress
$p_i$	Total load at i step
$q_w$	Discharge capacity of geocomposite
$q_{wp}$	Discharge capacity of geocomposite per unit width
$q_u$	Unconfine compression strength
$q_o$	Fitted value in $q_u$ equation
$R$	Pore radius
$S$	Constant value in Ladd equation
$S_c$	Primary settlement
$S_v$	Vertical spacing of geocomposite
$S_h$	Horizontal spacing of geocomposite
$s_u$	Undrained shear strength
$s_{u1}$	Undrained shear strength due to consolidation
$s_{u2}$	Undrained shear strength due to cementation effect
$\Delta s_u$	Increment of undrained shear strength
$s_{uo}$	Initial undrained shear strength
$T$	Temperature
$T_{max}$	Maximum torque
$t_g$	Thickness of geocomposite
$t$	Elapsed time
$t_i$	Time at $U_i$
$t_{jo}$	Imaginary time corresponding to $U_{jo}$
$T_v$	Time factor for vertical drainage
$u$	Excess pore water pressure
$U$	Average degree of consolidation
$U_{jo}$	Degree of consolidation at $t_i$
$w/c$	water-cement ratio
$w$	Width of geocomposite
$w_n$	moisture content
$w_c$	Water content of admixture with curing time of 28 days
$w_p$	Plastic limit
$w_L$	Liquid limit
$\varepsilon$	Strain
$\gamma_t$	Total unit weight of soil
$\gamma_{dmax}$	Unit weight at optimum water content
$\mu$	Factor for the effect of spacing

$V$	Pore volume intrusion of mercury
$\nu$	Cation valence
$\Delta e$	Reduction of void ratio
$\Delta p_j$	Incremental load of j step
$\Delta \sigma$	Stress increment due to surcharge
$\Delta t$	Time increment

# CHAPTER 1 INTRODUCTION

## 1.1 General background

In recent years, how to treat the surplus clayey soils generated from construction sites and dredged mud from harbors is one of the geoenvironmental problems. On the other hand, there is a shortage of sandy soils, such as decomposed granite from mountains, to be used as construction fill material. Therefore, if an effective technique can be developed to use the waste clayey soils as construction fill material, these two problems can be solved together. The most widely used method is to improve the mechanical properties of the clayey soil by adding cement or lime. But for high water content clayey soils, the resulting material will have a high void ratio and there is a concern about its long-term engineering properties. An alternative way is to treat the clayey soils with small amount of lime or cement (i.e., 2 ~ 6% by dry weight). There are two purposes for using light lime-/cement-treated clayey soils: (1) Mixing small amount of lime/cement to make soft clay enough strong for transportation. (2) Without lime/cement treatment, due to the high natural water content of clayey soils (>150%), the constructing embankment is impossible. With small amount of lime/cement (<4% cement or 2% lime), the aggregates/clusters of the treated soils stick together but still low undrained shear strength and therefore very easy to compress during the consolidation process. Then using the soil as embankment fill material with dual functions (drainage and reinforcement) geocomposite (Chai et al., 2011). The drainage effect can accelerate the self-weight consolidation of the clayey soils and the reinforcement effect can improve the stability of the embankment (Yamadera 1999; Zheng et al., 2009; Raisinghani and Viswanadham, 2010, 2011; Taechakumthorn and Rowe, 2012).

In case of placing geocomposite into cement or lime treated clayey soil, geocomposite needs to be made with geosynthetics of high alkaline resistance. Also in actual engineering practice, these may be a surface stability problem of an embankment, and it can be solved by either using high quality sandy soil at slope surface or wrapping each soil layer by geotextile at both sides.

## 1.2 Objective and scopes

There are numbers of publications on the behavior of cement or lime treated clayey soils (Brom et al, 1979; Terashi et al., 1979, 1983; Kawasaki et al., 1981; Bergado 1996; Tatsuoka et al., 1996; Uddin and Balasubramniam, 1997; Miura et al., 1998; Lorenzo et al., 2003; Horpibulsuk et al., 2004; Chai, J.C. and Miura, N. 2005). However for lime/cement lightly treated clayey soils, only few publications available in the literature (McCallister and Petry 1992; Locat et al., 1990, 1996; Yamadera 1999; Chew et al., 2004; Quang et al., 2011; Al-Mukhtar et al., 2012; Chai, J.C. and Quang D. N. 2011, 2012), and there are still unclear point on their physico-chemical and mechanical behaviour. The objectives of this study are: through a series of laboratory tests to investigate (1) physico-chemical and (2) mechanical properties of two types clayey soils in Japan.



The mechanical properties investigated are undrained shear strength and coefficient of consolidation, which is a function of permeability and coefficient of volume compressibility. In this study, permeability of lime and cement lightly treated clayey soils were investigated by laboratory flexible-wall permeameter and also determined indirectly by oedometer consolidation test results. Series of physico-chemical tests (e.g., pH measurement, Atterberg's limit, grain size distribution, electrical conductivity, and ion concentration test) and microstructure analysis (mercury intrusion porosimetry (MIP) and scanning electron microscope (SEM)) tests were conducted. After that, laboratory large scale model tests were conducted to investigate the geocomposite induced consolidation behavior of clayey soils with and without lime/cement additives. Then, using the laboratory measured  $s_u$  values from vane shear test and unconfined compression test, and permeability from laboratory flexible-wall permeability test, a suitable method for predicting  $s_u$  value of the clayey soil during an embankment construction is discussed. Finally, the proposed method has been applied to analyze two case histories in Japan.

The research works conducted can be classified into 3 groups: laboratory tests, large scale consolidation tests and proposed method for predicting undrained shear strength.

- (1) **Laboratory tests.** A series of physico-chemical tests: pH measurement, Atterberg's limit, particle size distribution, electrical conductivity, ion concentration, microstructure analysis (MIP and SEM), oedometer consolidation and permeability tests were conducted.
- (2) **Large scale consolidation tests.** Large scale model tests were done to investigate geocomposite induced consolidation of lime/cement lightly treated clayey soils under stepwise load.
- (3) **Proposed method for predicting undrained shear strength.** Proposed method for predicting undrained shear strength ( $s_u$ ) induced by consolidation and cementation effect were discussed.

### 1.3 Organization of thesis

As seen in Fig. 1-1, this dissertation contains seven chapters. The introduction (Chapter 1) describes the general background, objectives and scopes of research and organization of dissertation.

Chapter 2 reviews the literature regarding the previous study about physico-chemical properties, permeability, consolidation behaviour of lime/cement lightly treated clayey soils and various predicting methods of undrained shear strength.

Chapter 3 describes physico-chemical properties of treated clayey soils. The results of physico-chemical test: pH measurement, Atterberg's limit, grain size distribution, electrical conductivity, ion concentration test and microstructure analyses (MIP and SEM) test are discussed.

Chapter 4 presents the results of laboratory oedometer consolidation test and flexible-wall permeability test. The details of equipment, material used, test procedures, cases tested and interpretation of the results are given in this chapter.

Chapter 5 presents the details of large scale consolidation tests and results.

Chapter 6 discusses about the proposed method to predict excess pore water pressure and undrained shear strength of geocomposite induced consolidation under stepwise load. Then, the proposed method was applied to analyze two case histories in Japan.

Finally, the conclusions drawn from this study and recommendations for future works are given in Chapter 7.

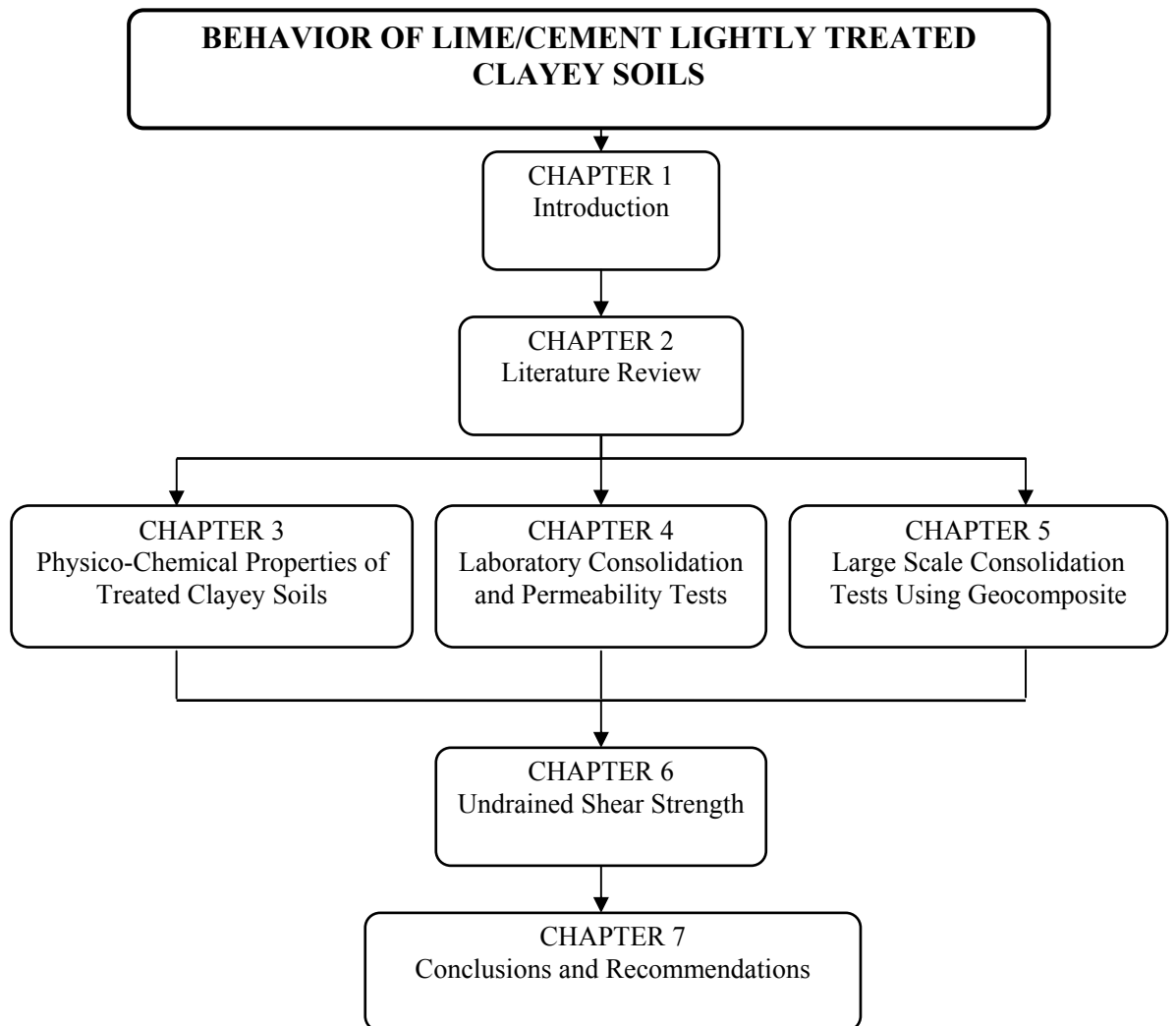


Fig. 1-1 Flow chart of this dissertation

## CHAPTER 2 LITERATURE REVIEW

### 2.1 Introduction

Mixing lime/cement with in-situ soils to form soil-cement columns start in the late 1970's in Japan (Okumura and Terashi, 1975; Terashi et al., 1979 and 1983; Kawasaki et al., 1981; and Suzuki, 1982). The fundamental mechanical properties and engineering behavior of the cement stabilized soils were investigated by several researchers (Terashi et al., 1979; Kawasaki et al., 1981; Bergado 1996; Tatsuoka et al., 1996; Uddin and Balasubramniam, 1997; Horpibulsuk et al., 2004; Chai, J.C. and Miura, N. 2005), and the method became one of the most widely used soft ground improvement technique. In recent years, how to treat the surplus clayey soils generated from construction sites and dredged mud from harbors is one of the geoenvironmental problems. On the other hand, there is a shortage of sandy soils, such as decomposed granite from mountains, to be used as construction fill material. Therefore, if an effective technique can be developed to use the waste clayey soils as construction fill material, these two problems can be solved together. The result of survey for the fiscal year of 2000 (Miki et al., 2005): approximately 208 million m<sup>3</sup> of waste soil from construction site in Japan (only 30% re-used for construction work). So, the question is how to treat the waste clayey soils from construction sites and dredged mud from harbours. And second reason is due to shortage of sandy soils for construction fill material. Liquefied soil stabilizing method (LSS method) was proposed by Miki et al. (2005). Mixing soil can be facilitated by turning cohesive soil into slurry by increasing its water content. The mixture can not be compacted but can be used to fill spaces closely due to its liquidity; strength can be developed after hardening, like placing concrete into a form (Fig. 2-1).

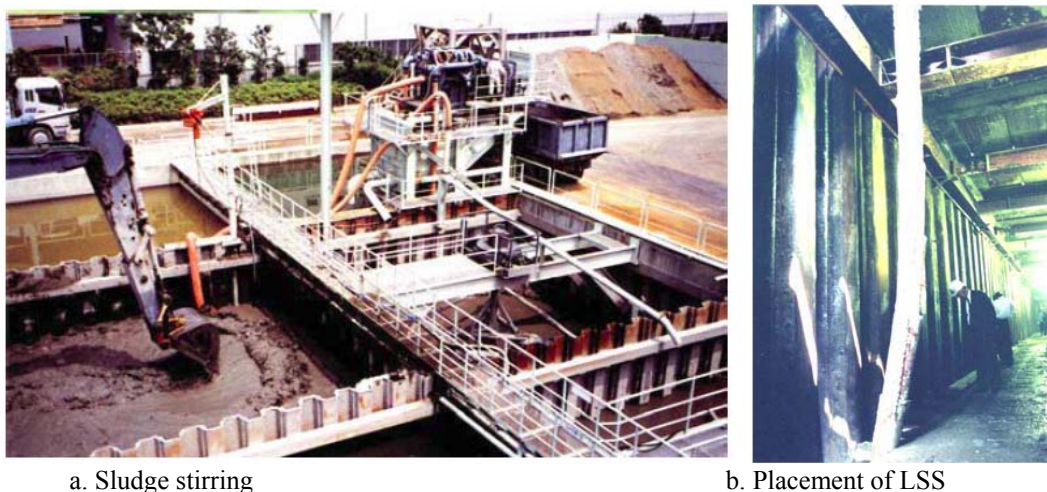


Fig. 2-1 Liquefied soil stabilizing method (LSS method, Miki et al., 2005)

Another method is pipe-line soil treatment system (Fig. 2-2). For the purpose of stabilization of dredged mud, pipe-line soil mixing methods are getting popularized in Japan. The pipe-line treatment system has developed as a kind of the pipe-line soil mixing methods. The system is called

“Kanro Mixer” installed on the way of dredging pipe-line and feeder devices for mixing materials. The system can be utilized for not only the consolidation of mud but also making the foam mixed soil, producing grainy soil and so on (Miki et al., 2005).

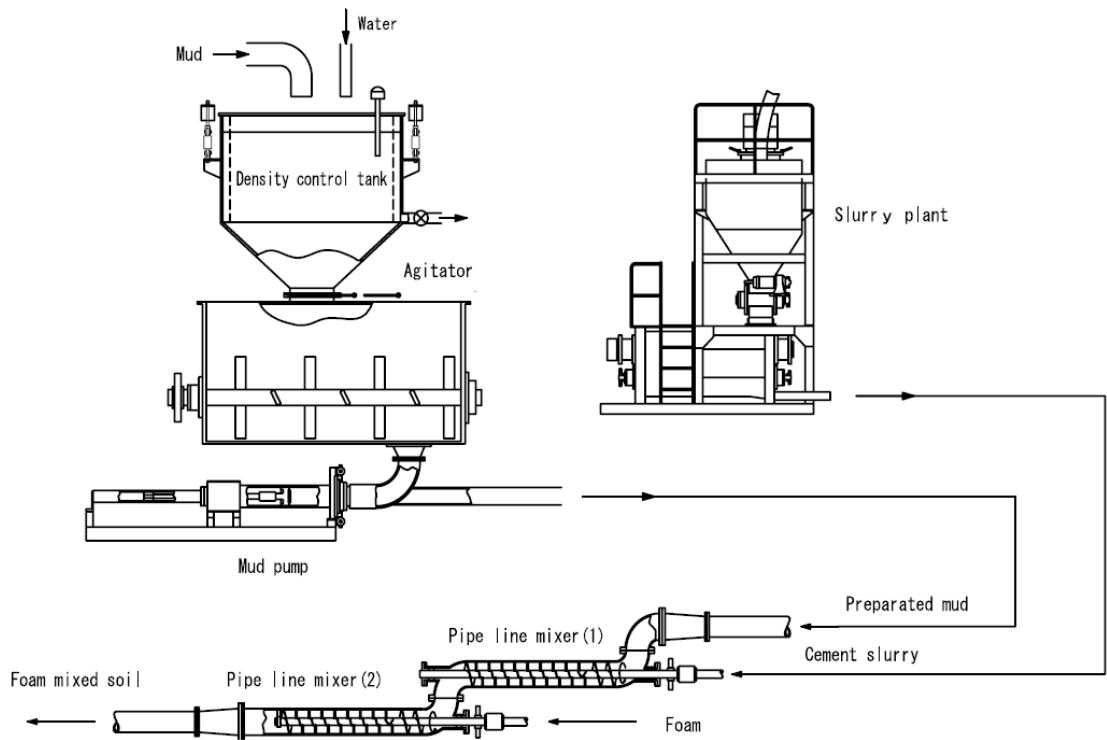


Fig. 2-2 Production system for foam mixed lightweight soil

Foam mixed soil has been used extensively in Japan for road widening and back-filling projects, but never throughout the entire road cross-section (Fig. 2-3). Cohesive soil taken in situ from the surface of the ground was used to make a high lightweight soil embankment. Geogrid layers were laid at uniform intervals to add reinforcement to the embankment. The slope faces are sprayed with a seed-mud-chemical mixture to create vegetation cover (Miki et al., 2005).



a. Embankment construction in progress



b. Completed embankment

Fig. 2-3 Light-weight banking method using in-situ surface soils (Miki et al., 2005)

Backfill as seep-proof structure: To protect the dredgings or waste soils from leaking through the rubble mound, it is necessary to place protection inside wharf. It was found that dredged soft soil after being treated with cement was a rational alternative for this protection at a depth of 20 to 40 m.

As shown in Fig. 2.4 and 2.5, it was decided to place the cement treated soil inside the wharf, with a layer thickness greater than 1.0 m and a slope about 1:3.

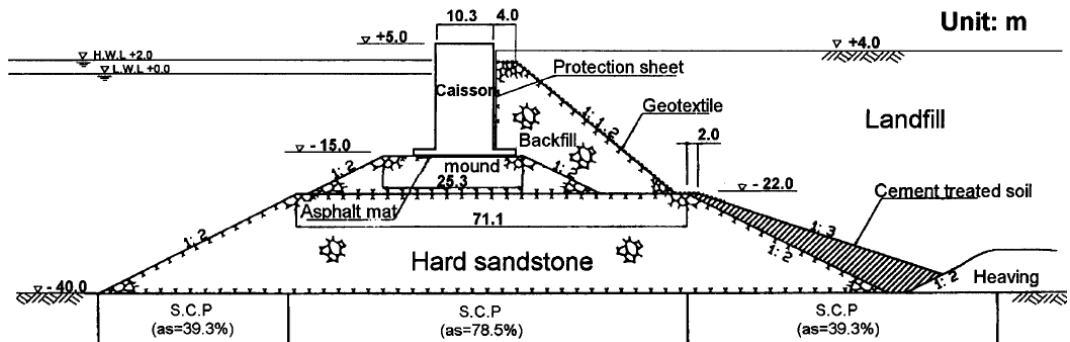


Fig. 2-4 Cement treated soil using as slope protection (Tang et al., 2001)

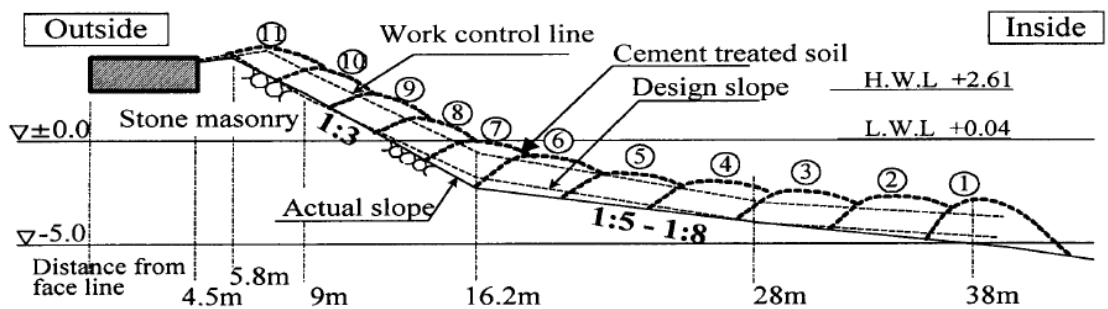


Fig. 2-5 Placement of cement treated soil along slope (Tang et al., 2001)

Recently, two stage methods for treatment the dredged mud or surplus clayey soils generated from construction sites was proposed. First stage is that clayey soils were mixed with a small amount of lime/cement to make them stronger enough for transportation. Then improve the mechanical properties of treated clayey soils by adding more lime/cement (Hino et al., 2008) (Fig. 2-6). Second stage is combination of lightly cement treatment with dual functions (reinforcement and drainage) horizontal geocomposite (Chai et al., 2011). The drainage effect can accelerate the self-weight consolidation of the clayey soils and the reinforcement effect can improve the stability of the embankment.



Fig. 2-6 Two stages construction method using lightly lime/cement treated clayey soils (Hino et al., 2008)

## 2.2 Physico-chemical analysis

**Effect of lime/cement on Atterberg Limit:** Locat et al., (1996) reported that the soil is classified as a plastic clay with a liquid limit of 67% and a plasticity index of 41%. After treatment with 5 and 10% lime, index properties have dramatically changed. For the samples treated with 5 and 10% lime, the liquid limit are, respectively, 181 and 213% and the plasticity indices are 124 and 139%, respectively (Table 2-1). These values still fall along the “A” line of the Casagrande plasticity chart.

Table 2-1 Consistency parameters determined on samples from SEDCON cells after a curing period of more than 100 days (Locat et al., 1996)

Lime (%)	w (%)	w <sub>L</sub> (%)	w <sub>P</sub> (%)	I <sub>P</sub> (%)	I <sub>L</sub>
0	89	67	26	41	1.53
5	341	181	57	124	2.29
10	351	213	74	139	1.99

The liquid limit increases significantly at low cement content (<10%) before dropping slightly at higher cement contents. As Fig. 2-7 shows, the rates of increase in the liquid and plastic limits with respect to the cement content are almost equal at low cement content. Chew et al., (2004) explained that this is consistent with the notion of water trapped with intra-aggregate pores. However, the rates of change of these two Atterberg limits at higher cement content are not the same. This suggests that the entrapped water hypothesis explains much, but not all, of the observed changes in the plastic and liquid limits. One possible reason for this is the deposition of cementation products onto the surfaces of the flocculated clay clusters, which would lower the surface activity of these clusters.

Horpibulsuk et al., 2010 reported that the adsorption of Ca<sup>2+</sup> ions onto the clay particle surface decreases the repulsion between successive diffused double layers and increases edge-to-face contacts between successive clay sheets. Thus, clay particles flocculate into larger clusters, which increase in the plastic limit with an insignificant change in the liquid limit (Table 2-2). As such, the plasticity index of the mixture results from the significant increase in the plastic limit.

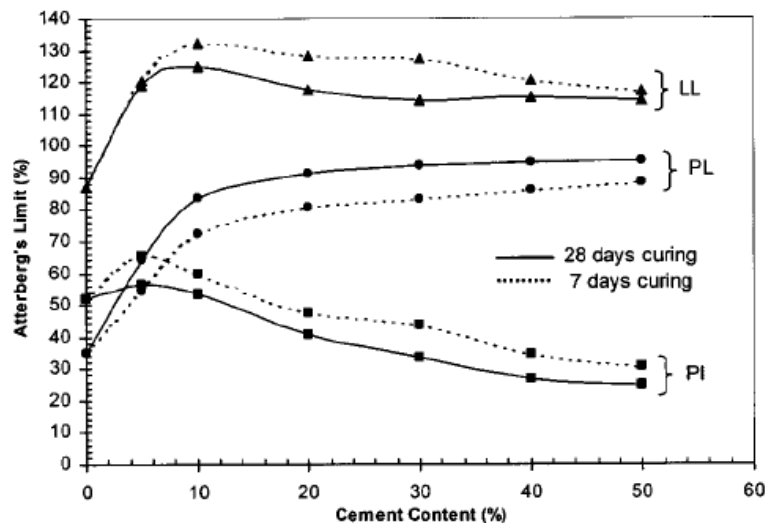


Fig. 2-7 Effect of cement content and curing time on Atterberg limit for treated clays ( $w_i = 120\%$ ) (Chew et al., 2004)

Table 2-2 Basic properties of the cemented samples in the active zones.

Cement (%)	Atterberg's limits (%)			Optimum water content (%)		$\gamma_{dmax}$ (kN/m <sup>3</sup> )	
	w <sub>L</sub>	w <sub>P</sub>	I <sub>P</sub> (%)	Standard	Modify	Standard	Modify
0	74.1	27.5	46.6	22.4	17.2	14.6	17.4
3	74.1	45.0	29.1	22.2	17.5	16.2	18.5
5	72.5	45.0	27.5	21.8	17.3	16.2	18.7
10	71.0	44.8	26.2	22.0	17.4	16.4	18.8

**Effect of lime/cement on Particle size and Pore size distribution:** Mercury intrusion porosimetry (MIP) has been used previously for examining the microfabric of various porous media and can provide quantitative information on the distribution of pores within the material (e.g. Delage et al., 1984; Choquette et al., 1987; Locat et al., 1996; Yamadera 1999; Kang et al., 2003; Tanaka et al., 2003; Chew et al., 2004). Such information can significantly improve the understanding of the macroscopic and engineering behaviour of soils. Diamond (1970) was one of the first to investigate the pore size distribution of clays using MIP analysis.

Locat et al., (1996) used the samples of Louiseville clay and mixed with various quantities of lime (0 - 10%) and had a varied water content (122 – 650%). Based on the results of MIP tests, it is reported that the addition of lime results in a rapid increase in mercury intrusion with the resulting very large pore sizes. This is due to artificial pore space created by cementation and increased flocculation. In this case, curves for 0% and 1% lime show few pores having a radius greater than 2  $\mu\text{m}$ . The distribution of the various pore sizes for treated specimens at lime concentrations greater than 1% all indicate a significant impact of the treatment. Adding lime will increase the flocculation potential of the soil-water mixture and also will, as pozzolanic reactions take place, provide an array of pore sizes at various scales, along with some additional effects on the connectivity with the intra-aggregate pore network (Fig. 2-8). Chew et al., (2004) conducted MIP test and laser diffraction test (Mastersizer Micro) to investigate pore and particle size distribution analyses of untreated and cement-treated clays. The particle size distribution curves of the samples, inferred from the MIP data using the method suggested by Carli and Motta (1985) and directly measured by laser diffraction method (Mastersizer Micro machine) indicate that there is a shift from predominantly clay-size particles to silt-size particles (Fig. 2-9).

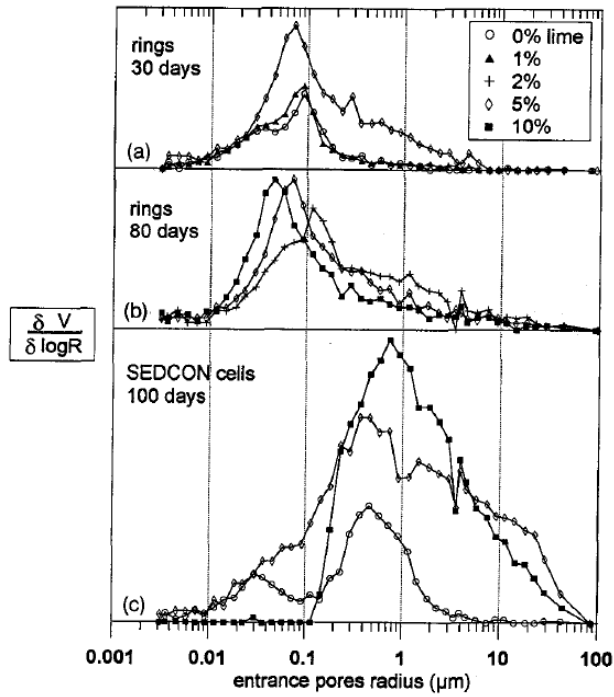
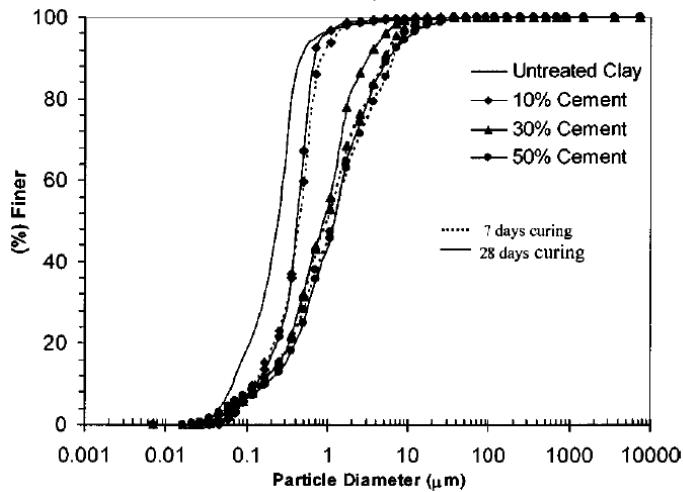
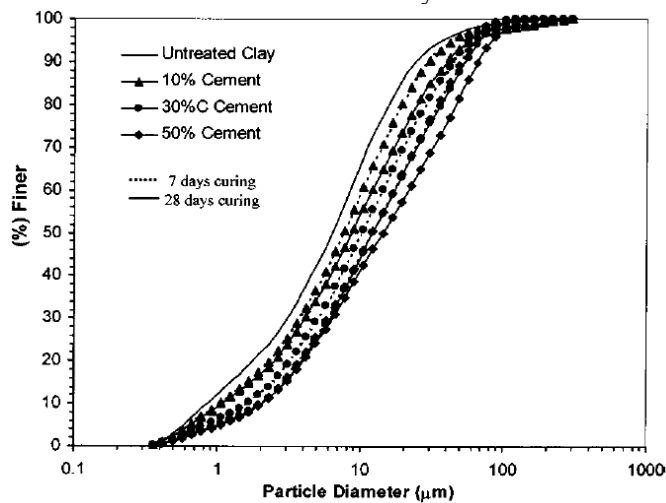


Fig. 2-8 The derivative of pore volume intrusion of mercury as a function of pore radius (Locat et al., 1996)



a. From MIP analysis



b. Measured by Mastersizer

Fig. 2-9 Effect of cement content and curing time on particle size distribution of treated clays (Chew et al., 2004)



**Scanning Electron Microscope (SEM) images of lime/cement treatment:** Scanning electron microscope images of clay samples were investigated by several researchers. Delage and Lefebvre (1984) investigated the soil structure of Champlain clay during the compression process using scanning electron microscope and porosimeter. During consolidation, most of the changes in microstructure network are related to a reduction maximum in the average entrance pore radius is shifted toward small values. Based on the SEM images, Choquette et al., (1987) indicated that secondary minerals from pozzolanic reaction are reticular particles and designated as CSH minerals (calcium silicate hydroxides). Lapierre et al., (1990) and later Locat et al., (1996) also observed the SEM image for the Louiseville clay in its remoulded state. As seen in Fig. 2-10, with 2% lime, flocculation is very visible, with aggregates of 1 – 5 $\mu$ m. Secondary minerals are not expected and are not visible at this lime concentration. Adding more lime content (i.e., 10%) it was believed that there are presence of secondary minerals such as CSH (calcium silicate hydroxides), CAH (calcium aluminate hydroxides). Yamadera (1999) also investigated the microstructure of 5%, 7.5% and 10% of cement mixed Ariake clay after 28 days of curing time obtained by SEM. It is clearly found that there are some structures produced by cement mixing, and the shape and arrangement seem to be granular soils (Fig. 2-11).

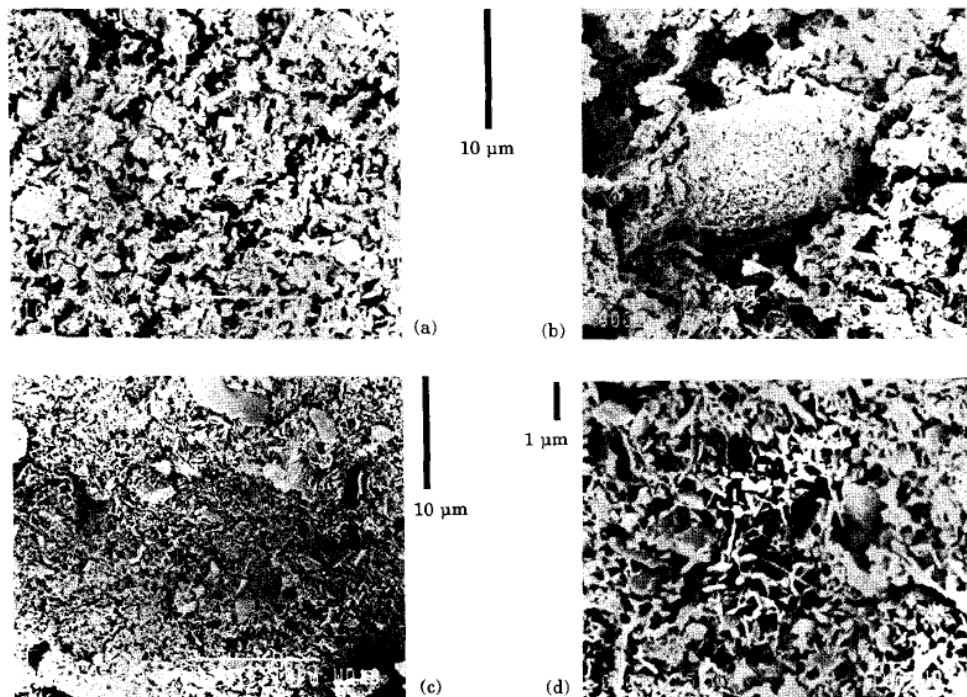


Fig. 2-10 Scanning electron microscope images: samples prepared in rings after 80 days of curing a) natural clay, b) treated with 2 % lime, c) and d) treated with 10 % lime (Locat et al., 1996)

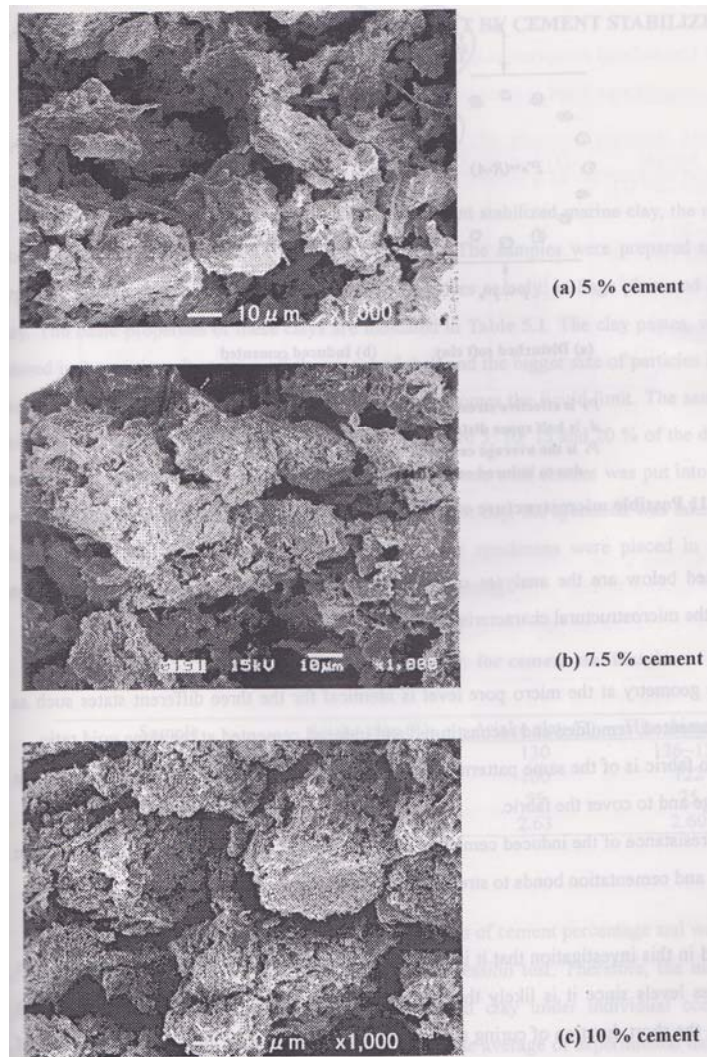


Fig. 2-11 SEM images: cement treated Ariake clay after 28 days of curing (Yamadera, 1999)

### 2.3 Consolidation and permeability

Several researches (McCallister and Petry 1992; Locat et al., 1996; Yamadera 1999; Chew et al., 2004; Al-Mukhtar et al., 2012) investigated the influence of lime or cement treatment on the hydraulic conductivity ( $k$ ) of the treated soils. When compared under the same void ratio ( $e$ ) condition, McCallister and Petry (1992) showed that the  $k$  values increase with the lime content up to 3%, and then decrease with the lime content. Locat et al. (1996) reported that lime treatment reduced  $k$  value of soil (Fig. 2-12). Yamadera (1999) conducted permeability test on 5% of cement-treated Ariake clay and indicated that the untreated and treated Ariake clay have almost the same  $k$  value (Fig. 2-13). Chew et al. (2004) reported that for the same  $e$  value, the cement treated soft Singapore marine clay had lower permeability than the untreated soft clay (Fig. 2-14). Al-Mukhtar et al. (2012) reported that the permeability increased substantially with the increase of lime content up to 4% and then decreases with 10% of lime. The hydraulic conductivity measurement was done with the falling head method, with observation made over a period of 24 h. So, for each consolidation test, five or six hydraulic conductivity measurements were made.

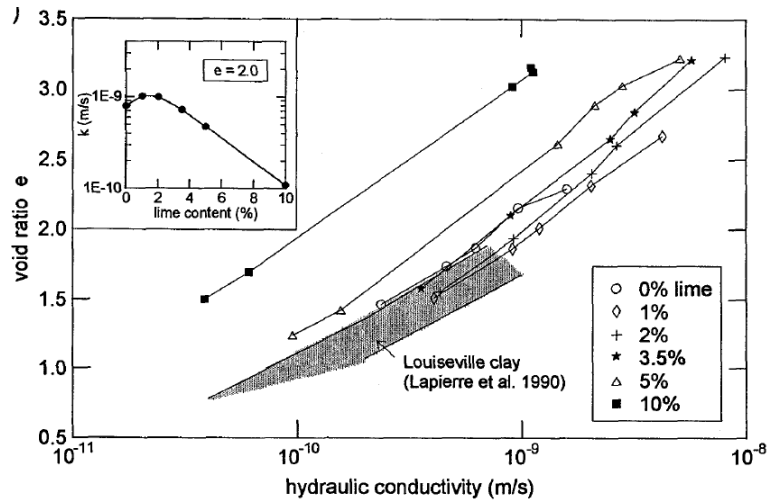


Fig. 2-12 Permeability curves vs. void ratio of lime treatment after 30 days of curing (Locat et al., 1996)

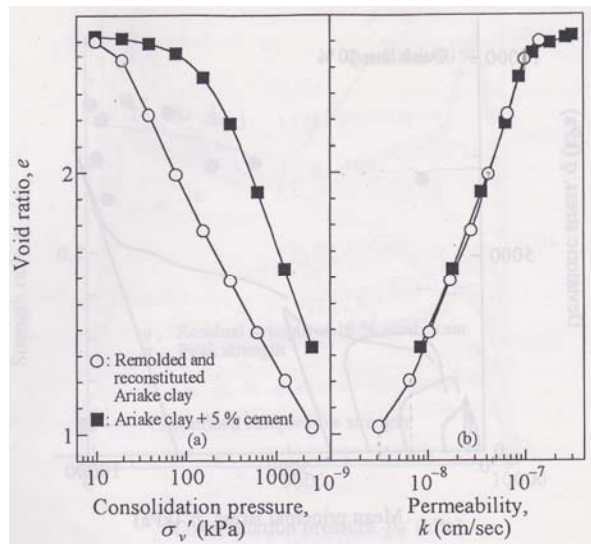


Fig. 2-13  $e - \log \sigma'_v$  and  $e - \log k$  relations in remolded and cement stabilized Ariake clay (Yamadera, 1999)

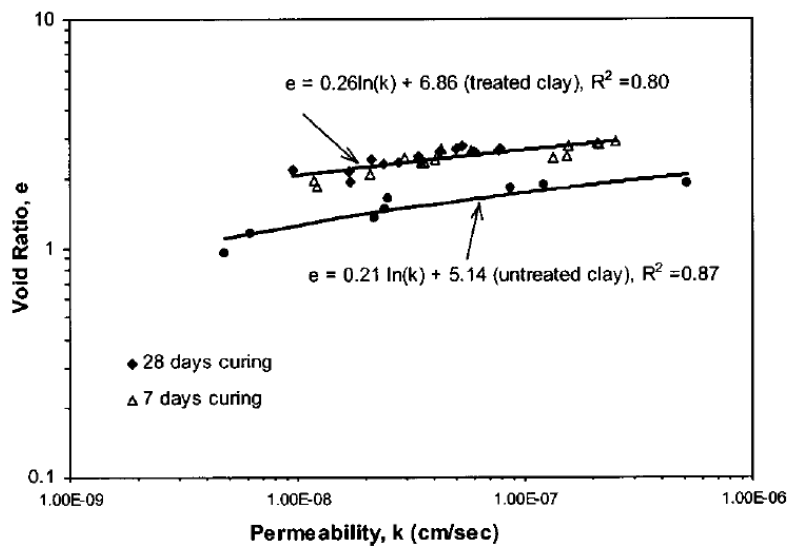


Fig. 2-14 Void ratio and permeability ( $e - \log k$ ) relationship of treated and untreated clay ( $w_i = 120\%$ ) (Chew et al., 2004)

## 2.4 Consolidation induced by geocomposite

Method of embankment construction with saturated or close to saturated clayey soil as backfill and improved by drainage/reinforcement geocomposite was investigated by previous researchers. The combined method of reinforcement using geosynthetics with improvement with addition of cement or lime is called “hybridized reinforcement”. Another way is formed by combining the geosynthetics with sand mat. This way is derived from the idea that was proposed by Yamanouchi and Miura (1967, 1971 and 1982) and has been called “multiple sandwich structure”. The sandwich structure was extended by Yasuhara et al., (2002). The geosynthetics are placed in between sand layers above and beneath, and is combined with the chemical hardening material (Fig. 2-15). A geocomposite in which a woven-geosynthetic sandwiched by a woven-geosynthetic has many advantages for reinforcing soft soils, such as the high tensile strength, high pull-out resistance and high permeability (Yasuhara et al., 2002). Due to the availability of the local fill material, the clayey sand or sandy clay with high water content was used as fill material. To accelerate the self-weight induced consolidation process of the fill material, drainage/reinforcement geocomposite was used. And there are several cases histories in Japan that embankments were successfully constructed using clayey backfill with geosynthetics such as Tatsuoka and Yamaguchi, (1986), Noto Airport (Nagahara et al., 2000; Inagaki et al. 2000), Shizuoka airport (Tatta et al., 2003), Kanto loam embankment (Yasuhara et al., 2003). Recently, Raisinghani et al. (2011) performed centrifuge model study on low permeable slope reinforced by hybrid geosynthetics and Taechakumthorn et al. (2012) also reported performance of a reinforced embankment on a sensitive Champlain clay deposit.

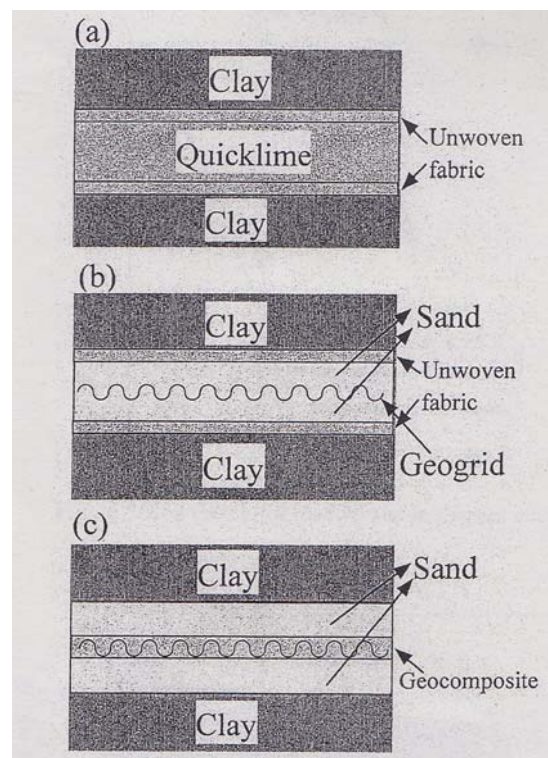


Fig. 2-15 Sandwich reinforcement (Yasuhara et al., 2001)

The new idea is combination of cement/lime lightly treated clayey soils using horizontal geocomposite as a dual function (reinforcement and drainage) was suggested by Chai et al. (2011). The drainage effect can accelerate the self-weight consolidation of the treated soils and the reinforcement effect can improve the stability of the embankment (Fig. 2-16). In this method, the undrained shear strength of the surface of embankment is normally low due to small self-weight loading. Therefore, the top layer (let's say 1.0m thickness) of embankment can be constructed with granular soils.

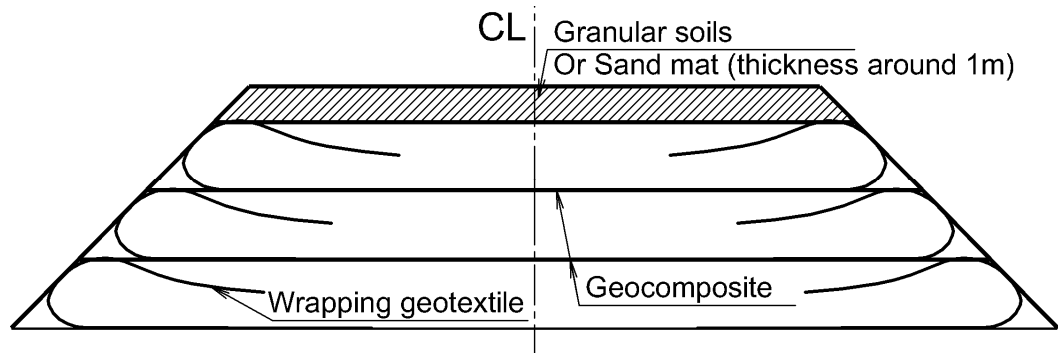


Fig. 2-16 Proposed model of geocomposite induced consolidation of clayey soils under stepwise load (Chai and Quang, 2013)

## 2.5 Predicting method of undrained shear strength

The value of  $S_u$  of a soil is a function of effective stress, stress history and the mechanical properties of the soil. Relationship has been plotted for the field vane test by many authors (Table 2-3), following Skempton (1957) who proposed the empirical expression:

$$S_{u(VST)} / p'_c = 0.11 + 0.0037PI \quad (2-1)$$

for normal consolidated clays. Another relationship is that given by Bjerrum (1973) for “Young” clays; that is, clays with  $OCR \approx 1$ . Jamiolkowski et al. (1985) present the results of the field vane undrained strength plotted as the ratio  $S_u / p'$  against OCR. These can be expressed in the form:

$$S_u / p' = S_1(OCR)^m \quad (2-2)$$

where  $S_1$  is the undrained shear strength ratio for normally consolidated clay (that is,  $OCR \approx 1$ ). Similar relationships have been presented for various laboratory undrained strength tests by Ladd et al. (1974) who concluded that  $m$  is typically 0.8 in simple shear tests. Mesri (1975) additionally multiplied the  $S_u / p'_c$  relation by Bjerrum's factor  $\mu$ , at corresponding values of  $I_p$ . This resulted in the almost constant field strength ratio, independent of plasticity, of  $\mu S_u / p'_c = 0.22(\pm 0.03)$ . Ladd (1991) proposed an empirical equation to calculate  $S_u$  value of clayey soils as follows:

$$S_u / p' = S (OCR)^m \quad (2-3)$$

where  $p'$  is vertical effective stress,  $OCR$  is over-consolidation ratio, and  $S$  and  $m$  are constants. Ladd (1991) proposed that the range for  $S$  is 0.162 to 0.25 and for  $m$  is 0.75 to 1.0.

Table 2-3 Empirical equations related to  $S_u$  and effective stress ( $p'$ ) (data from Das M., Advanced Soil Mechanics, 2008)

Reference	Relation	Remarks
Skempton (1957)	$S_{u(VST)}/p' = 0.11 + 0.0037 PI$	For normally consolidated clay Can be used in overconsolidated soil; accuracy $\pm 25\%$ ; not valid for sensitive and fissured clays.
Chandler (1988)	$S_{u(VST)}/p'_c = 0.11 + 0.0037 PI$	
Jamiolkowski et al. (1985)	$S_u/p'_c = 0.23 \pm 0.04$	For low overconsolidated clays.
Mesri (1989)	$S_u/p' = 0.22$	See Figure 7.70; for normally consolidated clays
Bjerrum and Simons (1960)	$S_u/p' = f(LI)$	
Ladd et al. (1977)	$\frac{(S_u/p')_{\text{overconsolidated}}}{(S_u/p')_{\text{normally consolidated}} (OCR)^{0.8}} =$	

PI, plasticity index (%);  $S_{u(VST)}$ , undrained shear strength from vane shear test;  $p'_c$ , preconsolidation pressure; LI, liquidity index; and OCR, overconsolidation ratio.

## 2.6 Summaries

The aim of this dissertation is to investigate physico-chemical and mechanical behaviour of lime-/cement-treated clayey soils. In the literature, there are some publications on these aspects, but there are still a lot of unclear points, especially on the permeability and undrained shear strength of the treated soils.

### 2.6.1. About permeability

Several researches investigated the influence of lime or cement treatment on the permeability ( $k$ ) of the treated soils. However, most direct measurement for  $k$  used a modified oedometer consolidation cell. This kind of device has a shortcoming that water may leak through the micro gaps between the rigid container wall and the treated soil specimen that form during the curing period. This leakage may be one of the possible reasons underlying the reported variations in the  $k$  values of treated soils.

### 2.6.2. Method for predicting undrained shear strength ( $s_u$ )

Method of embankment construction with saturated or close to saturated clayey backfill is used to dual function (reinforce and drainage) horizontal geocomposites. There are several case histories in Japan that embankments were successfully constructed using clayey backfill with geosynthetics.

Recently, for the design of a dual function geocomposite reinforced embankment with saturated or close to saturated clayey backfill, prediction of  $s_u$  values of the clayey backfill was proposed by Chai et al. (2011). However, for geocomposite induced consolidation of lime/cement lightly treated clayey soils using as embankment backfill, the effect of lime/cement on the prediction of the distribution of  $s_u$  values is still issue to be resolved.

Based on the above, two main objectives have been proposed for this study: (1) Propose flexible-wall permeameter for investigating permeability of lime/cement lightly treated clayey soils (2) Propose method for predicting undrained shear strength ( $s_u$ ) of geocomposite induced consolidation of lime/cement lightly treated clayey soils under stepwise load.

## CHAPTER 3 PHYSICO-CHEMICAL PROPERTIES OF TREATED CLAYEY SOILS

### 3.1 Introduction

Several researchers (Choquette et al., 1987; Locat et al., 1990, 1996; Yamadera 1999; Chew et al., 2004) investigated the influence of lime/cement treatment on the change of microstructure of clayey soils. Choquette et al. (1987) and Locat et al. (1990) reported that if enough lime is mixed with clay soil, the main dominant chemical reactions are (1) flocculation and (2) pozzolanic reactions. The flocculation results from the large increase in the electrolyte concentration ( $\text{Ca}^{2+}$ ). The pozzolanic reactions imply an attack on reactive minerals to form secondary products such as CSH (calcium silicate hydroxides) or CAH (calcium aluminate hydroxides). The MIP and the visible image of SEM test normally used to investigate the changing in microstructure before and after treatment. However, the effect of lime/cement treatment on particle size distribution and the thickness of DDL are still issues to be resolved. Therefore, to fully understand the effect of flocculation and cementation process of lime/cement treatment on the change of micropore network in soil structure, in this Chapter, series of physico-chemical properties tests, e.g. pH measurement, Atterberg limit, particle size distribution, electrical conductivity, ion concentration and microstructure of the soil-cement or soil-lime mixture were investigated.

### 3.2 Test methods

The Atterberg limit, pH measurement, electrical conductivity, ion concentration and particle size distribution tests were conducted according to JIS A 1205-2009, JGS 0211-2009, JGS 0212-2009, JGS 0261-2009 and JIS A1204-2009, respectively.

The basis of the mercury intrusion method conceived originally by Washburn (1921) and suggested later by Diamond (1970). Both MIP and SEM tests were prepared by freezing and vacuum drying method (Diamond, 1970; Delage and Lefebvre, 1984).

### 3.3 Materials used and specimen preparations

#### 3.3.1. Materials used

Two types of clayey soils were used in this study. One was Ariake clay sampled at about 2 m depth from the ground surface at Ashikari, Saga, Japan. Another was river bed deposits sampled at Nishiyoka, Saga, Japan which will be called dredged mud later. Some physical properties of the soils are listed in Table 3-1.

The chemical compositions of the cement and the quicklime used are listed in Table 3-2. Cement used is called US10 which is commonly used cement for soft ground improvement in Japan.



Table 3-1 Soil properties of clayey soils tested

		Ariake clay	Dredged mud
Moisture content, $W_n$	%	157	170
Liquid limit, $W_L$	%	133	147
Plastic limit, $W_P$	%	46.5	48.6
Plasticity index, $I_p$		86.5	98.4
Particle size distribution, %	Sand (2-0.075 mm)	0.2	0.2
	Silt (0.075-0.002 mm)	48.4	48.3
	Clay (<2 $\mu$ m)	51.4	51.5
pH		7.5	8.5
Ignition loss	%	8.5	11.8
Organic content	%	0.9	2.0

Table 3-2 Chemical composition of cement and quicklime used

	CaO %	SiO <sub>2</sub> %	Al <sub>2</sub> O <sub>3</sub> %	Fe <sub>2</sub> O <sub>3</sub> %	MgO %	K <sub>2</sub> O %	Na <sub>2</sub> O %	SO <sub>3</sub> %
Cement (US10)	60.7	19.2	4.8	2.5	1.2	-	-	7.3
Quicklime	92.0	1.4	0.6	0.3	1.0	<0.1	<0.1	<0.1

### 3.3.2. Specimen preparation

The clayey soils were mixed thoroughly by a laboratory mixing machine to obtain clay slurry with water content of about 157 and 170% for remolded Ariake clay and dredged mud, respectively. The pre-determined amount of the lime and the water with the same weight as the lime was directly added into the soil slurry, while in the case of using cement, cement slurry with a water/cement ratio ( $w/c$ ) of 1.0 was added to the clay slurry. After completion of the mixing, pH measurements of soil-lime-water mixture or soil-cement-water mixture were conducted according to the method of JGS 0211-2009.

For preparing the Atterberg limit, ion concentration, electrical conductivity, grain size, MIP and SEM tests samples, soils were put into a polyvinyl chlorite (PVC) cylindrical mold with a diameter of 75 mm and height of 200 mm. Then, the top and bottom of the mold were covered with vinyl plastic sheets to prevent moisture loss. The molds were then submerged in a container of water to cure the soil samples. After 28 days of curing time, samples for Atterberg limit, ion concentration, electrical conductivity, grain size, MIP and SEM tests were cut from the soils in the PVC cylinders.

### 3.4 Cases tested

For lime- and cement-treated samples, all samples were cured for 28 days before the tests. All cases tested are listed in Table 3-3. The results of micro structure tests (SEM and MIP) and chemical properties tests for pore water (EC and IC) are used to investigate the mechanism of the variation of permeability of the cement and the lime treated soils in Chapter 4.

Table 3-3 List of the physico-chemical tests

Tests	% lime or cement					
	0%	2%	4%	6%	8%	16%
Atterberg's limit test	√	√	√	√	√ <sup>b</sup>	
pH measurement	√	√	√	√	√	
Electrical conductivity test	√	√	√	√	√ <sup>b</sup>	
Ion concentration test	√	√	√			
SEM test	√	√			√	
MIP test	√	√	√	√	√	√ <sup>b</sup>

<sup>b</sup>Cement only.

### 3.5 Atterberg limit and pH measurement

The Atterberg limit of treated and untreated clay was conducted according to JIS A 1205-2009. Liquid limit test was determined using Casagrande liquid limit device (Fig. 3-1a). For plastic limit test, a 20-g or more portion of soil from the soil remaining after completion of the liquid limit test is selected. Reducing the water content of the soil to a consistency at which it can be rolled without sticking to the hands by spreading or mixing continuously on the glass plate. For the liquid limit and plastic limit tests, three tests were conducted and the averages of those are plotted in Fig. 3-2 and 3-3. As can be seen, the plastic limit increases with an increase of cement/lime content, and the rate of increase is higher at lower cement/lime content. The exact reason for this phenomenon is not very clear. Locat et al. (1990; 1996) and Chew et al. (2004) reported the similar phenomenon, and Locat et al. (1990, 1996) explained that the possible reason is: due to the effect of small amount of cement or lime, clusters of clay particles are formed with larger inner voids, which can held more water when the soil reaches its liquid limit than that of a soil without treatment.

For pH value measurement, 20 g of dry soil with the various amounts of lime/cement (from 2 - 8%) was put into 100 ml of distill water in a plastic bottle. Then the mixture was mixed by a stirring rod for 30 min. After mixing, the bottle was left on a table to let the sediment of the solid particles. After the solid particles and the liquid separated, the pH value of the liquid was measured following the method of JGS 0211-2009. Fig. 3-4 shows the pH value of the treated soil at various cement/lime contents. As can be seen, the pH values increase rapidly at less than 4% of cement content and 2% of lime content but the rate of increase is insignificant at higher cement/lime content. The increase of pH with an increase of cement/lime content is due to concentration of the Ca<sup>2+</sup> ion on the clay surface from cement hydration or slaking process, leading to form flocculated clay-cement matrix (Chew et al., 2004). Figure 3-4 also indicates the effect of curing time on pH values. For 28 days of curing time, the

pH values of lime/cement treatment decrease significantly due to changing in clay–water–electrolyte system.



a. Casagrande liquid limit device



b. pH measurement device

Fig. 3-1 Casagrande liquid limit device and pH measurement device

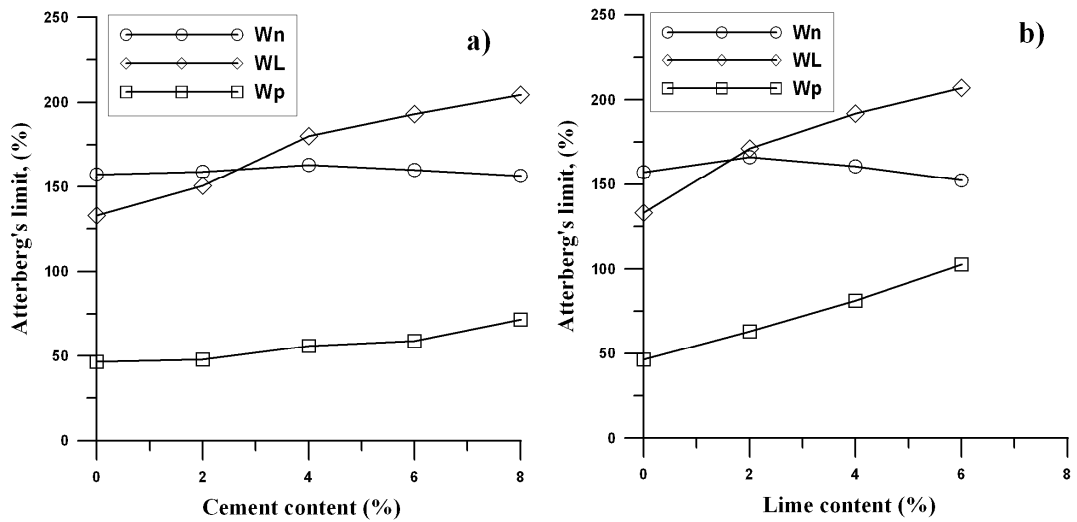


Fig. 3-2 Atterberg's limit of cement/lime treated Ariake clay

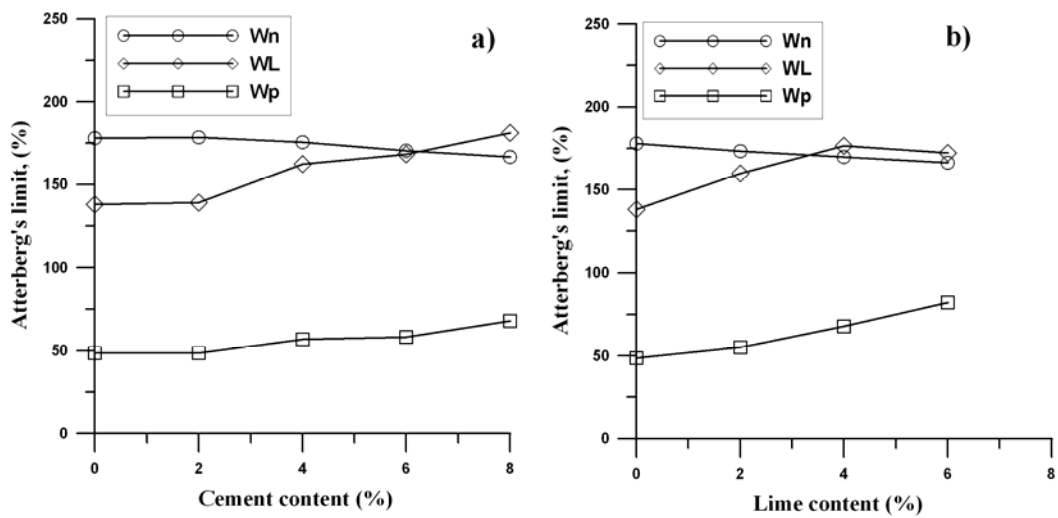


Fig. 3-3 Atterberg's limit of cement/lime treated dredged mud

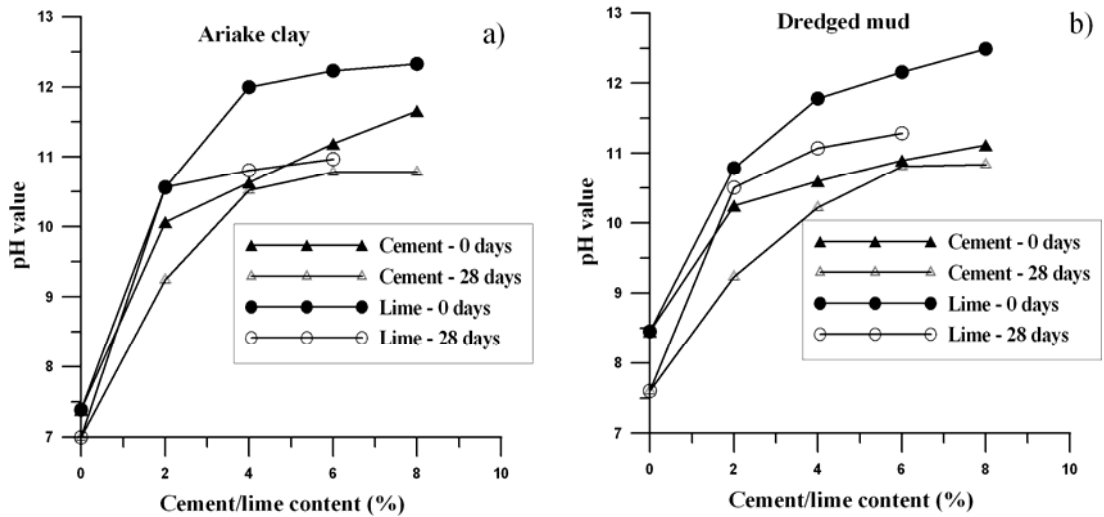


Fig. 3-4 pH measurement of cement/lime treatment

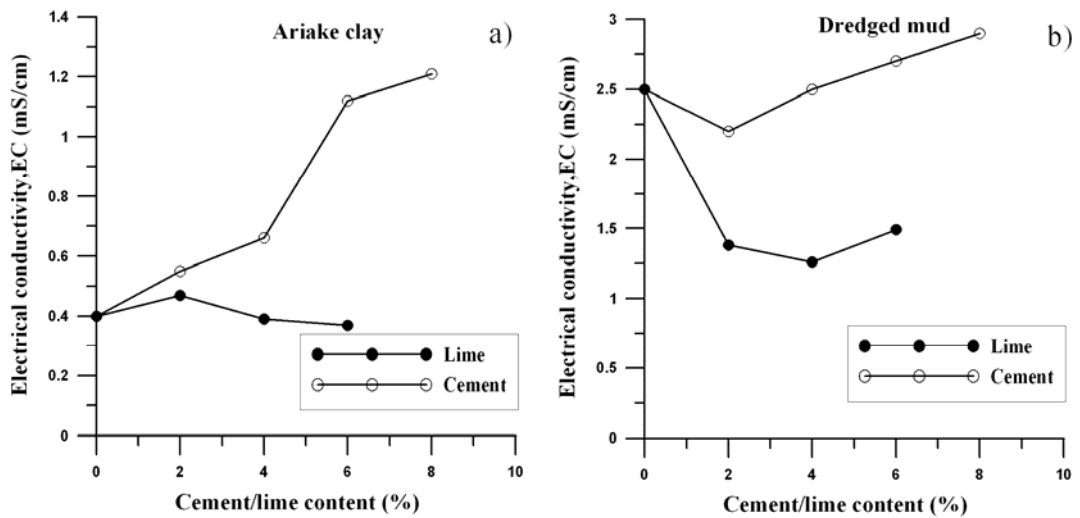


Fig. 3-5 Electrical conductivity of cement/lime treatment

### 3.6 Ion concentration and electrical conductivity

As seen in Fig. 3-5, for cement treatment, the electrical conductivity increased with the increase of cement content. On the contrary, for lime treatment, the electrical conductivity reduced substantially (dredged mud) or moderately (Ariake clay) with the increase of lime content. In addition, as shown in Table 3-4, for 2% and 4% of cement/lime treatment, ion concentration of  $\text{Ca}^{2+}$  cation increases 1.4 – 2.2 times comparing to untreated soil. However, it is important to note that for the lime treatment, the increase of ion concentration of  $\text{Ca}^{2+}$  cation is clearly lower than that of the cement treatment. Increasing in valence ( $\text{Na}^+ < \text{Ca}^{2+}$ ) and the ion concentration will suppress the midplane concentrations and potential between interacting plates, thus leading to a decrease in interplate repulsion and hence reducing the thickness of diffuse double layer (DDL). Even relatively small amounts of divalent or trivalent cations added to clay-water-monovalent electrolyte systems can have a significant influence on DDL interaction and physical properties (Mitchell, 1993). These values used for calculating thickness of DDL and were discussed later in Chapter 4.

Table 3-4 Effect of lime/cement on ion concentration in pore water

Ion concentration, mg/l	Ariake clay	2% cement	4% cement	2% lime	4% lime
Ca <sup>2+</sup>	170	294	366	230	301
Na <sup>+</sup>	381	229	206	187	206
Mg <sup>2+</sup>	485	14	7	11	4

### 3.7 Particle size distribution

This test method covers the quantitative determination of the distribution of particle sizes in soils following JIS A1204-2009. The distribution of particle sizes larger than 75 µm (retained on the No. 200 sieve) is determined by sieving analysis (Fig. 3-6a), while the distribution of particle sizes smaller than 75 µm is determined by a sedimentation process, using a hydrometer (Fig. 3-6b).



a. Sieves analysis

b. Hydrometer

Fig. 3-6 Particle size test using sieves analysis and hydrometer

As seen in Fig. 3-7 and Table 3-6, with a limited lime/cement content (less than 4%), there is a shift of predominant particles size from clay to silt and fine sand resulting from cementing the finer particles into bigger ones. For cases with lime content 4% or more and cement content 6% or more, the soil became hard and the grain size distribution test could not be conducted effectively.

Table 3-6 Effect of lime/cement on particle size distribution

Particle size distribution (%)	Ariake clay				Dredged mud			
	0%	2%-Cement	2%-Lime	4%-Cement	0%	2%-Cement	2%-Lime	4%-Cement
Sand (2-0.075mm)	0.2	2.3	9.1	2.3	0.2	0.8	1.5	2.3
Silt (0.075-0.002mm)	48.4	60.6	71.7	77.1	48.3	56.8	69.6	70.0
Clay (<0.002mm)	51.4	37.1	19.2	20.5	51.5	42.4	28.9	27.7

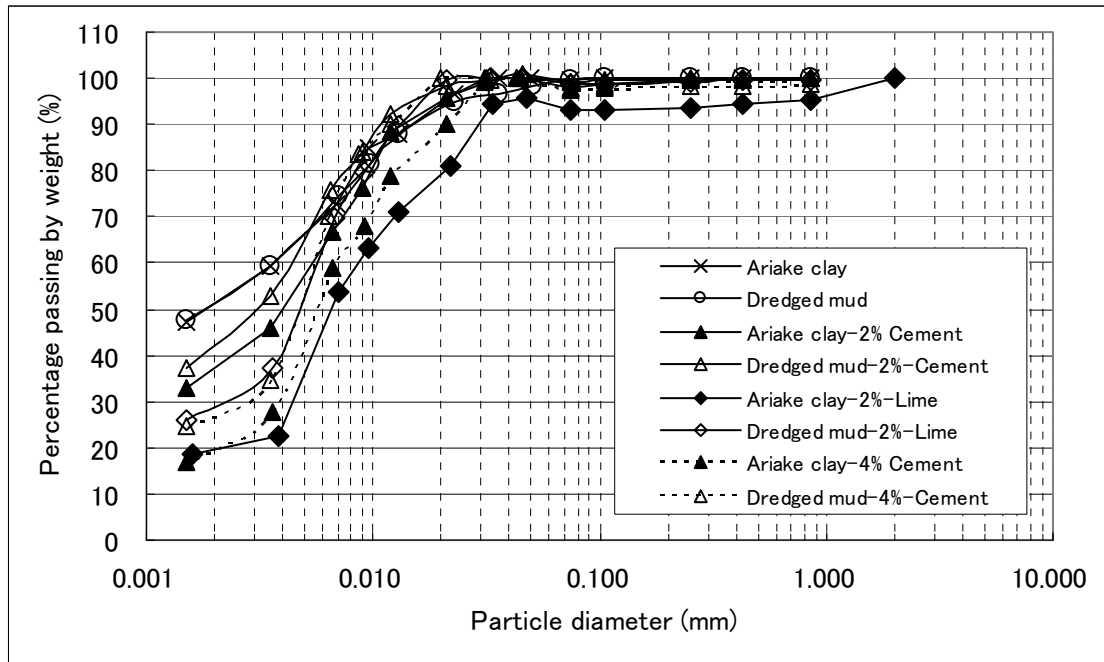


Fig. 3-7 Particle size distribution curves

### 3.8 Pore size distribution from mercury intrusion porosimetry (MIP) tests

#### 3.8.1. Testing method and procedure

The soil samples for MIP test were prepared by freezing and vacuum drying method (Delage et al., 1984; Kang et al., 2003; Tanaka et al., 2003). In freeze drying, a soil specimen was trimmed in 3 mm thick and 3-4 cm long of stick shape with iron wire. Then, immersed into liquid nitrogen ( $-210^{\circ}\text{C}$ ) for instant freezing to avoid formation of crystallized ice in pores which leads to volumetric increase. After that, the frozen specimens were transferred to the vacuumed chamber of freeze dryer and sustained for about 48 hours. MIP analyses of untreated and treated soils were conducted using mercury intrusion porosimeter (Micromeritic instrument) (Fig. 3-8). Mercury was intruded into the voids by applying pressure. By assuming pores are cylindrical shape, the pore diameter is calculated with capillary theory proposed by Washburn (1921).

$$d_p = -4\sigma \cos \theta / p \quad (3-1)$$

Where,  $\sigma$  is surface tension of mercury (N/m)

$d_p$  is diameter of pore intruded (m)

$p$  is applied external pressure (Pa)

$\theta$  is contact angle of mercury with solid ( $^{\circ}$ )



Fig. 3-8 MIP apparatus (Micromeritics instrument)

### 3.8.2. Results

As seen in Fig 3-9 and 3-10, the pore size range of remolded Ariake clay is about 2 - 10  $\mu\text{m}$ . When treated by the cement or the lime, the most pore sizes are in the range of 0.1 - 10  $\mu\text{m}$ . For remolded dredged mud, the pore size range is about 1 - 5  $\mu\text{m}$  (Fig. 3-11). When treated by cement, the dominant pore size reduced in the range of 0.5 - 5  $\mu\text{m}$  (Fig. 3-11) and for lime treated ones, the dominant pore size is in range of 0.05 - 5  $\mu\text{m}$  (Fig. 3-12). However, the dominant pore size reduced significantly with the increase of the cement or the lime content. The lime-treated samples have a faster reduction rate, and the pore sizes are distributed in a wider range. For example, for the untreated Ariake clay's sample, the dominant pore size is about 4  $\mu\text{m}$ , while for 8% the cement-treated case, it is about 0.5  $\mu\text{m}$ . It is worth to mention that the void ratios of the samples used for MIP tests are not exactly the same. Generally, the cement- and lime-treated samples have a smaller initial  $e$  value. This partially explains the fact that the pore size distributions as shown in Fig. 3-9 to 3-12, for the cement- and lime-treated samples are different from those for the untreated samples.

Assuming the sample has been completely saturated and the density of the pore water is approximately  $1\text{g/cm}^3$ , the total measured pore volume will be equal to the water content in the soil. Delage and Lefebvre (1984) used this same method to check the link between the natural water content of soft clay and the total intruded pore volume measured by MIP analysis. However, since the limitation of the maximum practical pressure of the apparatus, possibly leaving some miniature pores and isolated pores surrounded by solids unintruded, the water content and therefore, void ratio using MIP method underestimates about 18% comparing with the measured values (Fig. 3-13).

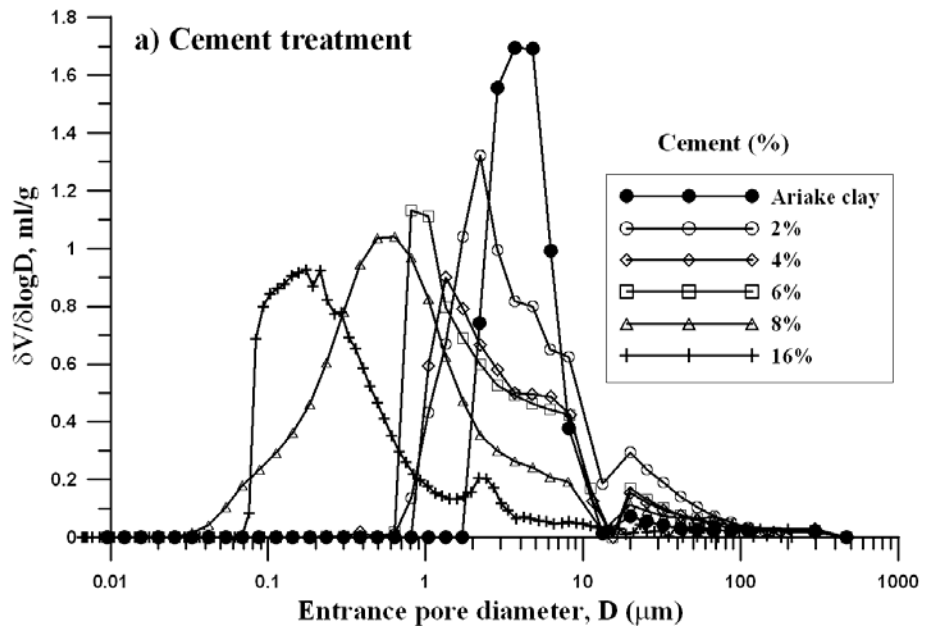


Fig. 3-9 Effect of cement treatment on pore size distribution curves of treated Ariake clay

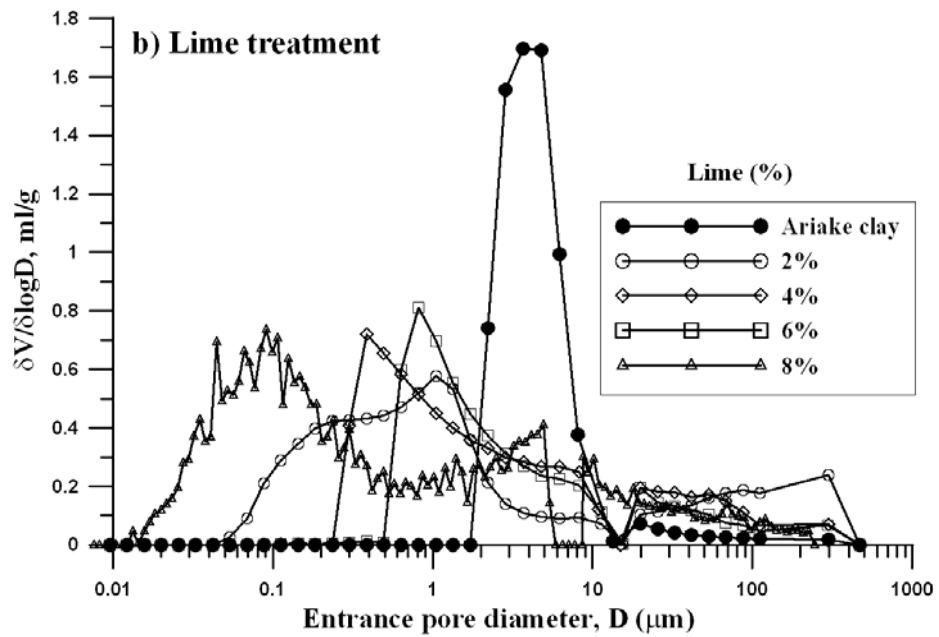


Fig. 3-10 Effect of lime treatment on pore size distribution curves of treated Ariake clay



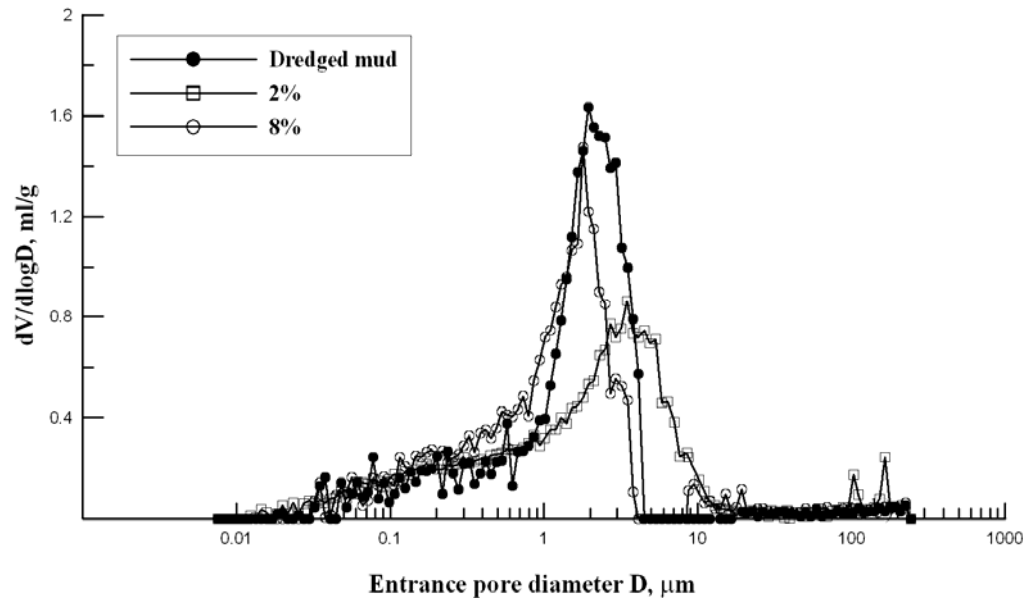


Fig. 3-11 Effect of cement treatment on pore size distribution curves of treated dredged mud

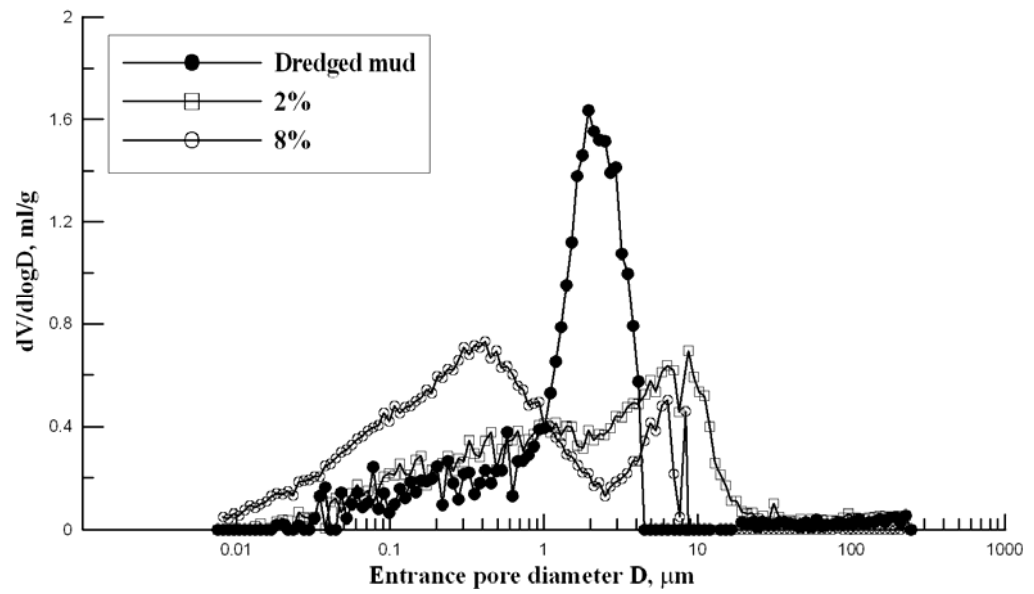


Fig. 3-12 Effect of lime treatment on pore size distribution curves of treated dredged mud

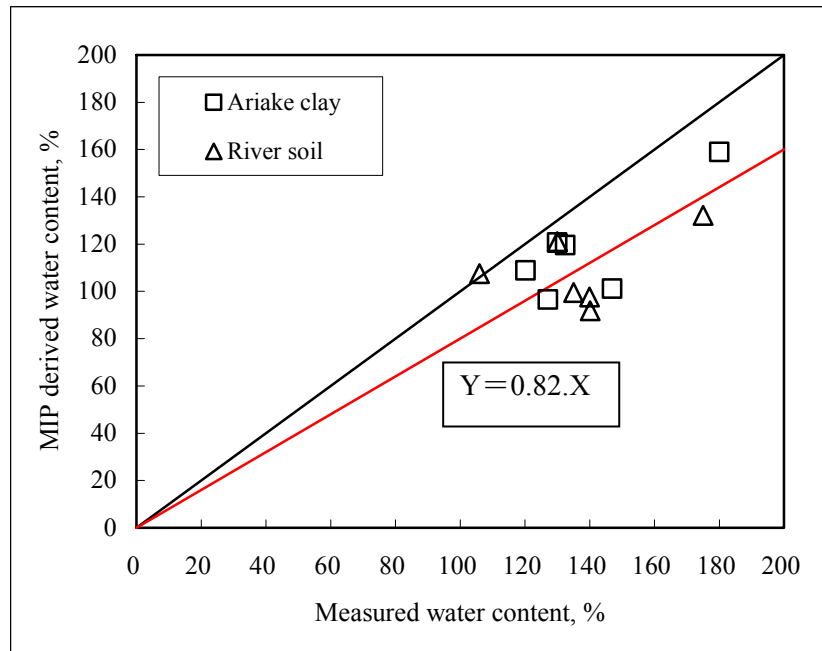


Fig. 3-13 Comparison between measured and MIP derived water content

### 3.9 Scanning electron microscope (SEM)

#### 3.9.1. Testing method and procedure

The soil samples for SEM test were prepared by freezing and vacuum drying method (Delage et al., 1984; Locat et al., 1996; Kang et al., 2003; Tanaka et al., 2003; Chew et al., 2004). SEM analysis of untreated and treated soil samples was conducted using JEOL-5800 machine (Fig. 3-14). Soil samples used for microanalyses were carefully cut in 3-5 mm wide sticks with an iron wire and rapidly put into liquid nitrogen slush at  $-210^{\circ}\text{C}$ . While frozen, the samples were broken to expose a fresh surface and put into a vacuum desiccator. For SEM testing, samples were coated with a gold-platinum layer.



a. SEM apparatus



b. Freezing drying equipment

Fig. 3-14 SEM apparatus (JEOL-5800 machine) and freezing drying equipment

### 3.9.2. Results

SEM images for the untreated and treated Ariake clay samples are shown in Fig. 3-15 and 3-16. Comparing with the case of without additives (Fig. 3-15a and 3-16a), for the cases of adding 2% additives, the inter-aggregate pores volumes were still remained (Figs. 3-15b, 3-15c and 3-16b, 3-16c). For the cases of 8% of the lime content, it was believed that the inter-aggregate pores were filled by the products of the additives (Figs. 3-15d, 3-15e and 3-16d, 3-16e) such as CSH (calcium silicate hydrate), CAH (calcium aluminate hydrate) and CASH (calcium aluminat silicate hydrate). However, the adequate technique to determine the types of secondary minerals is still not clear. So, in this study, the secondary minerals were only guessed visually from “cloud bonds” by scanning electron microscope (SEM) images.

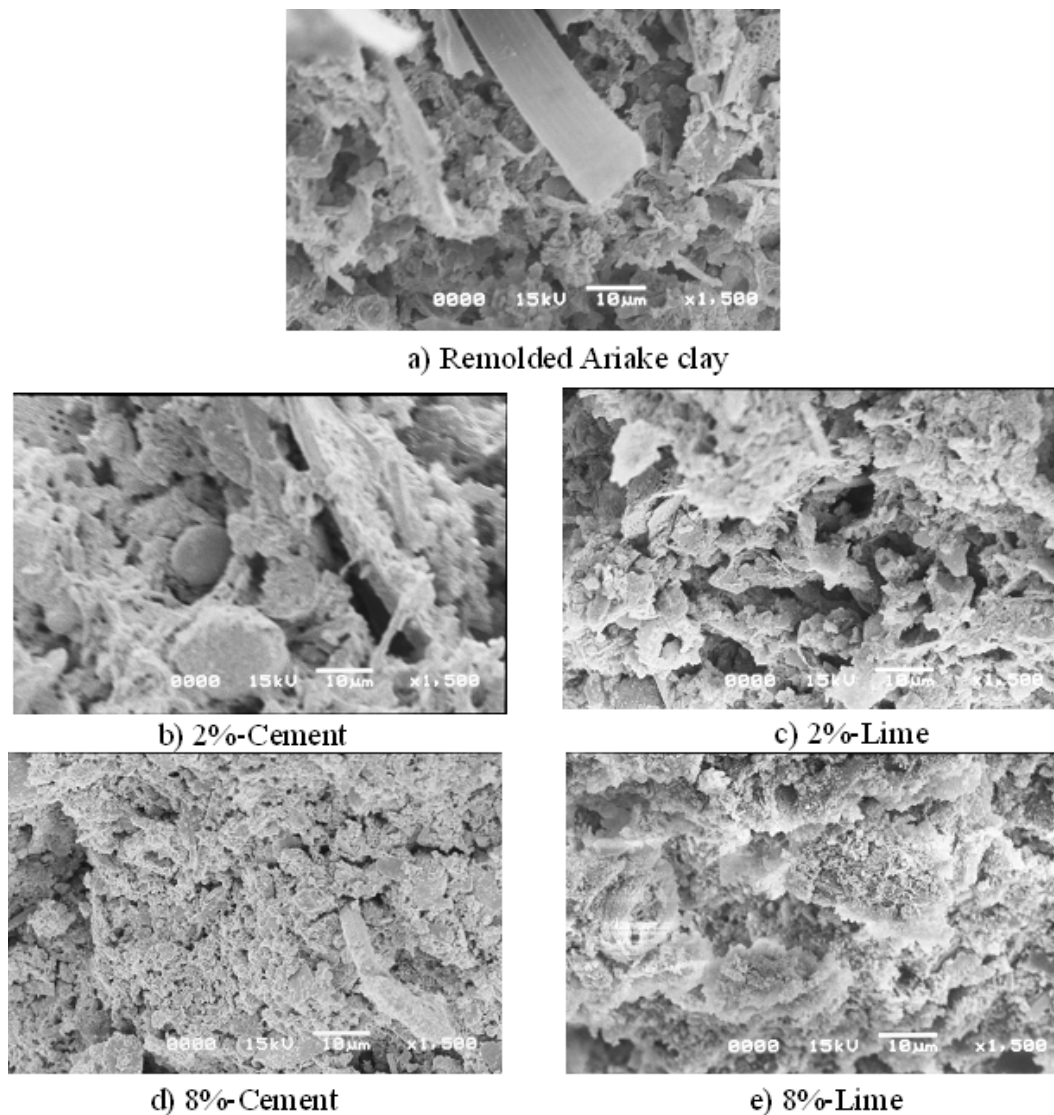
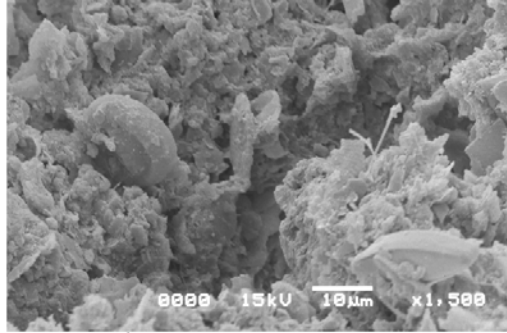
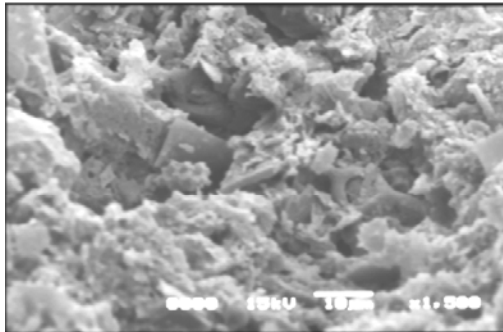


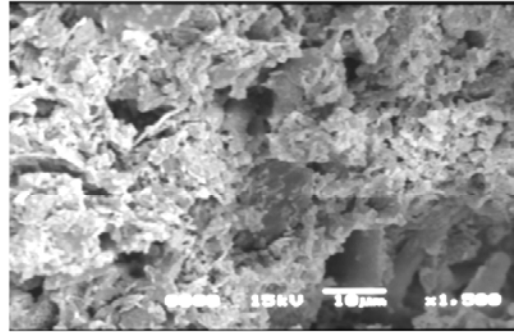
Fig. 3-15 SEM images of treated and untreated Ariake clay



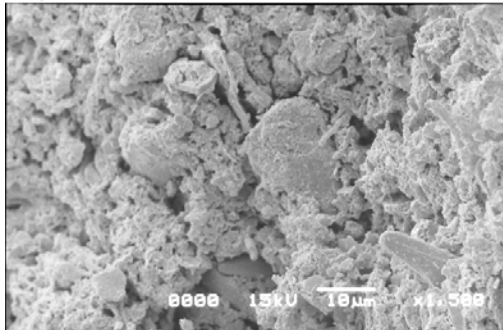
a) Remolded dredged mud



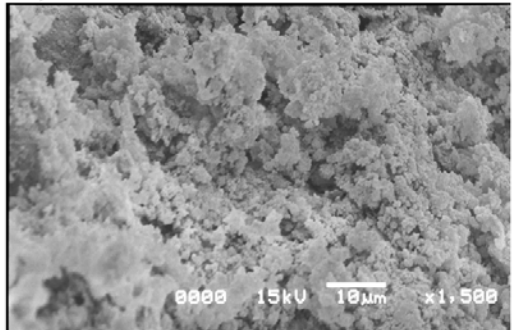
b) 2%-Cement



c) 2%-Lime



d) 8%-Cement



e) 8%-Lime

Fig. 3-16 SEM images of treated and untreated dredged mud

### 3.10 Mechanism of the effect of cement and lime additive on particle size distribution

From the particle size distribution test results and SEM images, it is proposed/speculated that with the amount of cement less than 4% or 2% for lime, lots of clay particles were cemented together and formed aggregates/clusters but there are no or very less inter-aggregate/clusters bonds (Fig. 3-17a). With the increase of the amount of the additives, the cementation products will bind the aggregates together and fill the inter-aggregate pores (Fig. 3-17b) and the soil will become stronger with obvious increase on shear strength (it will be investigated in detail in next Chapter)

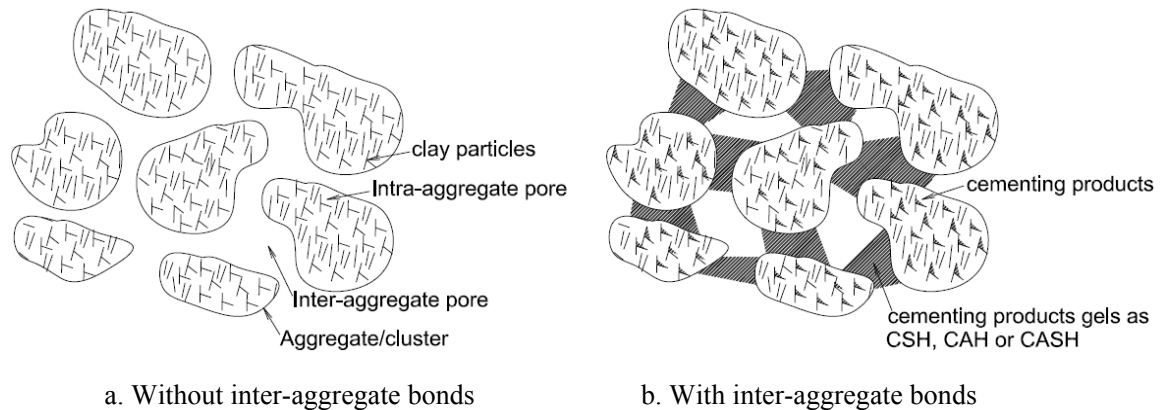


Fig. 3-17 Cementing process

### 3.11 Summaries

The physico-chemical properties of lime and cement lightly treated clayey soils were investigated by particle size distribution, pH measurements, Atterberg limit, electrical conductivity, ion concentration, mercury intrusion porosimetry (MIP) and using the images of scanning electron microscope (SEM) tests. Two clayey soils, remolded Ariake clay and dredged mud from an estuary were tested. Based on the test results, the following conclusions can be drawn.

(1) When the cement additive is less than 4% or 2% for lime, there were obvious changes in particle size distribution from clay to silt and fine sand resulting from cementing the finer particles into bigger aggregates/clusters.

(2) The dominant pore size reduced significantly with the increase of the cement or the lime content. The lime treated samples have a faster reduction rate, and the pore sizes are distributed in a wider range.

(3) The further SEM image analysis indicates that the change of the mechanical properties is related to the change of microstructure of the soils.

(4) Due to the effect of cementation of lime/cement treatment, the changing of pore size distribution and thickness of diffuse double layer (DDL) are clear.

(5) The lime treatment was much more effective than that the cement. The pH values of the soil-lime-water mixture was higher than that of the soil-cement-water mixture indicating more pozzolanic reaction occurred in lime treatment.

## CHAPTER 4 LABORATORY CONSOLIDATION AND PERMEABILITY TESTS

### 4.1 Introduction

As discussed in Chapter 2, several researches have investigated the influence of lime or cement treatment on the permeability ( $k$ ) of the treated soils. However, there are still no unified understanding. Some researchers reported that the treated soil has a higher  $k$  value than the untreated soil. In comparisons under the same void ratio ( $e$ ) condition, McCallister and Petry (1992) showed that the  $k$  values increase with the lime content up to 3%, and then decrease with the lime content. Al-Mukhtar et al. (2012) reported that the permeability increased substantially with the increase of lime content up to 4% and then decreases with 10% of lime. Meanwhile, some results indicated that the treated soil has a lower  $k$  value than the untreated soil. For Louiseville clay, Locat et al. (1990, 1996) reported that lime treatment reduced  $k$  value of soil. Chew et al. (2004) reported that for the same  $e$  value, the cement treated soft Singapore marine clay had lower permeability than the untreated soft clay. However, Yamadera (1999) conducted permeability test on 5% of cement-treated Ariake clay and indicated that the untreated and treated Ariake clay were almost identical to those of untreated soils. Further, most direct measurement for  $k$  value used a modified oedometer consolidation cell. This kind of device has a shortcoming that water may leak through the micro gaps formed during curing period between the rigid wall of the container and a treated soil specimen. So, the flexible-wall permeability cell was proposed to investigate permeability of lime and cement lightly treated clayey soils. The test results are compared with the values deduced from the oedometer consolidation test results. The discussions are made on the effect of cement or lime additives on  $k$  value as well as coefficient of consolidation ( $c_v$ ) and consolidation yield stress ( $p_y$ ). And the possible mechanisms are investigated.

### 4.2 Permeability and oedometer tests

#### 4.2.1. Flexible-wall permeameter and consolidometer

Schematic illustrations of flexible-wall permeameter are shown in Fig. 4-1 and 4-2. The system consists of three main parts: permeameter cell, consolidation pressure applying system, hydraulic gradient application and flow system. The cell was made of acrylic plastic with 150 mm in diameter and 170 mm in height. The cell pressure was applied by air pressure. The soil sample is 60 mm in diameter and 20 mm in height. The sample was set in a rubber sleeve which is fixed on the top and the bottom pedestals. The vertical pressure to soil sample was applied through Bellofram cylinder system using air pressure. During the test, the vertical displacement of the soil sample was measured by a LVDT and pore water pressure was monitored by a pore water pressure transducer. Head difference on the soil sample was applied using air pressure through a burette (100ml), which was connected to the bottom of the sample. During permeability test, water flow from the bottom to

the top of the sample, and flow rate was measured from the water level in the burette (amount of inflow).

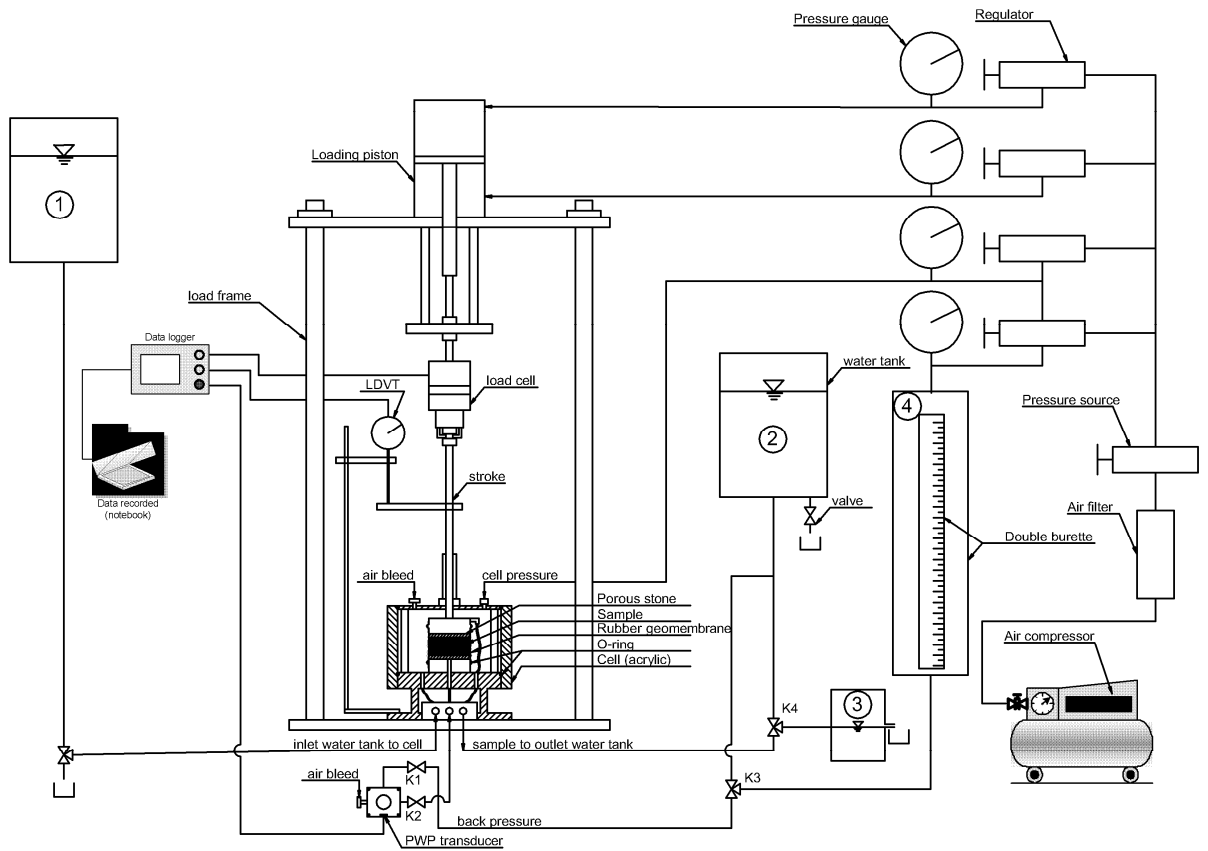


Fig. 4-1 Schematic illustration of flexible-wall permeameter



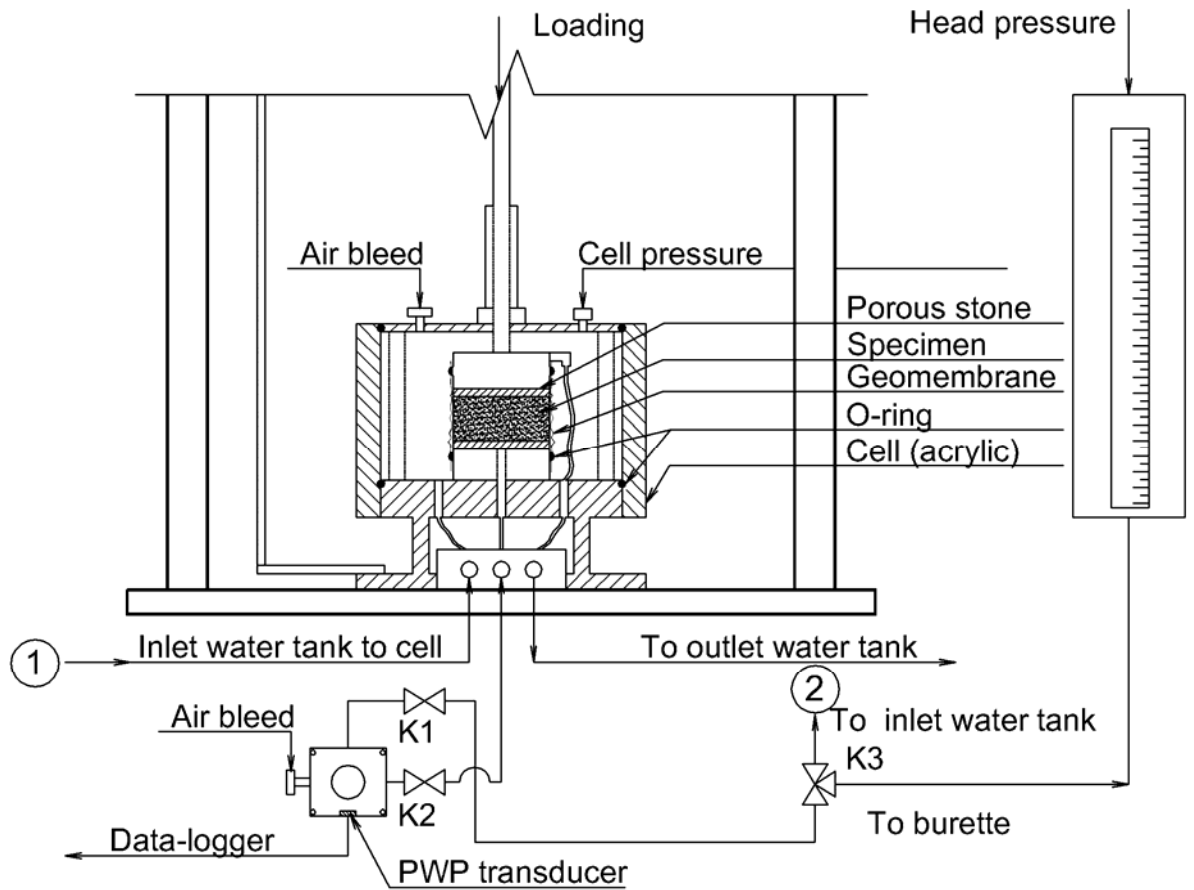


Fig. 4-2 Detail of flexible-wall permeameter

The load frame and consolidometer used were shown in Fig. 4-3. The vertical displacement was measured by LVDT transducer. The incremental load consolidation test was carried out according to Japanese Industrial Standard (JIS A1217-2009) with increment loading ratio (LIR) = 1, two-way drainage and loading intervals of 24h.



Fig. 4-3 Load frame and consolidometer

#### 4.2.2. Procedure for flexible-wall permeability test

##### (1) *Sample preparation:*

The clayey soils were mixed thoroughly by a laboratory mixing machine to obtain clay slurry with water content of about 157 and 170% for remolded Ariake clay and dredged mud, respectively. In case of using the cement, cement slurry with a water/cement ratio ( $w/c$ ) of 1.0 was added to the clay slurry. While in case of using the lime, the pre-determined amount of the lime together with water of the same weight as the lime was directly added into the soil slurry (lime/water ratio of 1.0 also). After thoroughly mixing again, soil was put into a PVC cylindrical mold with a diameter of 75 mm and height of 200 mm. The top and the bottom of the mold were sealed with vinyl plastic sheet to prevent moisture loss. The molds were then submerged in a water container to cure the soil samples. All samples were cured for 28 days prior to consolidation and permeability testing. In case of untreated soil samples, the samples were first consolidated under a pressure of 10 kPa to prepare them for further tests.

##### (2) *Test set-up:*

- a) Cut soil specimen from the pre-cured or pre-consolidated soil sample using a cutter 60 mm in diameter and 20 mm in height.
- b) Saturate the specimen under 30 kPa vacuum pressure using a container to which a vacuum pressure can be applied. The magnitude of vacuum pressure required to achieve a high degree of saturation and to prevent considerable specimen deformation was determined through several trials.
- c) Fix a rubber membrane to the bottom pedestal using an O-ring and a filter paper, and place the specimen on the filter paper.
- d) Install the filter paper, porous stone and top pedestal on top of the specimen, stretch the rubber membrane over the top pedestal, and fasten it with an O-ring.
- e) Install the acrylic cylinder (permeability cell) and fill it with distill water from the inlet water tank as shown Fig. 4-2.
- f) Connect load application and measurement systems.

##### (3) *Pre-consolidation:*

Pre-consolidate the specimen under approximately no lateral deformation ( $K_0$ ) condition by following procedure.

- a) Apply pre-determined vertical consolidation pressure ( $P_L$ ) to the specimen and the same magnitude cell pressure ( $P_{cell}$ ) (confined pressure).
- b) Open drainage valves to consolidate the specimen under two-way drainage condition.
- c) Gradually reduce cell pressure from  $P_L$  to  $P_L/2$  using following equation

$$P_{\text{cell}} = P_v/2 + u_a/2 \quad (4-1)$$

where  $u_a$  is estimated average pore water pressure in the specimen by Terzaghi's one-dimensional consolidation theory. Equation (1) is derived assuming at-rest earth pressure coefficient ( $K_0$ ) of 0.5. The pre-consolidation test is lasted for 24 hours.

**(4) Permeability test:**

a) Lock the upper pedestal to prevent any vertical movement and maintain the confining cell pressure.

b) Connect the water flow system.

c) Apply 50 kPa pressure to the water in the burette, which is connected to the inlet valve. Simultaneously, increase the cell pressure by 50 kPa to prevent specimen bulging. The 50 kPa pressure difference generates a hydraulic gradient ( $i$ ) of approximately 250 over approximately 20 mm of specimen thickness.

d) Open the outlet valve and record the water level in the burette periodically until the measured flow rate becomes steady (duration of 10 - 24 hrs).

After the permeability test, the current specimen is consolidated under a higher pressure, and a new permeability test is conducted; i.e., the pre-consolidation and permeability test procedures are repeated. In this way, the relationship between the void ratio ( $e$ ) and permeability ( $k$ ) can be determined in a single specimen.

**4.2.3. Procedure for oedometer consolidation test**

**(1) Sample preparation:**

For oedometer test, the sample preparation is the same with permeability test. After desired curing time, the samples were cut from the soil in PVC cylindrical molds by the stainless steel consolidation ring with 60 mm in diameter and 20 mm in height.

**(2) Test procedure:**

a) Install the filter paper on the bottom pedestal, and put the specimen on the filter paper.

b) Install filter paper, porous stone and top pedestrian.

c) Place the consolidometer in the loading device and apply a seating pressure of 5 kPa.

d) Place LVDT transducer to measure the vertical displacement of specimen.

b) Apply an increment loading ratio LIR=1 by doubling the pressure on the soil to obtain values of approximately 9.8, 19.6, 39.2, 78.5, 157, 314, 628 etc. kPa.

c) At given load increment, record the change in height at time intervals of approximately 6, 9, 15, 30 s; 1, 1.5, 2, 3, 5, 7, 10, 15, 20, 30 and 40 min; 1, 1.5, 2, 3, 6 and 24 h.

#### 4.2.4. Cases tested

All the tests conducted are summarized in Table 4-1. Permeability discussed here are calculated from the oedometer consolidation results and they are compared with the directly measured values. The results of microstructure tests (SEM and MIP) using specimens after permeability test were further investigated, and chemical properties tests for pore water (EC and IC) in Chapter 3 are also used to study the mechanism of the variation of permeability of the cement and the lime treated soils.

Table 4-1 Summary of the tests conducted

Tests	% lime or cement					
	0%	2%	4%	6%	8%	16%
Permeability test	√	√	√	√	√	√ <sup>c</sup>
Oedometer test	√	√	√	√	√	
MIP test	√	√	√	√	√	√ <sup>b</sup>
SEM test		√ <sup>a</sup>		√ <sup>a</sup>	√ <sup>b</sup>	√ <sup>b</sup>

<sup>a</sup>Lime only, <sup>b</sup>Cement only, <sup>c</sup>Exclude lime treated dredged mud.

### 4.3 Oedometer consolidation test results

#### 4.3.1. Apparent consolidation yield stress ( $p_y$ )

Figure 4-4 shows the typical one-dimensional compression curves for dredged mud and Ariake clay treated with 2 – 8% cement or lime and cured for 28 days, respectively. It can be seen that in term of  $p_y$ , the lime treatment had much more effect than that of the cement for both the soils. For example, for 6% cement treated dredged mud, the  $p_y$  value was about 30 kPa, while for 6% of the lime, the  $p_y$  value was more than 300 kPa. Moreover, the  $p_y$  values of the Ariake clay were much higher than that of the dredged mud, which is considered primarily due to the different initial water content as well as organic content and pH value of the soils (Table 3-1). The relationships of  $p_y$  versus lime/cement content are given in Fig. 4-5. It is clearly shown that the increase of  $p_y$  with the increase of the amount of the admixture is non-linear. Finally, the results of oedometer tests demonstrate that the small amount (< 4%) of cement had not much effect on  $p_y$  values for both the dredged mud and the Ariake clay.

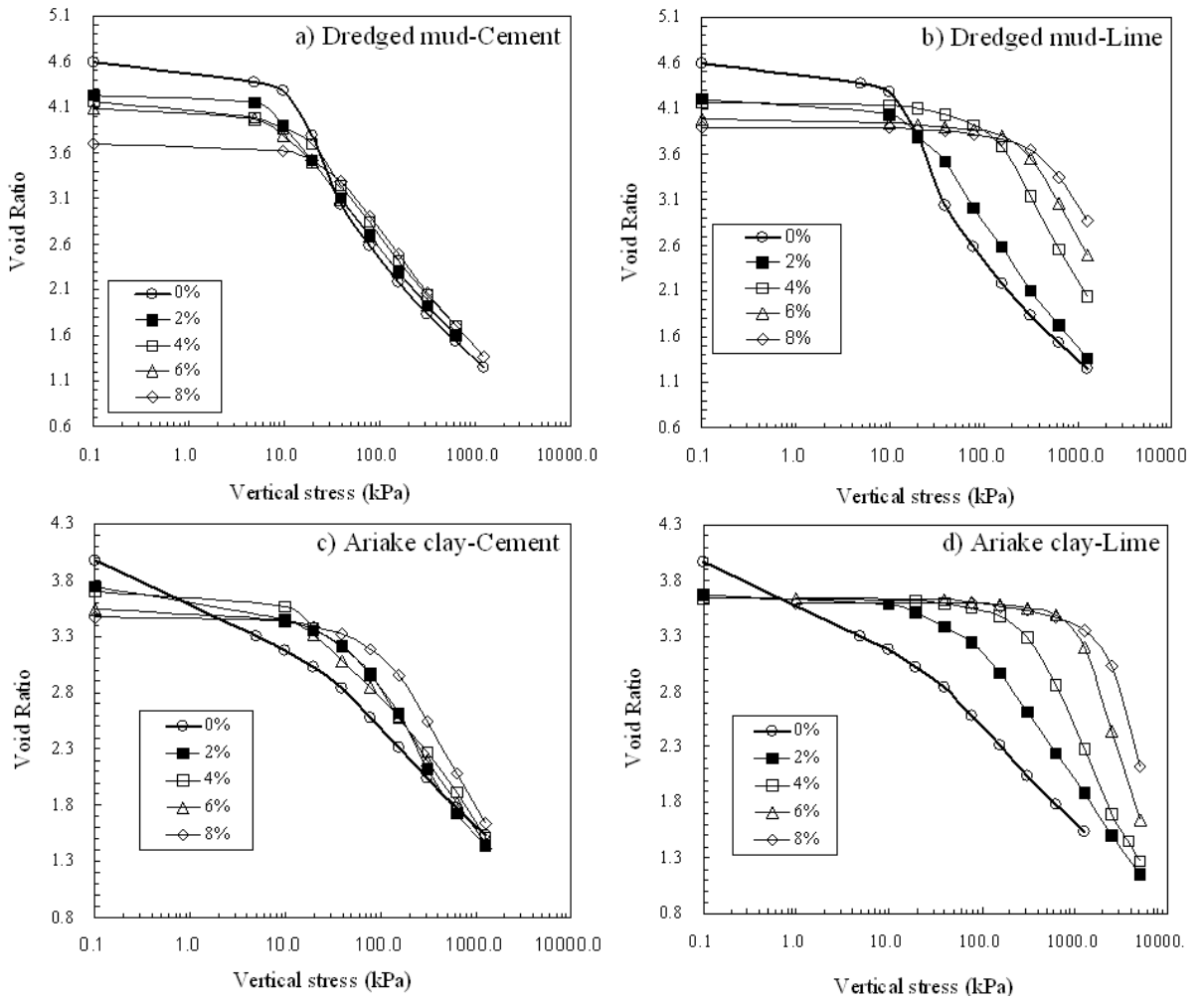


Fig. 4-4 Oedometer compression curves of untreated and treated soils with curing time of 28 days

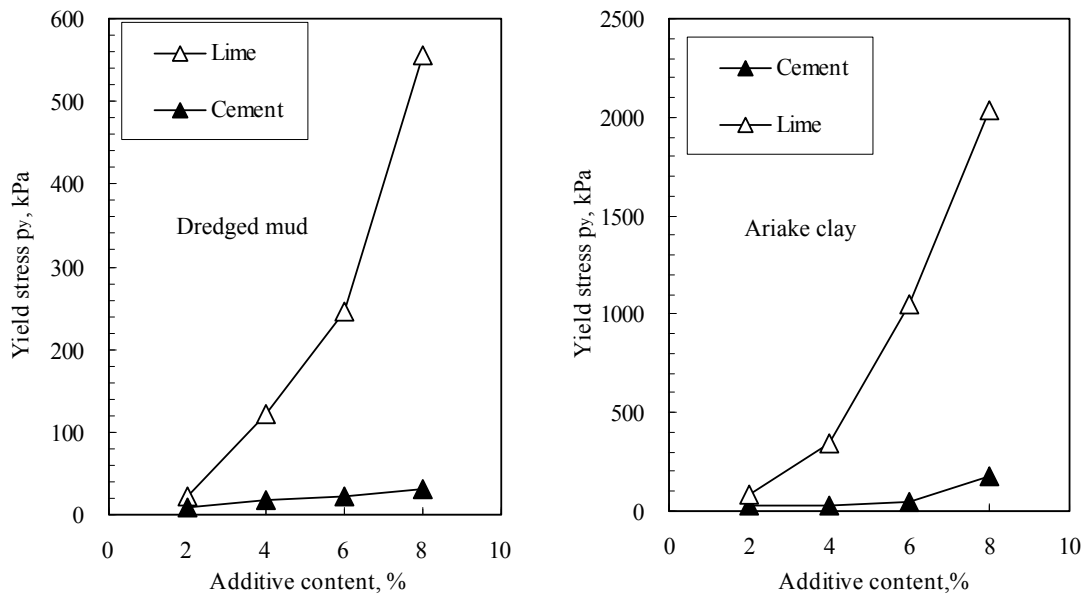


Fig. 4-5 Yield stress and water content vs. cement or lime content with curing time of 28 days

### 4.3.2. Compression and secondary compression indexes ( $C_c$ and $C_{\alpha}$ )

As shown in Fig. 4-6 that with the increase of the admixture, the compression index ( $C_c$ ) is also increased. For the same range of the admixture,  $C_c$  increases faster for the lime treatment than that of the cement treatment. It indicates that the increase of  $C_c$  values is consistent with the increase of yielding stress ( $p_y$ ). The behaviour of treated soils changes from ductile to brittle when increasing the amount of lime/cement content. In contrast, secondary compression index ( $C_{\alpha}$ ) decreases significantly with the increasing of the amount of the cement or lime as shown in Fig. 4-7. So, it is worth to mention that lime/cement treated soft clayey soils can reduce the secondary consolidation settlement significantly.

### 4.3.3. Coefficient of vertical consolidation ( $c_v$ )

Figure 4-8 and 4-9 show the variation of  $c_v$  with average effective vertical stress  $\sigma'_v$  under different lime/cement content for dredged mud and Ariake clay, respectively. The values of  $c_v$  from the oedometer consolidation test are determined by the Taylor method ( $\sqrt{t}$  method) (where  $t$  is time). From the results, in the overconsolidated range, the data are scattered, but in the virgin consolidation range there is a clear trend for  $c_v$  to increase with the increase of lime/cement content for both treated soils. Further, the tendency of increase in  $c_v$  value for lime treated soils is more higher than that of cement treated soils. So, it implies that when clayey soils treated by lime/cement, the  $c_v$  value increases with the increase of the amount of additive content, and therefore increases the degree of consolidation of treated soils.

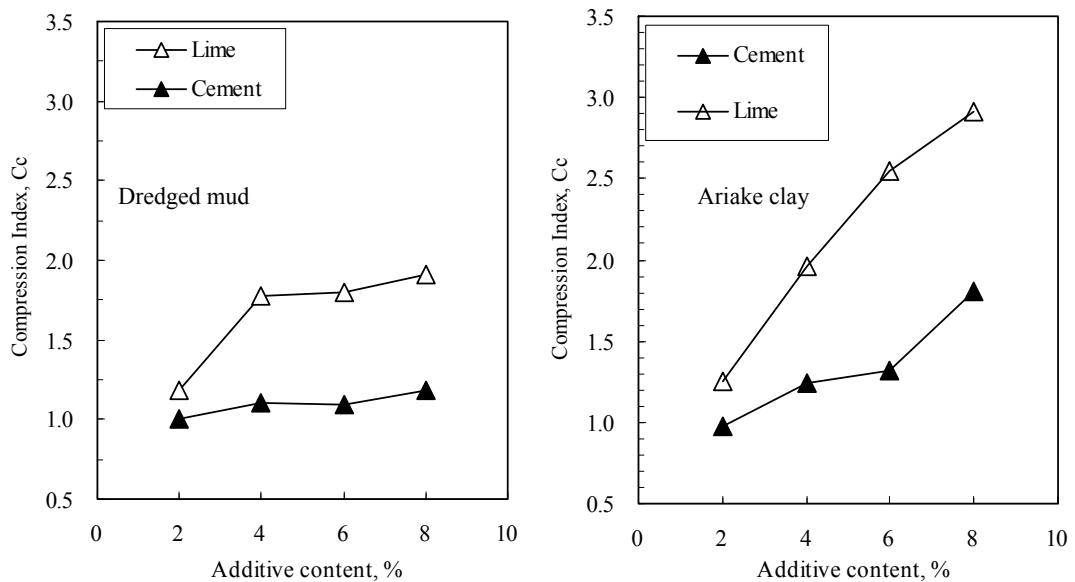


Fig. 4-6 Compression index vs. cement and lime content with curing time of 28 days

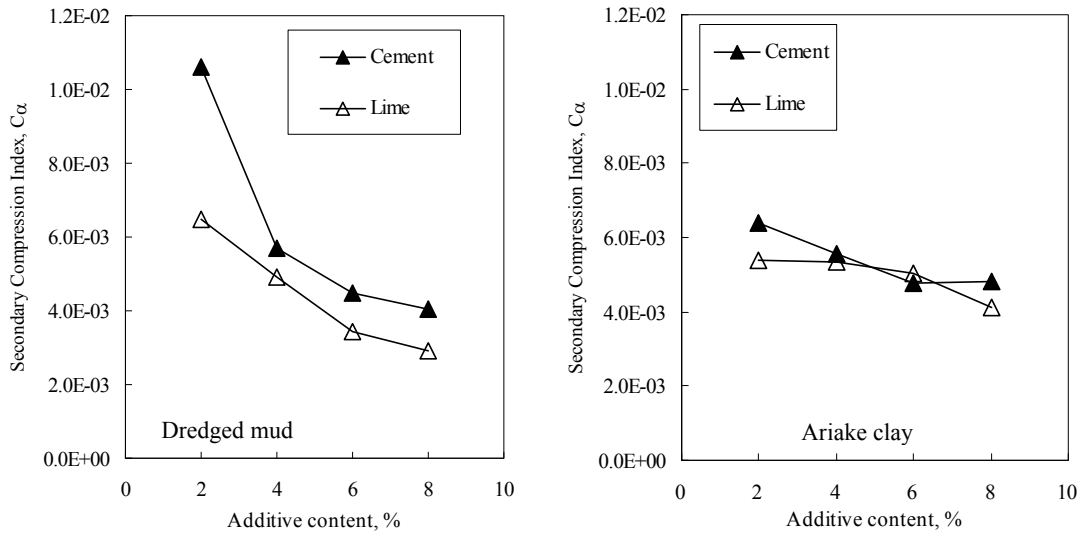
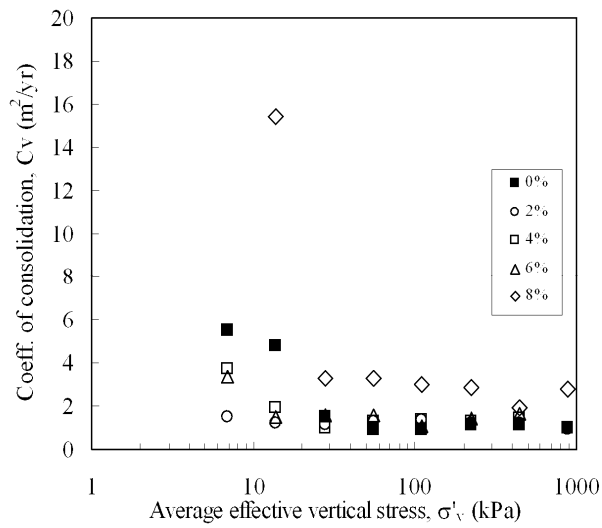
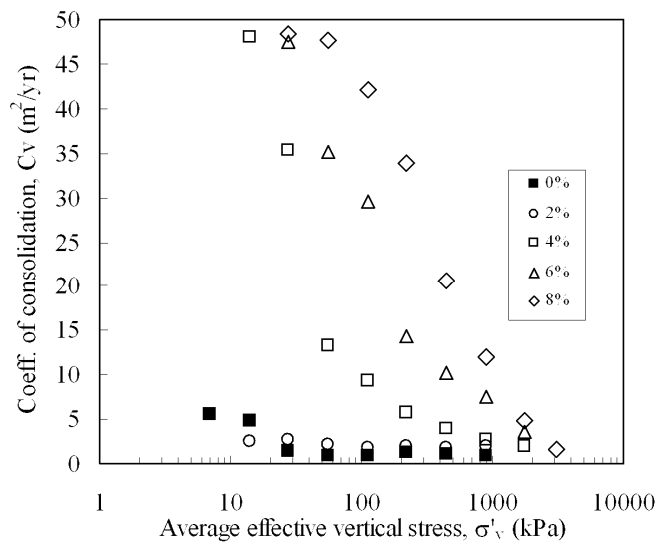


Fig. 4-7 Secondary compression index vs. cement and lime content with curing time of 28 days

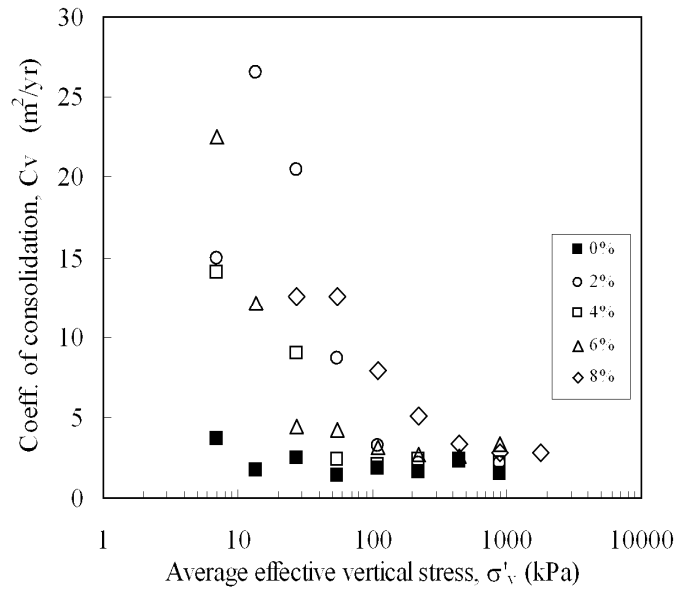


a) Cement-treated dredged mud

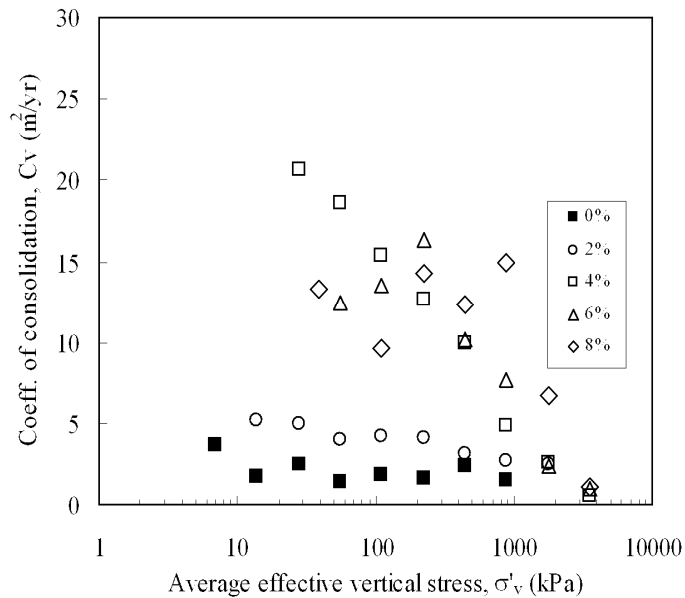


b) Lime-treated dredged mud

Fig. 4-8  $c_v - \sigma'_v$  relation of lime-/cement-treated dredged mud with curing time of 28 days



a) Cement-treated Ariake clay



b) Lime-treated Ariake clay

Fig. 4-9  $c_v - \sigma'_v$  relation of lime-/cement-treated Ariake clay with curing time of 28 days

#### 4.4 Permeability test results

##### 4.4.1. Permeability

The void ratio ( $e$ ) versus permeability ( $k$ ) relationships, defined by both the flexible-wall permeameter tests and the results calculated from the oedometer tests, are depicted in Figs. 4-10 and 4-11, which show the Ariake clay treated with cement and lime, respectively. Figs. 4-12 and 4-13 show the results of the dredged mud. Based on these figures, the following observations can be made.

(1) Although these values are scatters, the  $e$ - $\log(k)$  relationships in the cement-treated soils are comparable with those in the untreated soils for cement contents up to approximately 8% (Figs.



4-10 and 4-12). For the lime-treated soils, there is an obvious reduction in  $k$  value with increases in lime content above 4% (Figs. 4-11 and 4-13).

(2) The  $e$ - $\log(k)$  relationship is nearly linear, which implies that Taylor's (1948)  $e$ - $\log(k)$  relationship can be applied to the cement- and lime-treated soils.

(3) The directly measured  $k$  values are similar and comparable to those calculated from the results of the oedometer tests. However, the results from the oedometer test appear more scattered than those from the direct measurements.

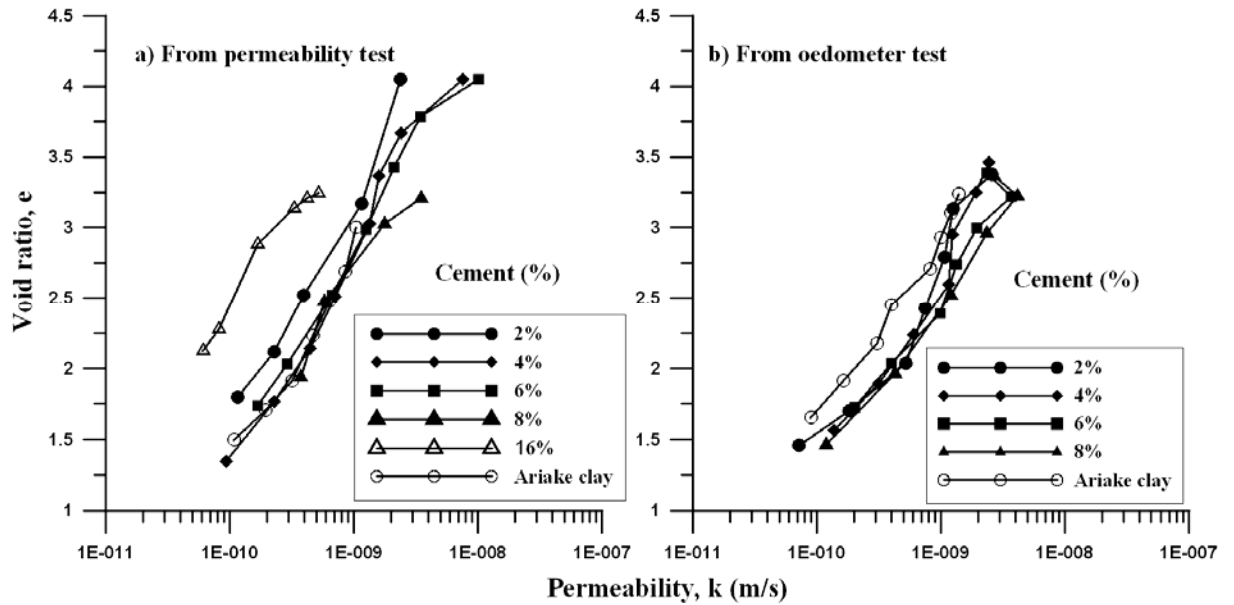


Fig. 4-10 Permeability of cement treated Ariake clay

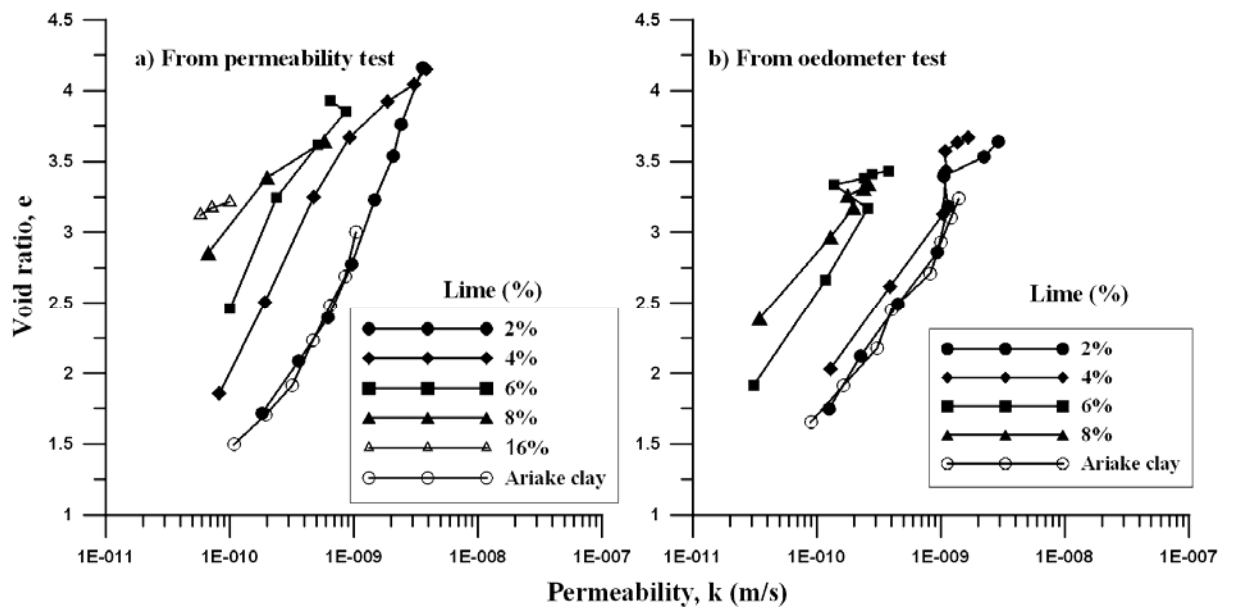


Fig. 4-11 Permeability of lime treated Ariake clay

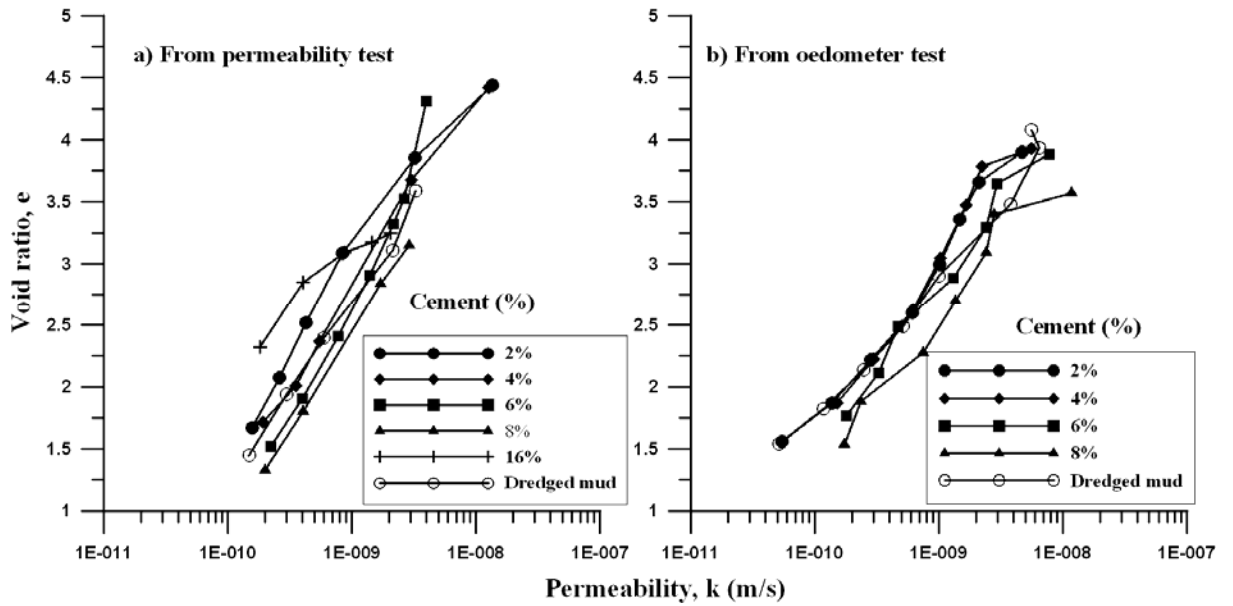


Fig. 4-12 Permeability of cement treated dredged mud

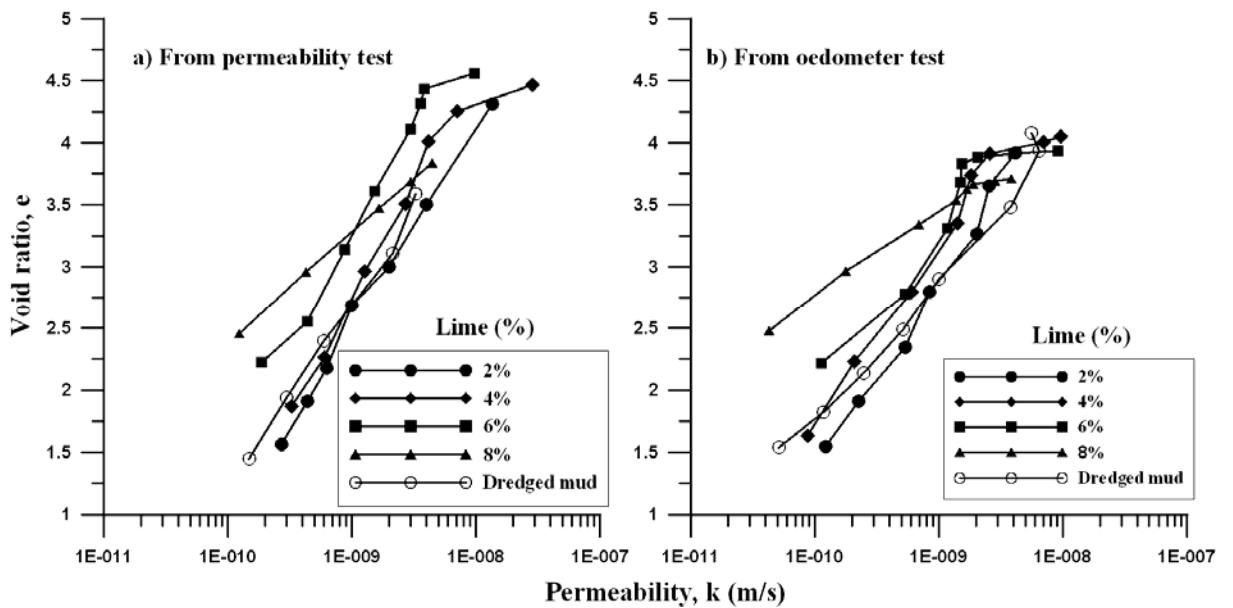


Fig. 4-13 Permeability of lime treated dredged mud

#### 4.4.2. Factors affecting permeability

Investigations of the strength of the treated soils have indicated that the lime treatment is more effective than the cement treatment (Chai and Quang, 2013). The results shown in Figs. 4-10 to 4-13 raised the question of why the permeability of the lime-treated soils is obviously different from that of the cement-treated soils, as well as the question of what factors influence the change in  $k$  values. Fundamentally, the permeability of a porous medium is a function of the void ratio ( $e$ ), the microstructure of the pores (sizes and distribution) and the properties of the pore water. Under identical void ratio ( $e$ ) conditions, the effect of  $e$  can be excluded.

### **(1) Pore Size Distribution and SEM pictures**

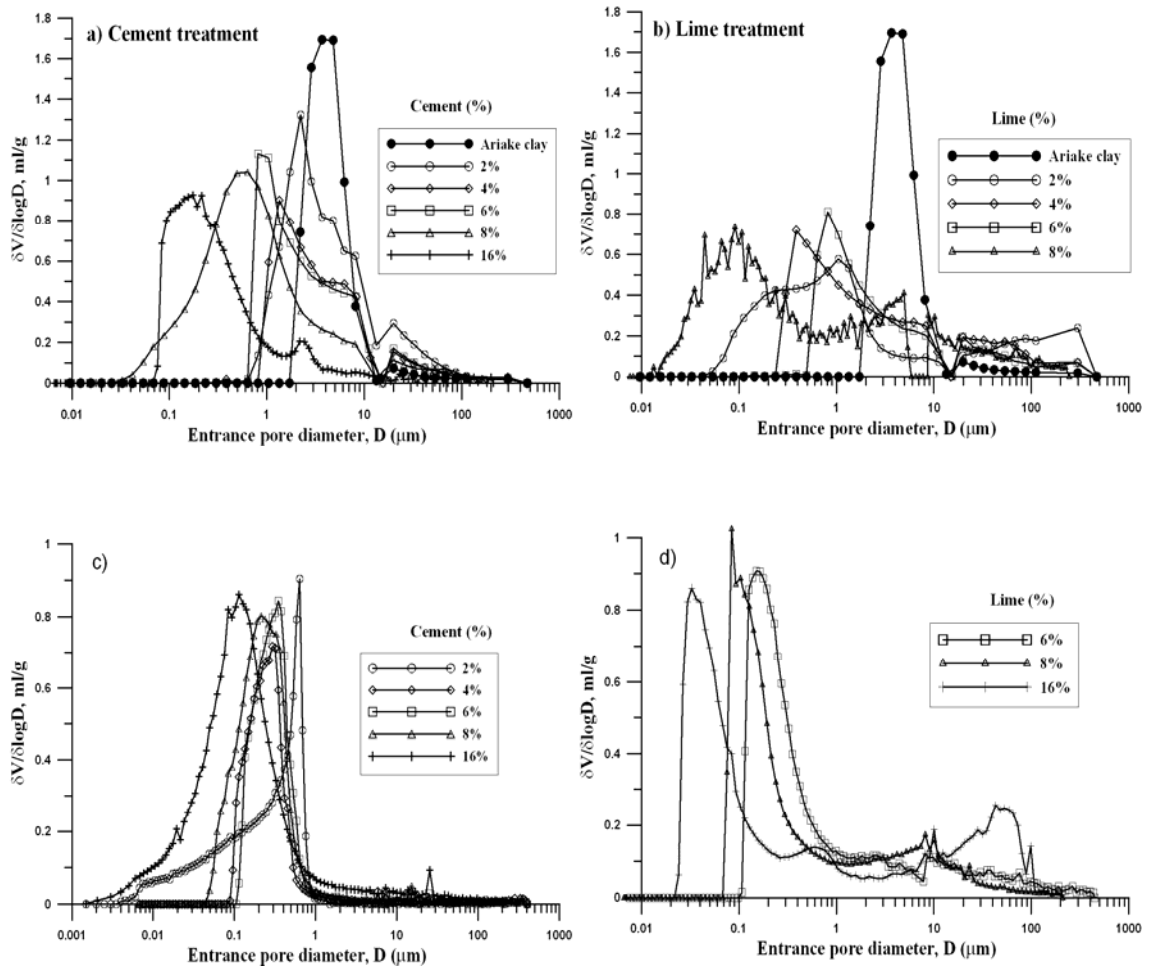
For a given void ratio, larger pore sizes and more uniform pore distribution are associated with higher permeability. The sizes and distributions of the pores of the treated and untreated soils were investigated using mercury intrusion porosimetry (MIP). The soil samples for the MIP test were prepared by freezing and vacuum drying (Delage and Lefebvre, 1984; Kang et al., 2003; Tanaka et al., 2003).

As shown in Figs 4-14a and 4-14b, the pore size range of the remolded Ariake clay is approximately 2 - 10  $\mu\text{m}$ . In soils treated with the cement or the lime, most pore sizes are in the range of 0.1 - 10  $\mu\text{m}$ . The vertical axis in Fig. 14 is the ratio of the increment volume ( $\delta V$ ) injected into a unit mass of sample to the logarithmic increment of pore diameter ( $\delta \log D$ ). The dominant pore size decreased significantly with the increase in the cement or the lime content. The lime-treated samples exhibited a faster reduction rate and a wider pore size distribution. As shown in Fig. 14(a), the dominant pore size for the untreated sample is approximately 4  $\mu\text{m}$ , whereas for the 8% cement treated sample, it is approximately 0.5  $\mu\text{m}$ . The void ratios of the samples used for MIP tests are not exactly identical. Generally, the cement- and lime-treated samples have a smaller initial  $e$  value. This partially explains the fact that the pore size distributions, as shown in Figs 4-14a and 4-14b, for the cement- and lime-treated samples are different from those for the untreated samples. For the treatments with up to 8% of the cement and 4% lime, the  $e - \log(k)$  relationships are comparable to those of the untreated samples. Figs 4-14c and 4-14d show the variation of pore size distribution of lime/cement treated clayey soil after completion of flexible-wall permeability test. Generally, due to the effect of consolidation process, the dominant pore size shifts from the range of 0.1 - 10  $\mu\text{m}$  to 0.02 - 1  $\mu\text{m}$ . The pores whose diameter is larger than 1  $\mu\text{m}$  were broken, and consequently transformed into smaller pores having diameter between 0.02 - 1  $\mu\text{m}$ . This causes the reduction of the pore size of treated soil after consolidation process.

The pores in clayey soils can be divided into two types: intra-aggregate pores and inter-aggregate pores. It has been postulated that when a small amount of cement or lime is added, the cementation products formed by the pozzolanic reactions will fill the intra-aggregate pores or cement several small aggregates into a larger one. However, the entire sample is not yet bound together. With the increase in the amount of additives, the cementation products will bind the aggregates together and fill the inter-aggregate pores. It is widely believed that the  $k$  value of a clayey soil is mainly controlled by the inter-aggregate pores. When the cementation products begin to fill the inter-aggregate pores, even under identical void ratio conditions,  $k$  value will begin to decrease.

The SEM pictures of 2%, 8% and 16% the cement-treated samples, and 2%, 6% , 8% and 16% the lime-treated samples are compared in Fig. 4-15. Considering the “cloud” shaped parts as cementation products, there are some cementing products can be observed for the 2% and 8% cement and 2% lime-treated samples, but there are many open inter-aggregate pores not being filled by the cementation products. However, for the 16% cement, and 6%, 8% and 16% lime-treated samples, the entire cross-section appears to be covered by the cementation products.

To confirm the above observation, the pore size distributions of the samples after the flexible-wall permeability test and the  $e - \log(k)$  relationships of the 16% cement and the 6% and 8% lime-treated samples are compared in Figs. 4-16a and 4-16b, respectively. The values of  $k$  and the pore size distributions were similar and comparable. The 16% cement-treated sample had a slightly smaller main pore size (Fig. 4-16a) but larger  $k$  values for  $e > 3$  (Fig. 4-16b). This may be due to the influence of the chemical properties of the pore water, which will be discussed later.



a) & b) Before permeability test; c) & d) After permeability test

Fig. 4-14 Pore size distributions of cement-/lime-treated and untreated Ariake clay

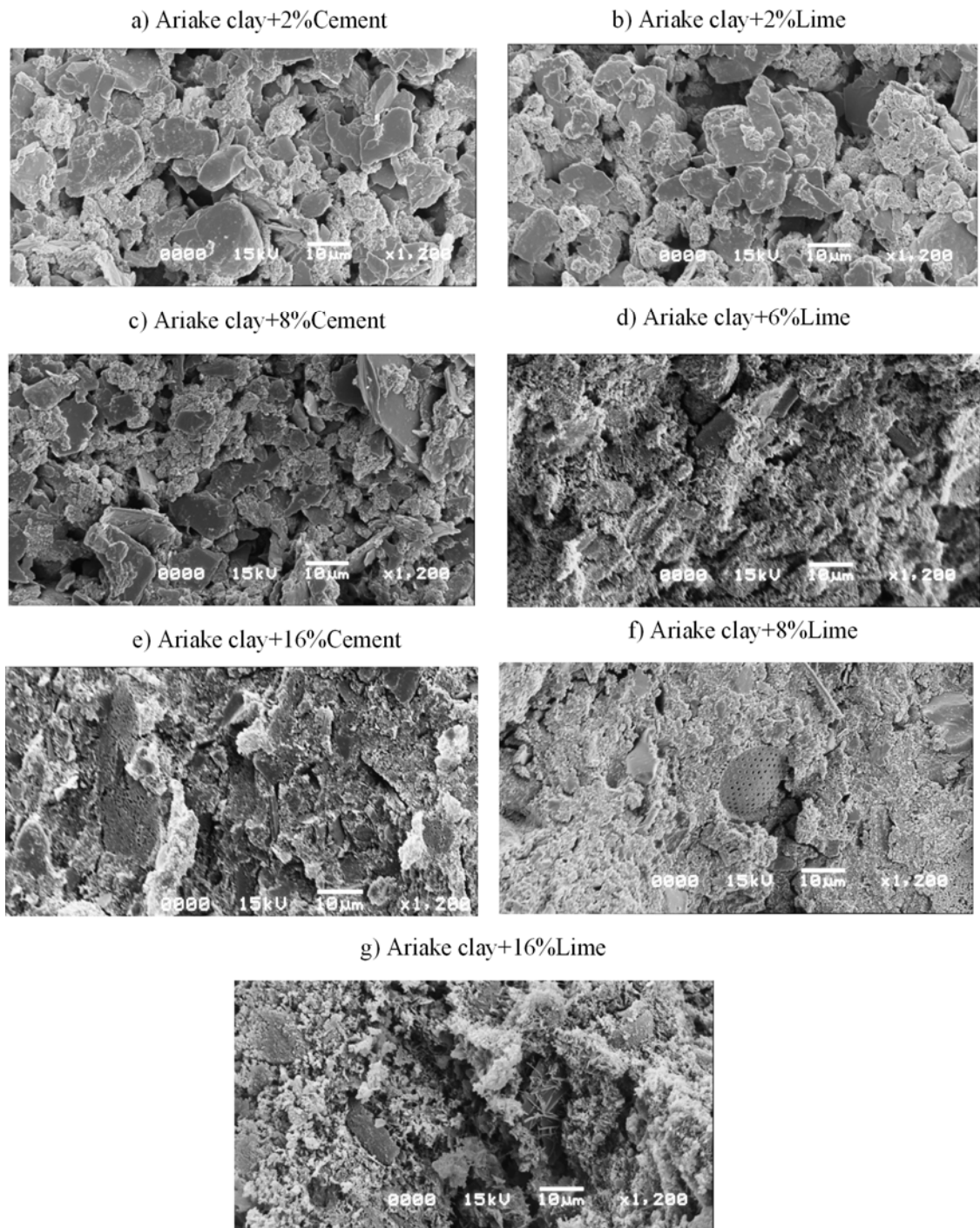


Fig. 4-15 SEM images of lime/cement treated Ariake clay after permeability test

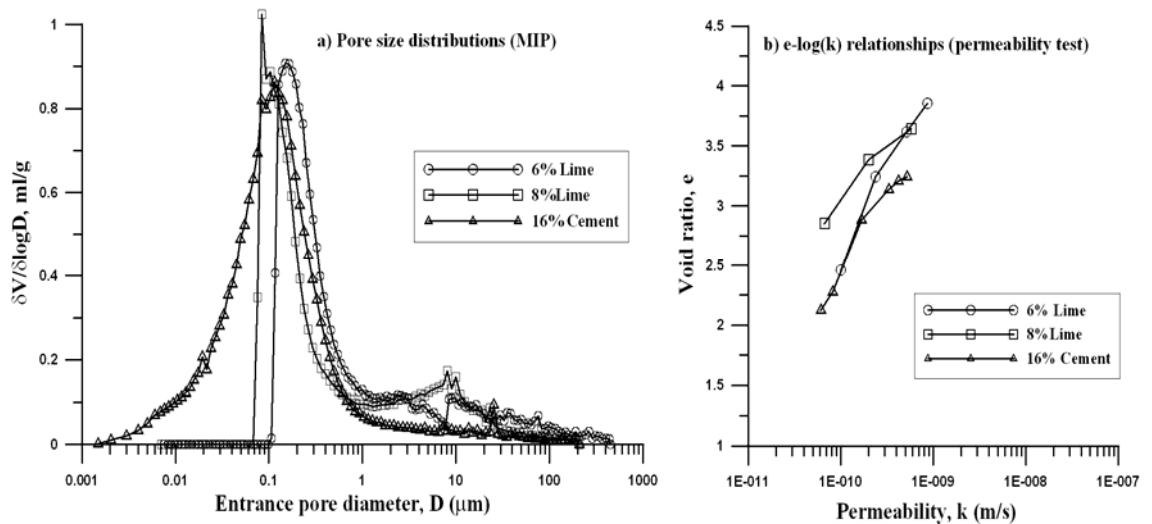


Fig. 4-16 Comparison of variations of pore size distributions and permeability

The strain-stress curves from the unconfined compressive tests for the 16% cement-treated and the 6% and 8% lime-treated Ariake clay samples are compared in Fig. 4-17. These curves are also similar and comparable (especially for the 8% lime- and 16% cement-treated samples). The unconfined compressive strength ( $q_u$ ) is an indicator of intra- and inter-aggregate bonds. Therefore, the results shown in Fig. 4-17 support the argument that similar inter-aggregate bonds will result in similar  $e$ - $\log(k)$  relationships.

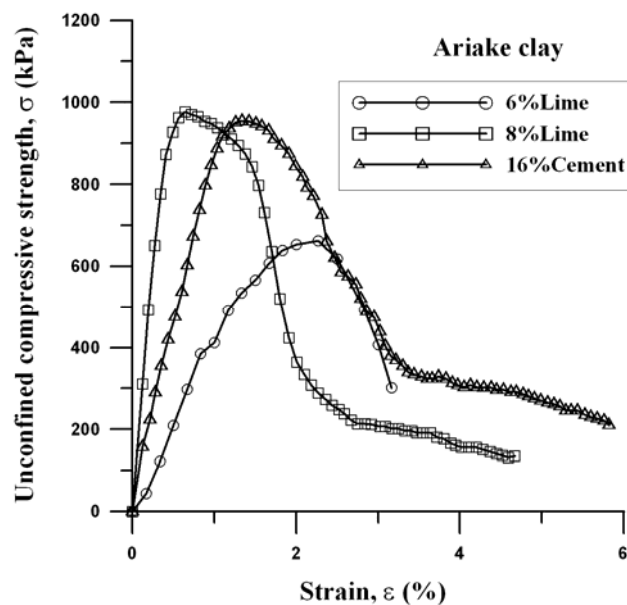


Fig. 4-17 Strain—stress curves of unconfined compressive test

From the above discussion, it can be stated that the pore size distribution is a dominant influential factor for  $e$ - $\log(k)$  relationship. When cementation products start to fill inter-aggregate pores,  $k$  value will reduce even compared under the same  $e$  value condition.

## (2) *Thickness of Diffuse Double Layer*

Clay particles carry negative charges at their surfaces. To balance the negative charges, cations will be attracted to surround the clay particles to form an electric double layer. The water within the double layer cannot move freely. For a given void ratio, thicker double layers are associated with smaller spaces for water to move freely and effectively and therefore smaller  $k$  values (Anandarajah, 2003; Schmitz and Robrecht, 2006). However, the thickness of the double layer cannot be measured directly. A semi-quantitative estimation can be calculated to investigate the possible effect of the DDL on the  $k$  value.

The thickness ( $1/K$ ) of the DDL depends on the type of clay mineral, electrolyte concentrations and the valences of the ions present in the pore water (e.g., Mahanta et al., 2012), and it can be approximated by the following equation (Mitchell, 1993):

$$\frac{1}{K} = \left( \frac{\varepsilon_0 D k T}{2 n_0 e^2 \nu^2} \right)^{1/2} \quad (4-1)$$

where  $n_0$  is the electrolyte concentration,  $\nu$  is the valence of the cation,  $D$  is the dielectric constant of the medium,  $T$  is the temperature ( $^{\circ}\text{K}$ ), and  $\varepsilon_0$ ,  $k$  and  $e$  are constants.  $\varepsilon_0$  is the vacuum permittivity ( $8.8542 \times 10^{-12} \text{ C}^2 \text{ J}^{-1} \text{ m}^{-1}$ ),  $k$  is the Boltzmann constant ( $1.38 \times 10^{-23} \text{ J}^{\circ}\text{K}^{-1}$ ), and  $e$  is the electronic charge ( $1.602 \times 10^{-19} \text{ C}$ ).

The concentrations of  $\text{Ca}^{2+}$ ,  $\text{Na}^{+}$  and  $\text{Mg}^{2+}$  in the pore water of the Ariake clay samples are listed in Table 4-2. The concentration of  $\text{Ca}^{2+}$  is used to calculate the  $n_0$  values and subsequently  $\nu = 2$ . Assuming the temperature is  $20^{\circ}\text{C}$ , then  $T = 293^{\circ}\text{K}$ .  $D$  is estimated with the following equation:

$$D = \frac{\alpha}{EC} \quad (4-2)$$

where  $\alpha$  is a constant and  $EC$  is the electrical conductivity of the pore water.

For distilled water, assuming  $D = 80$ , and  $EC$  was measured as  $105 \mu\text{S}/\text{cm}$ ; thus,  $\alpha = 8400 \text{ cm}/\mu\text{S}$ . For the cases considered,  $D$  values are estimated using the  $\alpha$  and the measured  $EC$  values and plotted in Fig. 3-5; these values are also listed in Table 3-4 in Chapter 3. For the 2% and 4% cement and lime additions to the Ariake clay samples, the estimated values of  $1/K$  are listed in Table 4-2. The cement-treated samples have relatively smaller  $1/K$  values. Consequently, under identical microstructure conditions, the cement-treated samples tend to exhibit a higher permeability. The results in Fig. 4-16 support this argument, i.e., that the 16% cement-treated sample had smaller pores than the 8% lime-treated sample (Fig. 4-16a) but had higher  $k$  values (Fig. 4-16b).

Table 4-2 Estimated thickness of DDL

	EC( $\mu\text{S/cm}$ )	D	$\nu$ ( $\text{Ca}^{2+}$ )	IC(mg/l)	$n_o$	1/K( $\text{A}^\circ$ )
Ariake clay	400	21	2	170	$9.14 \cdot 10^{23}$	19.9
2%Cement	550	15.3	2	294	$1.58 \cdot 10^{24}$	12.9
4%Cement	660	12.7	2	366	$1.97 \cdot 10^{24}$	10.6
2%Lime	470	17.9	2	230	$1.24 \cdot 10^{24}$	15.8
4%Lime	390	21.5	2	301	$1.62 \cdot 10^{24}$	15.1

EC is electric conductivity, IC is ion concentration.

#### 4.5 Summaries

A systematic test program was conducted on the effect of cement/lime on the yield stress ( $p_y$ ), compression and secondary compression index ( $C_c$  and  $C_\alpha$ ) and coefficient of vertical consolidation ( $c_v$ ) and permeability ( $k$ ) of untreated and treated soils. The coefficient of permeability of lime and cement lightly treated clayey soils was investigated by laboratory flexible-wall permeability test and also calculated indirectly from oedometer consolidation test results. Based on the test results, the following conclusions can be drawn:

(1) For 2 – 8% of the lime or the cement added, relationship between  $p_y$  and the amount of the lime or the cement additive is non-linear.

(2) With the increase of the amount of the lime or the cement additive,  $C_c$  values were increased, and the lime-treated soils had more increase than that of the cement-treated ones. However,  $C_\alpha$  values decreases significantly with the increasing of the amount of the cement or lime.

(3) When treated by lime/cement, the  $c_v$  values increase substantially with the increase of the amount of additive content, and for the lime-treated soils, the magnitude of increase is more higher than the cement-treated soils.

(4) The pore size distribution of the soil is the main factor influencing the  $k$  value. Under identical void ratio ( $e$ ) conditions, when the amount of cement or lime added is large enough that the cementation products formed during the pozzolanic reactions begin to fill the inter-aggregate pores, the  $k$  value begins to decrease. For the conditions tested, the threshold values are 8% the cement and 4% the lime by dry weight.

(5) The chemical properties of the pore water also affect the  $k$  value through their influence on the thickness of the diffuse double layer (DDL). Cement-treated soils tend to have a thinner DDLs and higher  $k$  values than the lime-treated soils with similar microstructures.



## CHAPTER 5 LARGE SCALE CONSOLIDATION TESTS USING GEOCOMPOSITE

### 5.1 Introduction

To investigate consolidation behavior of lime/cement lightly treated clayey soils induced by horizontal geocomposite under stepwise load, it is desirable to carry out many laboratory large-scale tests or full-scale trial embankment with the proper instrumentations to monitor consolidation process, e.g. settlement, excess pore water pressure, etc. Unfortunately, full-scale field tests are expensive and only a small number of such tests can be done. Therefore, the large scale model box was designed to simulate the consolidation behaviour of a geocomposite reinforced plain strain “unit cell”.

This chapter contains the details of the devices for the large-scale model test, the procedures of laboratory test and the test results.

### 5.2 Laboratory model test

#### 5.2.1. Equipment

The model test is designed to simulate the behavior of a geocomposite improved plane strain “unit cell” as illustrated in Fig. 5-1, which represents a part of an embankment. The model box is made of steel with dimensions of 0.6 m in length, 0.3 m in width and 1.0 m in height. On the front wall (0.3 m in width and 1.0 m in height), two drainage slots (outlets) were installed at 0.25 m and 0.5 m vertical distance from the bottom, which enables the test can be conducted with either 0.5 m or 1.0 m vertical spacing ( $S_v$ ) of geocomposites. But in this study, all model tests were conducted with 1.0 m vertical spacing ( $S_v$ ). Ideally, only the drainage through the geocomposite is allowed. However, the sealing between the top loading plate and the walls of the model box was not perfect and during the tests, water leakage at the top surface was observed. Therefore, we consider the behavior of soil layer below the geocomposite is closer to the field condition.

The load from the embankment fill above the “unit cell” was simulated by stepwise surcharge load applied through two Bellofram cylinders using air pressure. During the test, the vertical displacement of the model ground was measured by a LVDT. Two piezometers were installed in the model ground (one above and one below the geocomposite) to monitor the excess pore water pressure variations. The data from LVDT and piezometers were recorded by a data-logger.

Figure 5-2a shows the longitudinal cross-section of the set up of the model test. The soil above the geocomposite was about 0.45 m thick and below was about 0.5 m ( $S_v \approx 1.0$  m for the bottom layer). Regarding the plan layout of the geocomposite, there are two options, i.e., (1) continuous sheet and (2) strip material. The model test was conducted for the case of using strip type geocomposite (Fig. 5-2b).

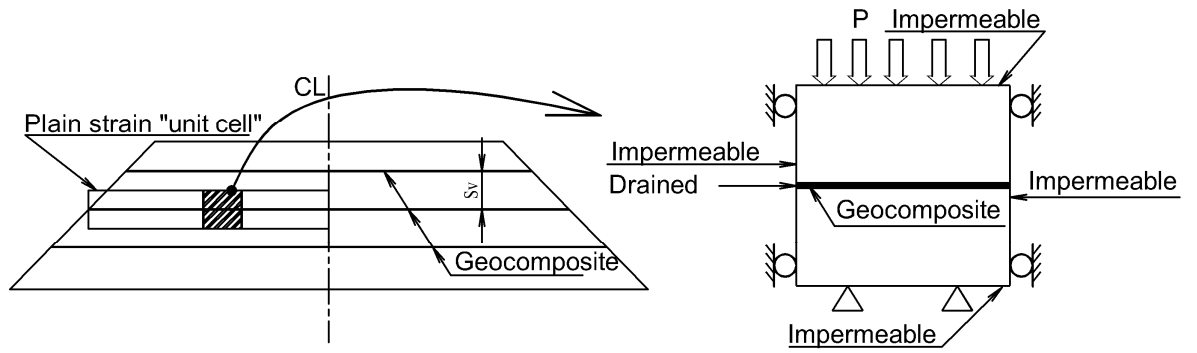
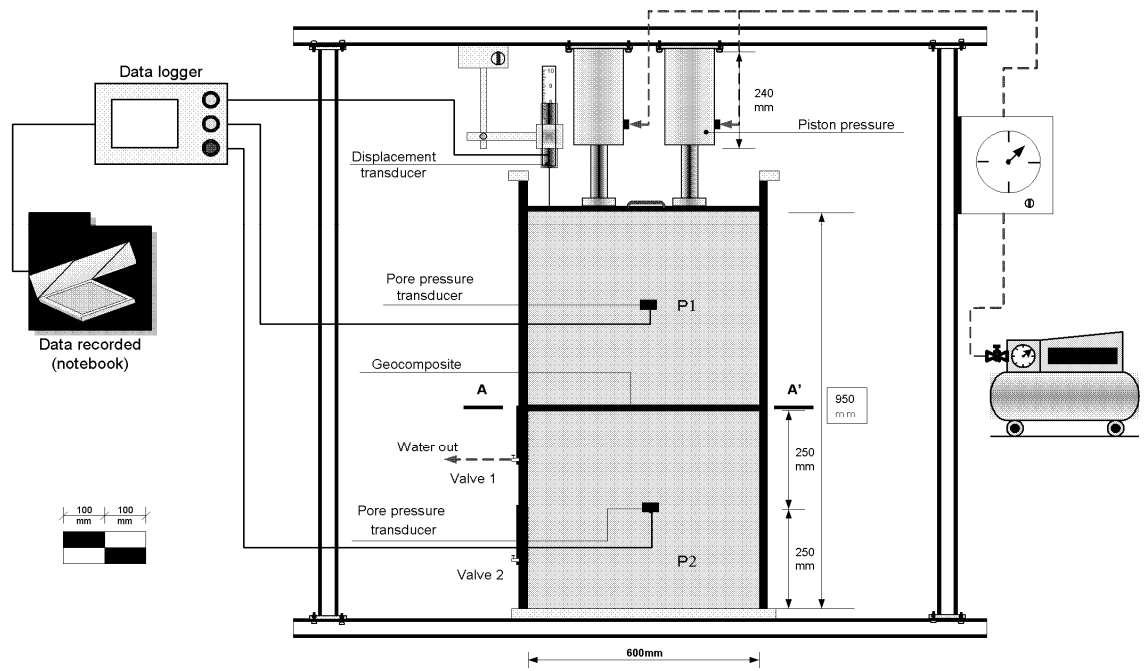
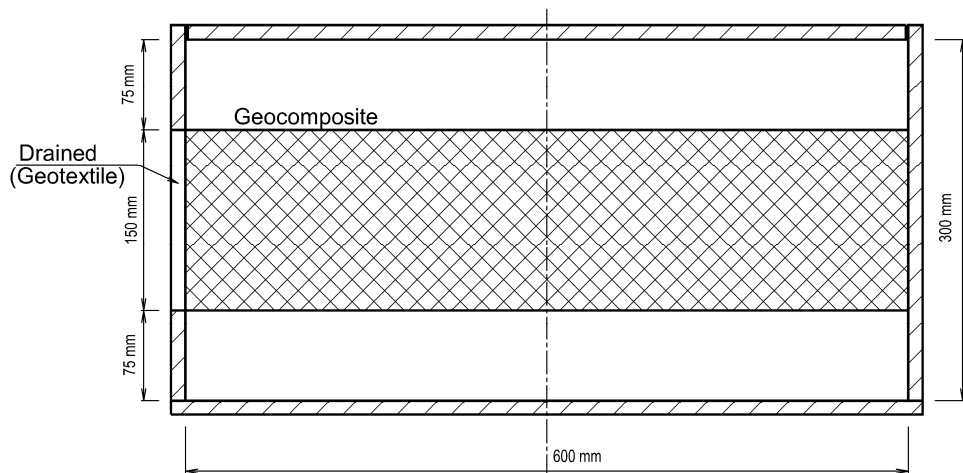


Fig. 5-1 Illustration of geocomposite reinforced plain strain "unit cell"



a. Cross sectional view



b. Enlarged plan view of A – A' section

Fig. 5-2 Large scale model test set-up

Table 5-1 Soil properties of natural, cement- and lime-treated Ariake clay and dredged mud

		Ariake clay			Dredged mud		
		Disturbed soil	4% cement	2% lime	Disturbed soil	4% cement	2% lime
Moisture content, $w_n$	%	150	151	152	150	152	153
Liquid limit, $w_L$	%	133	180	171	138	162	160
Plastic limit, $w_P$	%	46.5	56	63	48.6	57	55
Plasticity index, $I_p$		86.5	124	108	89.4	105	105
Total unit weight, $\gamma_t$	kN/m <sup>3</sup>	13.4	13.7	14.1	1.30	13.4	13.4
Void ratio, $e_o$		3.94	3.86	3.74	4.2	4.00	4.10
Particle size distribution, %	Sand (2-0.075mm)	0.2	2.3	9.1	0.2	2.3	1.5
	Silt (0.075-0.002mm)	48.4	77.3	71.7	48.3	70	69.6
	Clay (< 2 $\mu$ m)	51.4	20.3	19.2	51.5	27.7	28.9
pH		7.5	10.6	10.3	8.5	10.2	10.5
Ignition loss	%	8.5	-	-	11.8		

### 5.2.2. Test procedure

#### (1) Set-up:

- a) Install geotextile in the drainage slot on the front wall of the model box as drainage material.
- b) Apply a thin layer of silicon grease on the inner walls of the model box to reduce friction between soil and the model box.
- c) Put remolded clayey soil slurry into the model box layer by layer with a layer thickness of about 0.1 m. After each layer was placed, the soil was stirred by a stainless steel rod carefully and uniformly to avoid any possible trapped air bubbles. When the soil reaches to the pre-determined heights, strip geocomposite and two piezometers,  $P1$  &  $P2$ , were installed (Fig. 5-2a).
- d) After the model ground reaches to the designed thickness, place one layer of geomembrane on the top of the model ground to prevent free drainage at the top surface.
- e) Place steel loading plate on the top of the geomembrane and install two Bellofram cylinder systems for applying vertical pressure.
- f) Connect LVDT and piezometers to data-logger.

In case of clayey soil lightly treated by cement or lime, the remolded soil was mixed thoroughly by a mixing machine to obtain clay slurry with water content of about 150%. Then, for cement treatment, cement slurry at a water-cement ratio ( $w/c$ ) of 1.0 was added to the clay slurry and mixed uniformly. For lime treatment, clay slurry was mixed with pre-determined amount of the lime. After that, amount of water equivalent to water-lime ratio of 1.0 for the amount of the lime used was added to the mixed soil and mixed uniformly again. For laboratory model test, the clayey soil after mixing with cement/lime was put in the plastic bucket and covered by plastic bag to prevent moisture

loss. Then, cured about 01 month before placing in the model box. The remaining procedures were the same as for the remolded clayey soil. Some of the physical properties of 4% cement- and 2% lime-treated soils are listed in Table 5-1 also. There is a significant increase in liquid limit for the treated soils although the percentage of clay particles ( $< 2 \mu\text{m}$ ) was reduced. The exact reason for this phenomenon is not very clear. Locat et al. (1990, 1996) and Chew et al. (2004) reported the similar phenomenon and Locat et al. (1990, 1996) explained that the possible reason is: due to the effect of small amount of cement or lime, clusters of clay particles were formed with larger inner voids, which can held more water when the soil reaches its liquid limit than that of a soil without treatment.

### ***(2) Apply the stepwise load and monitoring:***

To simulate an embankment construction process, the vertical pressure was applied stepwise, and for each loading step, a load increment of 8 kPa was applied instantaneously followed a consolidation time increment of 5 days. The loading rate is within the range of practical construction rate of 0.05 - 0.1 m/day in Saga region, Japan. The total load applied was 72 kPa which is equivalent to the load of approximately 4 m height embankment. During the test, settlement of the model ground and excess pore water pressures at two locations inside the model ground were monitored.

### ***(3) Properties of the model ground after consolidation:***

After the consolidation test, the soil samples from the model ground were taken every 0.1 m in the vertical direction, the water content ( $w_n$ ) and undrained shear strength ( $s_u$ ) were measured.  $s_u$  value was measured using a laboratory mini-vane with a diameter of 20 mm and height of 40 mm.

#### **5.2.3. Materials used**

The properties of two types of clayey soils, i.e. Ariake clay and dredged mud were shown in Table 5-1. The chemical composition of cement and quicklime used were also described in Table 3-2 in Chapter 3.

The properties of the geocomposite used are given in Table 5-2. The confined in clay (confining pressure  $\sigma_n = 100$  kPa) discharge capacity of the geocomposite was about 25,000  $\text{m}^3/\text{year}/\text{m}$  (Chai et al., 2011), and under a strain rate of 20 %/min, the short-term tensile strength was about 52.7 kN/m.

#### **5.2.4. Cases tested**

Totally 6 cases were tested as listed in Table 5-3 for both clayey soils. Case-1 used remolded Ariake clay, Cases-2 and 3 used cement or lime lightly treated Ariake clays, respectively. For dredged mud, Case-4 is remolded soil, Cases-5 and 6 are cement- and lime-treated soil, respectively. The adopted loading conditions and the spacing for geocomposite were the same.

Table 5-2 Structure and index properties of geocomposite

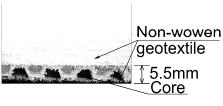
Structure (Photo)	Material	Mass per unit area (g/m <sup>2</sup> )	Tensile strength (kN/m)
	Filter: polyester Core: polyolefin- resin	1170	52.7

Table 5-3 List of tested cases

Case	Soil type	Initial water content, %	Thickness of model ground (m)	Total load (kPa)	Load increment (kPa)	Time interval between two loading steps (day)
1	Remolded Ariake clay	150	0.95	72	8	5
2	Ariake clay + 4% cement <sup>a</sup>	151	0.95	72	8	5
3	Ariake clay + 2% lime <sup>a</sup>	152	0.95	72	8	5
4	Remolded dredged mud	150	0.95	72	8	5
5	Dredged mud + 4% cement <sup>a</sup>	152	0.95	72	8	5
6	Dredged mud + 2% lime <sup>a</sup>	153	0.95	72	8	5

<sup>a</sup>By dry weight.

### 5.3 Laboratory vane shear test for model grounds

#### 5.3.1 Equipment and specimen preparation

For determining the undrained shear strength of reconstituted clayey soils, the laboratory vane shear test was conducted. A laboratory mini-vane with a diameter of 20 mm and height of 40 mm as shown in Fig. 5-3 was used and the strain rate adopted is 3°/min.

To perform the test, the vane is pushed into the soil and torque is applied at the top of the torque rod. The torque is gradually increased until the cylindrical soil of height  $h$  and diameter  $d$  fails. The maximum torque  $T_{\max}$  applied to cause failure is the sum of the resisting moment at the top,  $M_T$ , bottom,  $M_B$ , of the soil cylinder, and the resisting moment at the side of the cylinder,  $M_S$ . Thus

$$T_{\max} = M_S + M_T + M_B \quad (5-1)$$

Where,

$$M_S = \pi dh \frac{d}{2} s_u \quad \text{and} \quad M_T = M_B = \frac{\pi d^2}{4} \frac{2}{3} \frac{d}{2} s_u \quad (5-2)$$

Assuming uniform undrained shear strength distribution around the vane and with a value of  $s_u$ , so,

$$T_{\max} = \pi s_u \left[ \left( dh \frac{d}{2} \right) + 2 \left( \frac{d^2}{4} \frac{2}{3} \frac{d}{2} \right) \right] \quad (5-3)$$

or

$$s_u = \frac{T_{\max}}{\pi \left[ \left( D^2 \frac{H}{2} \right) + \frac{D^3}{6} \right]} \quad (5-4)$$

Normally, standard vanes used have  $h/d = 2$ . In such cases, Eq. (5-4) can be simplified to the form

$$s_u = \frac{6T_{\max}}{7\pi d^3} \quad (5-5)$$



Fig. 5-3 Laboratory mini vane shear device

### 5.3.2. Test results of the model grounds

For the laboratory large scale model tests described in Chapter 5, after completion of large scale model test, the soil samples from the model ground are taken every 0.1 m in the vertical direction, the water content ( $w_n$ ) and undrained shear strength ( $s_u$ ) are measured. The results of measured undrained shear strength of large scale consolidation test were shown in Figure 5-9 and 5-10 for lime-/cement-untreated/treated Ariake clay and dredged mud, respectively.

## 5.4 Large scale model test results

### 5.4.1. Settlement

The settlement-time curves together with loading histories are shown in Fig. 5-4 and Fig. 5-5 for lime-/cement-treated Ariake clay and dredged mud, respectively. For the lime/cement treatment, the cases (Cases-2 and 3) for Ariake clay and Cases-5 and 6 for dredged mud, the settlement of treated soils are smaller than that of untreated soils. Further, the settlement of lime-/cement-treated dredged mud is higher than that of Ariake clay. The reason is because the lime-/cement-treated Ariake clay has higher shear strength than the lime-/cement-treated dredged mud. As listed in Table 5-4, the average reductions of void ratio ( $\Delta e$ ) are 1.34, 0.98, 0.85, 1.35, 1.23 and 1.11 for Cases-1, 2, 3, 4, 5 and 6, respectively. For Ariake clay, the initial dry densities of three model grounds were 5.3, 5.6 and 5.6 kN/m<sup>3</sup>, and due to geocomposite induced consolidation, the average dry densities increased to 7.2, 6.7 and 6.7, respectively. For dredged mud, the initial dry densities of three model grounds were 5.2, 5.3 and 5.3 kN/m<sup>3</sup>, and due to geocomposite induced consolidation, the average dry densities increased to 6.7, 6.9 and 6.5, respectively. It is noticed that due to the leakage at the top surface, the degree of consolidation and therefore the amount of compression of the soil layer above the geocomposite is larger than that of the layer below it. After the consolidation tests, the distribution of the final water content with depth in the model ground was measured, and the results indicate that the average difference of final water content between the upper and lower layers is about 5%. However, for the remolded Ariake clay, the difference is about 20% and for remolded dredged mud, that is about 10%. Therefore, for the cement or lime lightly treated cases, the increase of the dry density of the lower layer is slightly lower than the average values, and for the case without cement/lime treatment, the increase of dry density of the lower layer is considerably less than the average value. The reason considered is that the cement-/lime-treated soils have a higher coefficient of vertical consolidation ( $c_v$ ) (Fig. 4-8 and 4-9 in Chapter 4) and therefore, increase the degree of consolidation of the cement-/lime-treated soils. The results presented above imply that combination of light cement/lime treatment and using geocomposite can result in a denser and stronger embankment with clayey fill material comparing with cases of cement/lime treatment alone without consolidation induced deformation. Further, it is worth to mention that constructing an embankment with clay as fill material without using geocomposite, due to the drainage capacity of clay itself, during construction process, the degree of self-weight induced consolidation of embankment will be very low and practically an embankment may not be able to be built.

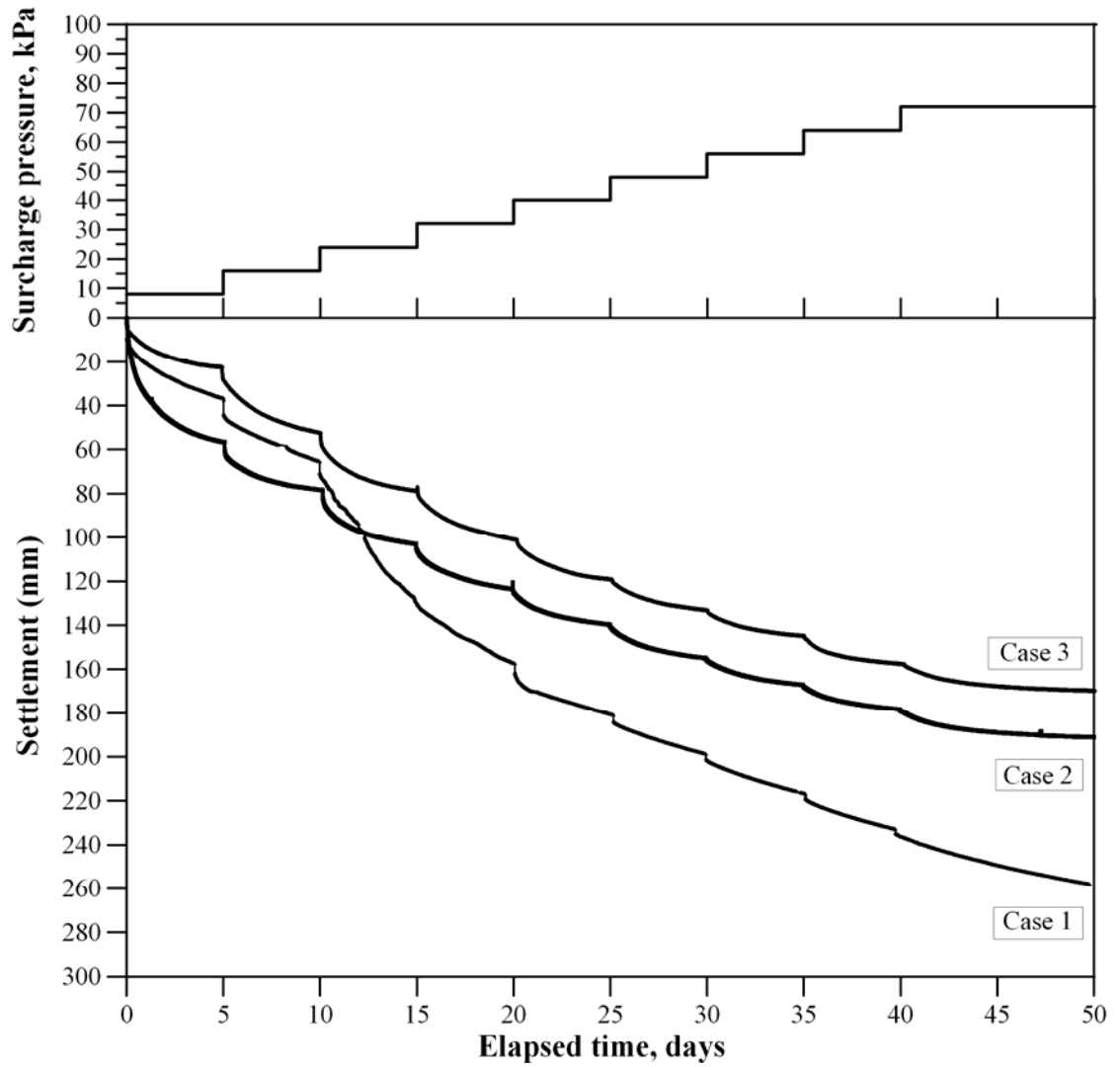


Fig. 5-4 Surface vertical settlement of Cases 1, 2 and 3



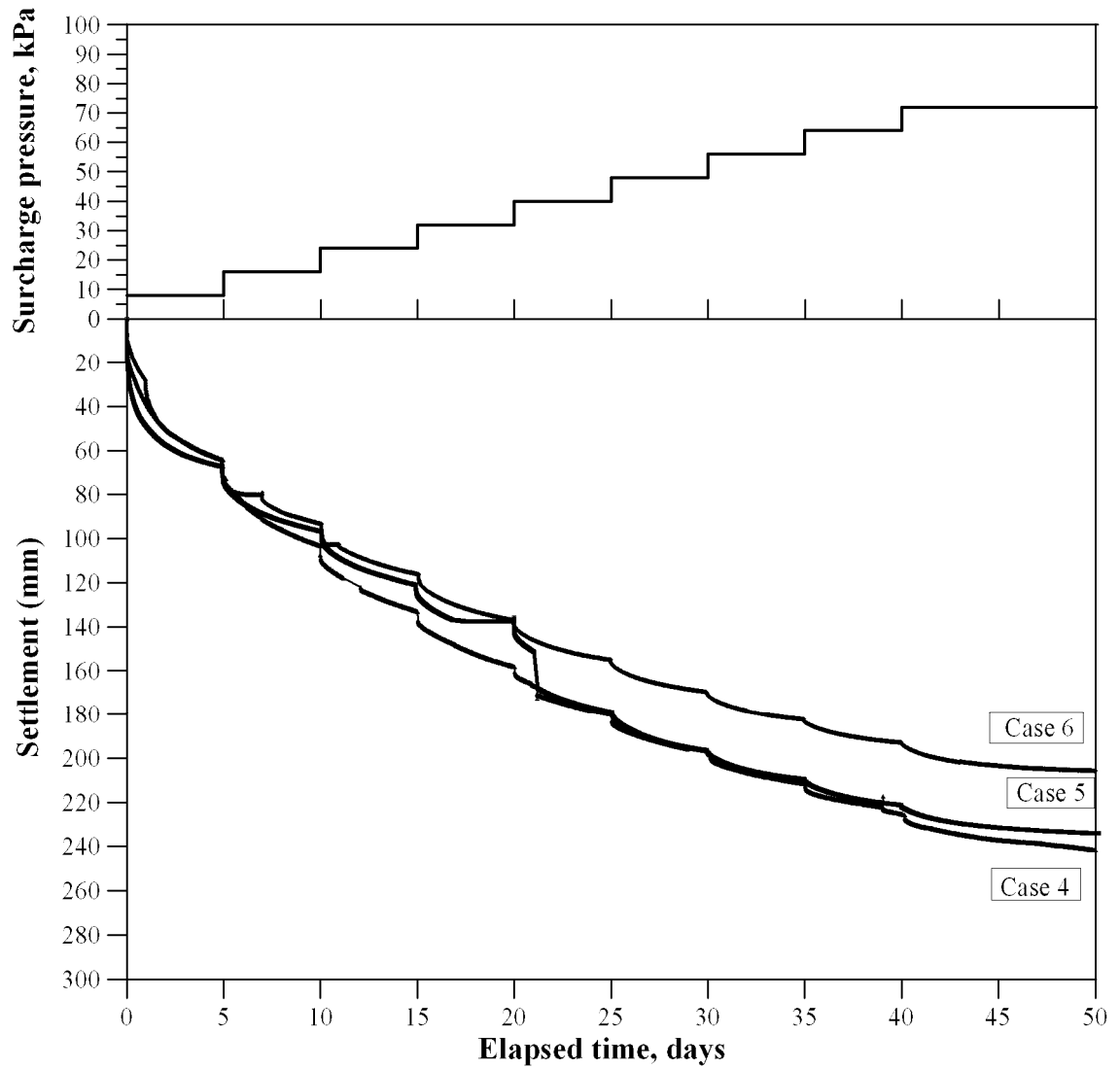


Fig. 5-5 Surface vertical settlement of Cases 4, 5 and 6

Table 5-4 Reduction of void ratio for tested cases

Parameter	Unit	Case-1	Case-2	Case-3	Case-4	Case-5	Case-6
Initial void ratio, $e_o$		3.94	3.86	3.74	4.2	4	4.1
Initial height of model ground, $H_o$	m	0.95	0.95	0.95	0.95	0.95	0.95
Settlement, $S_c$	m	0.258	0.192	0.170	0.246	0.234	0.206
Reduction of void ratio, $\Delta e$		1.34	0.98	0.85	1.35	1.23	1.11
Final void ratio, $e_f$		2.60	2.88	2.89	2.85	2.77	2.99

#### 5.4.2. Variation of excess pore water pressure ( $u$ )

The variations of measured excess pore water pressures ( $u$ ) are shown in Fig. 5-6 and Fig. 5-7 for lime-/cement-treated Ariake clay and dredged mud, respectively. For Case-3, there was a problem for piezometer  $P2$ , and the measurements are not included in the figure. It can be seen that there were gradual build up of  $u$  values during the test. For Ariake clay, the highest  $u$  value measured for Case-1 is about 43 kPa, and 18.2 and 14.6 kPa for Cases-2 and 3, respectively and for dredged mud, the

highest  $u$  value measured for Case-4 is about 20 kPa, and 15 and 17 kPa for Cases-5 and 6, respectively.

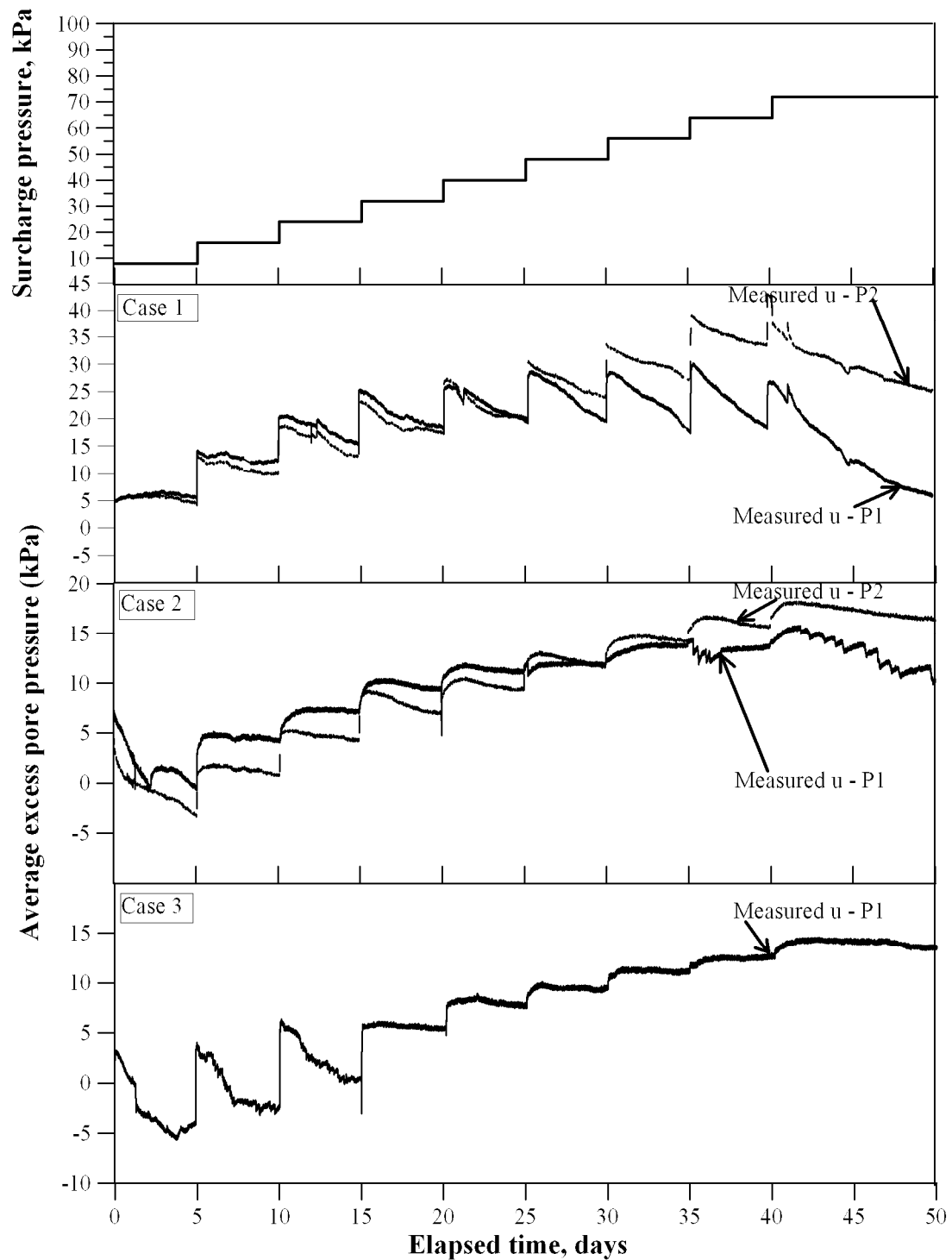


Fig. 5-6 Comparison between measured and predicted excess pore pressure of Cases 1, 2 and 3

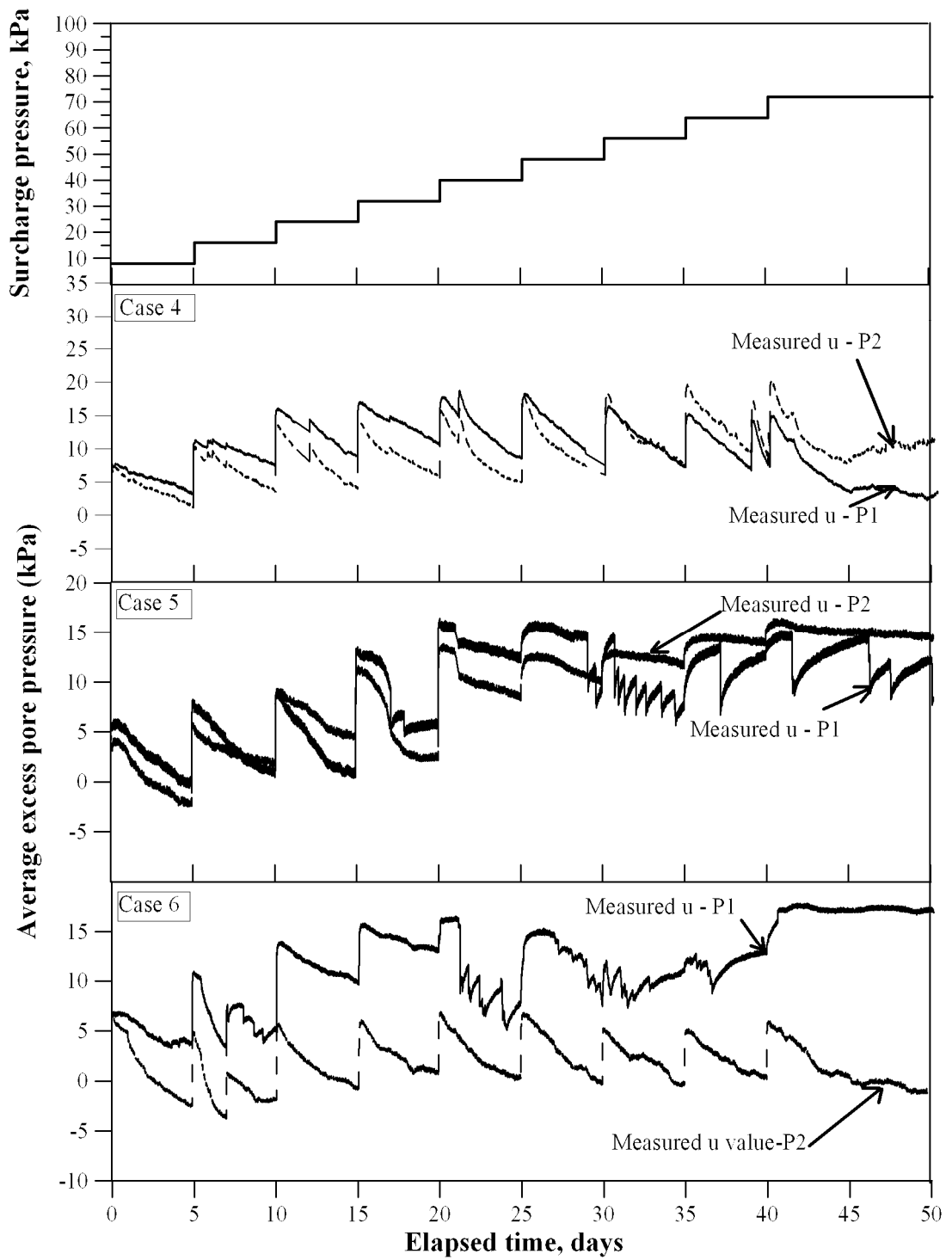


Fig. 5-7 Comparison between measured and predicted excess pore pressure of Cases 4, 5 and 6

Therefore, for Ariake clay, these values are corresponding to about 60%, 25% and 20% of the total applied load, and for dredged mud, these values are corresponding to about 30%, 21% and 24% of the total applied load. For Cases-1, 2, 4 and 5, the  $u$  values of  $P2$  are higher than that of  $P1$ . During the test, water leakage from the top surface of the model ground affected the consolidation process of the soil layer above the geocomposite, i.e., the top surface was not a perfect undrained boundary. Another point is that for Cases-2, 3 and Cases-5, 6 at the early stage, there are negative pore water pressures measured. The reason considered is due to the reaction of added lime or cement with water, which adsorbed certain pore water from the soil and caused certain suction pressure with a small magnitude, i.e. less than -5 kPa. To investigate the negative pore water pressure due to the effect of lime/cement during curing time, the treated soil was put into a chamber with a pore pressure transducer placed in the middle of it and the variation pore water pressure was monitored. The height of this chamber is about 0.7 m and excess pore water pressure was measured during curing time without applying any loading. The result of  $u$  values were shown in Fig. 5-8. As seen in this Figure, the negative excess pore pressures of Ariake clay treated with 4% of cement content were measured. The magnitude of the negative pore pressure is about -3 kPa.

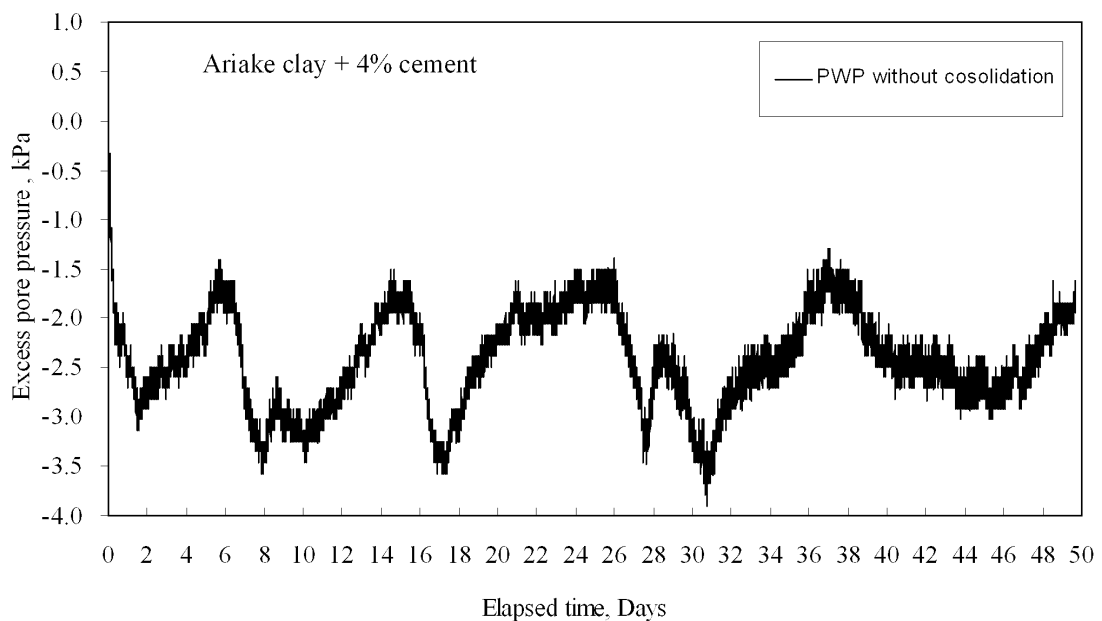


Fig. 5-8 Excess pore water pressure without consolidation during 50 days of curing time

#### 5.4.3. Undrained shear strength ( $s_u$ )

Figure 5-9 and 5-10 show the measured initial and final  $s_u$  values for both lime-/cement-treated Ariake clay and dredged mud. Both the initial and the final  $s_u$  values of the cases using the cement- and lime-treated soils are higher than that of the untreated soil (Cases-1 and 4). It is considered that the increase in  $s_u$  values for Cases-1 and 4 are due to the geocomposite induced

consolidation, but for Cases-2, 3, 5 and 6, the increase in  $s_u$  is the results of consolidation as well as cementation effect of the lime or cement added.

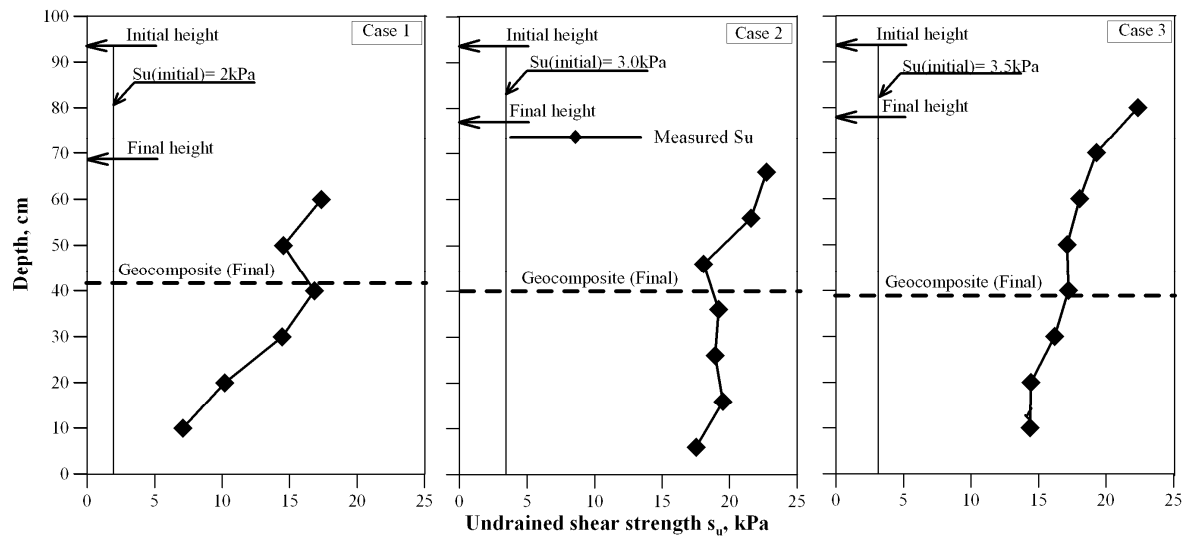


Fig. 5-9 Increase of undrained shear strength ( $s_u$ ) of Cases 1, 2 and 3

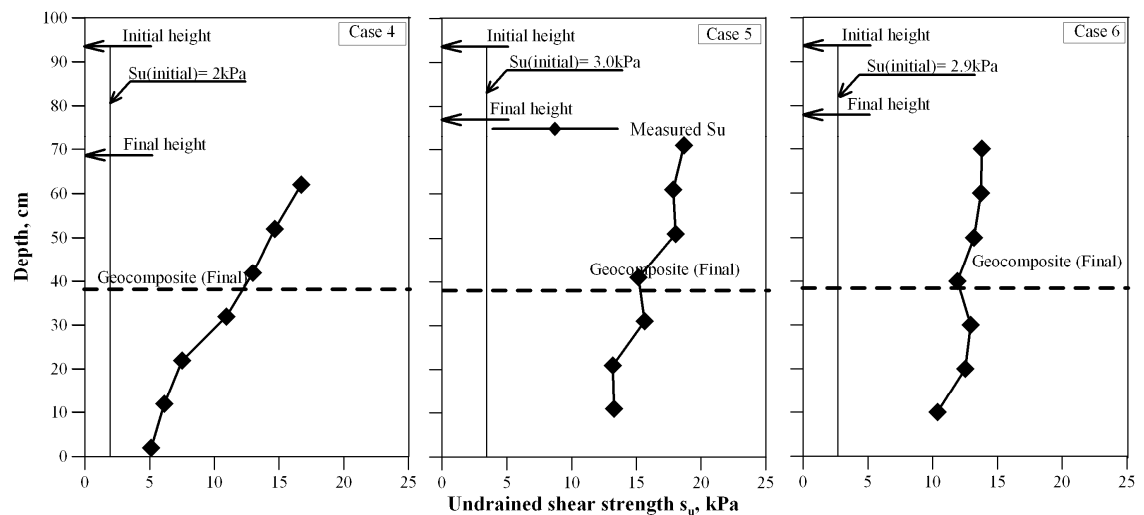


Fig. 5-10 Increase of undrained shear strength ( $s_u$ ) of Cases 4, 5 and 6

For all cases, the  $s_u$  values of the soil layer above the geocomposite are generally higher than that of the soil layer below the geocomposite. It is considered that the phenomenon is caused by partial drainage effect at the top surface as well as the friction between the soil and the wall of the model box.

Except the effect of drainage condition, the friction between the soil and the wall of the model box may be the cause for the measured  $s_u$  values reduced with depth. Although silicon grease was smeared on the wall, the soil/wall interface was not a friction free one. Direct shear tests were conducted for the interface between the soil and the grease painted steel plate. The direct shear box has a shear area of 0.2 m x 0.2 m. For the interface shear test, the upper box with a thickness of 50 mm was filled with the clay soil and the lower box was replaced by a steel plate (the same material for making the model box). The shear rate adopted was 2 mm/min. From the test results, an interface friction angle

of  $\delta \approx 3^\circ$  was obtained. Assuming lateral earth pressure coefficient at rest ( $K_0$ ) of 0.5, and considering the final thickness of the model ground of about 0.75 m, the interface friction can reduce the vertical consolidation stress of about 14 kPa at the bottom of the model.

From the results presented above, it can be seen that the geocomposite with about 1.0 m vertical spacing is effective for providing drainage path for partial consolidating saturated or close to saturated clayey soil during an embankment construction. Especially for using cement or lime lightly treated soil, the maximum pore water pressure generated in the model ground was only 20 – 30% of the applied load. Yasuhara et al. (2002, 2003) conducted model loading test on drainage geotextile reinforced clayey soil. They concluded that only the geotextile is not sufficient to provide drainage path for consolidating the clayey soil, and suggested to use sandwich arrangement: sandwich the geotextile within two sand layers. Chai and Miura (2002) also reported that the transmissivity of geotextile reduced significantly with elapsed time when confining it in clay. The model test results of this study show that for a geocomposite with drainage channels having high clay-confined discharge capacity, it can provide sufficient drainage capacity for consolidating clayey soil, and in this case there is no need to use the sandwich technique, which can simplify the construction procedure and therefore reduce the cost.

## 5.5 Summaries

Geocomposite induced consolidation and therefore strength increase of clayey soils with and without cement or lime additives have been investigated by laboratory large scale model (0.3 m x 0.6 m x 1.0 m) tests and analyses. Based on the results of the tests and the analyses, the following conclusions can be drawn.

1) *Effect of geocomposite on the degree of consolidation.* Geocomposite has a high confined in clay discharge capacity can be a sufficient drainage path for accelerating the consolidation rate of clayey soil. For the conditions adopted: loading rate of 1.6 kPa/day and geocomposite vertical spacing of about 1.0 m, at the end of loading, the average degree of consolidations were from 64 to 90%.

2) *Effect of combined cementation and consolidation.* Combination of light cement/lime treatment and using geocomposite can result in a denser (reduce void ratio and therefore increase density) and stronger embankment (increase undrained shear strength) with clayey fill material comparing with cases of cement/lime treatment alone without consolidation induced deformation.

## CHAPTER 6 UNDRAINED SHEAR STRENGTH

### 6.1 Introduction

To use saturated clayey soils with and without cement/lime treatment as construction material, one of important issues is predicting its undrained shear strength ( $s_u$ ) during and after construction. In case of combining lime/cement treatment and using dual function (reinforced and drainage) geocomposite (Chai et al., 2011), both the effect of cementation and consolidation on  $s_u$  value have to be considered. In this Chapter, the proposed method for predicting undrained shear strength ( $s_u$ ) will be discussed. The proposed method was applied to analyze laboratory large scale model tests and two case histories in Japan.

### 6.2 Unconfined compression test for cement/lime treated samples

#### 6.2.1. Equipment and specimen preparation

The load frame for unconfined compression test is shown in Fig. 6-1. Vertical displacement is measured by a LVDT. The strain rate is 1%/min.

The procedure for specimen preparation is explained in Chapter 3. The mixed soils were put in disposable plastic molds which is 50 mm in diameter and 100 mm in height. Soils were put layer by layer and possible entrapped air was eliminated by lightly beating the molds. The top and bottom of the mold were then covered with vinyl plastic sheets to prevent moisture loss. Finally, the samples were cured in a room with temperature of  $20\pm 2^\circ\text{C}$  and humidity of 70%. The tests were conducted according to JIS A1216-2009.

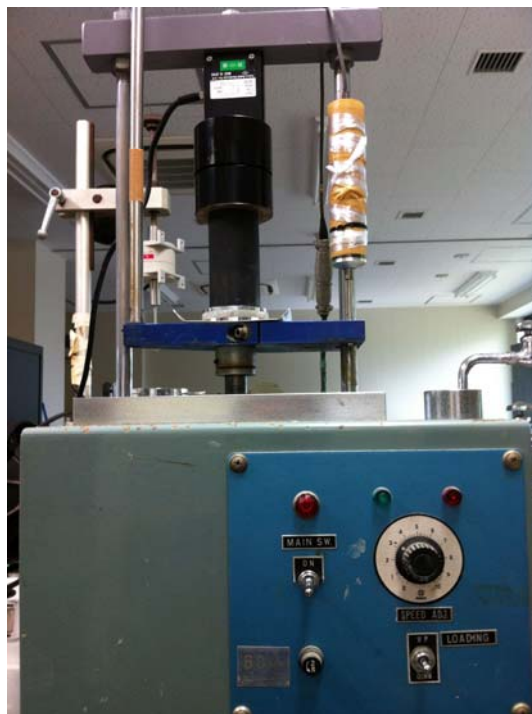


Fig. 6-1 Unconfined compression apparatus

### 6.2.2. Test results

The stress-strain curves for the samples cured for 28 days are given in Figs. 6-2 and 6-3 for the dredged mud and the Ariake clay, respectively. It can be seen that the unconfined compression strength ( $q_u$ ) values of the lime-treated soils are much higher than that of the cement-treated soils. For the lime-treated specimen, the initial stiffness increased with the amount of the lime added, but the failure strain was not changed much with a value of about 3 – 4%. However, for the cement-treated soils, the behavior changed from ductile to brittle when the amount of the cement added increased from 2 to 16%.

Furthermore, when the cement additive is less than 4% or 2% for lime content, there are obvious changes in particle size distribution (Fig. 3-7 in Chapter 3) but insignificant change in the  $q_u$  values of the samples.

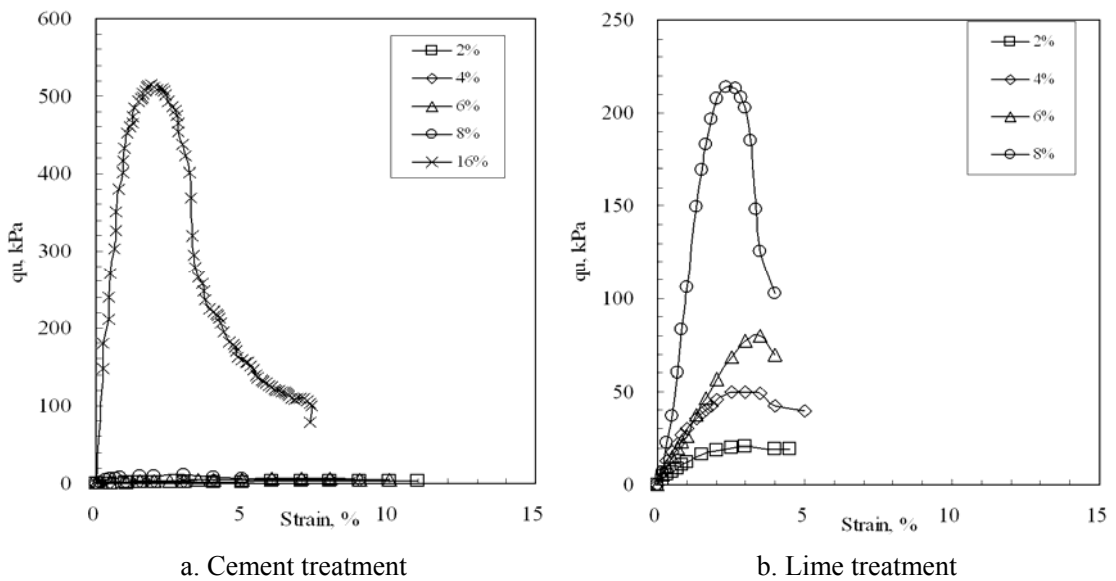


Fig. 6-2 Unconfined compressive strength curves of the dredged mud with curing time of 28 days

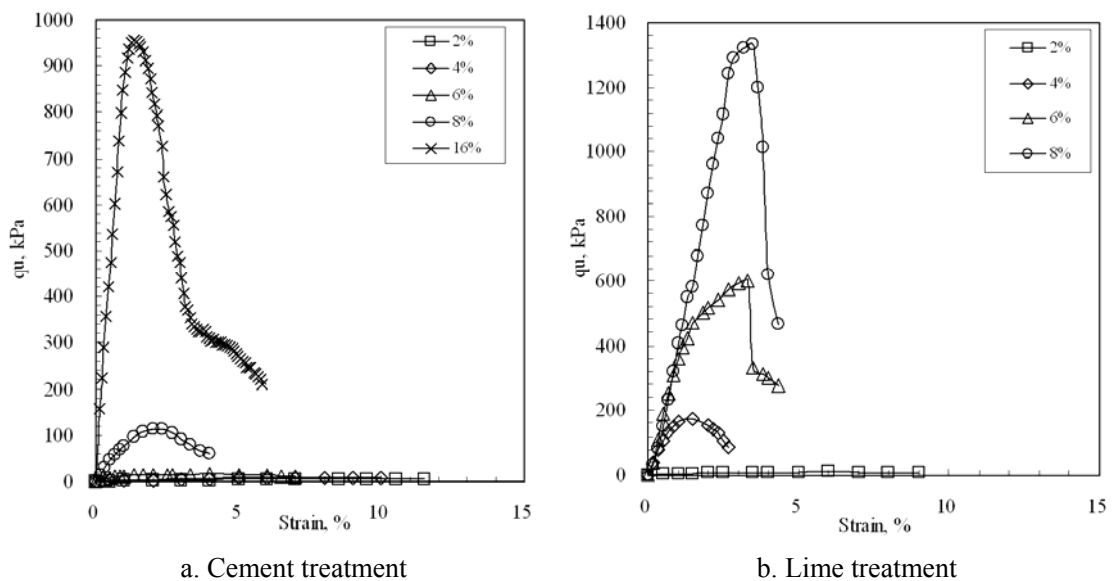


Fig. 6-3 Unconfined compressive strength curves of the Ariake clay with curing time of 28 days



Several previous researchers (Bergado et al. 1996; Tang et al. 2001) reported that the relationship between  $q_u$  and cement or lime content is linear. However, less than 16% of cement or lime treatment, the relationship is non-linear as shown in Figs. 6-4 and 6-5. It is shown that improvement is not effective when adding 2% of lime or 4% of cement. A possible reason is due to the higher organic content of the soils tested (Table 3-1 in Chapter 3). Humic substances such as humic acid are principal components of organic materials in high organic content soils. With the presence of humic acid, when lime or cement is added, the lime or cement may react with the humic acid, and may obstruct the dissolved silica ( $\text{SiO}_2$ ) and alumina ( $\text{Al}_2\text{O}_3$ ) in clay to react with the calcium hydroxide ( $\text{Ca}(\text{OH})_2$ ). Consequently, the cementing products such as calcium silicate hydrate (CSH), calcium aluminate silicate hydrates (CASH) and calcium aluminate hydrates (CAH) may not be formed and thus the strength of lime and cement treated soils will be low. With further increase of the amount of lime and/or cement, the strength of the treated soil is increased.

As shown in Figs. 6-6 and 6-7, the  $q_u$  values of the treated Ariake clay are about 7 times of those of the treated dredged mud at a cement content of 8%. However, with the lime treatment, the strengths of the treated Ariake clay are only 3 times of those of the treated dredged mud with a lime content of 8%. But, the strengths of the samples with 2% cement are almost the same as that of 2% lime treated samples. The results also clearly indicate that the  $q_u$  values increased rapidly for curing time less than 28 days.

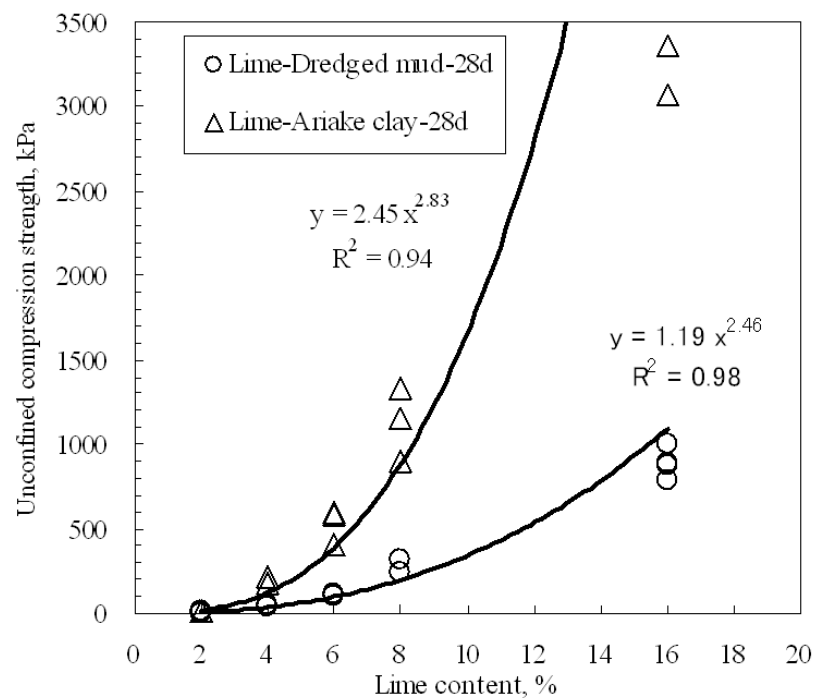


Fig. 6-4 Non-linear relationship between unconfined compression strengths vs. lime content

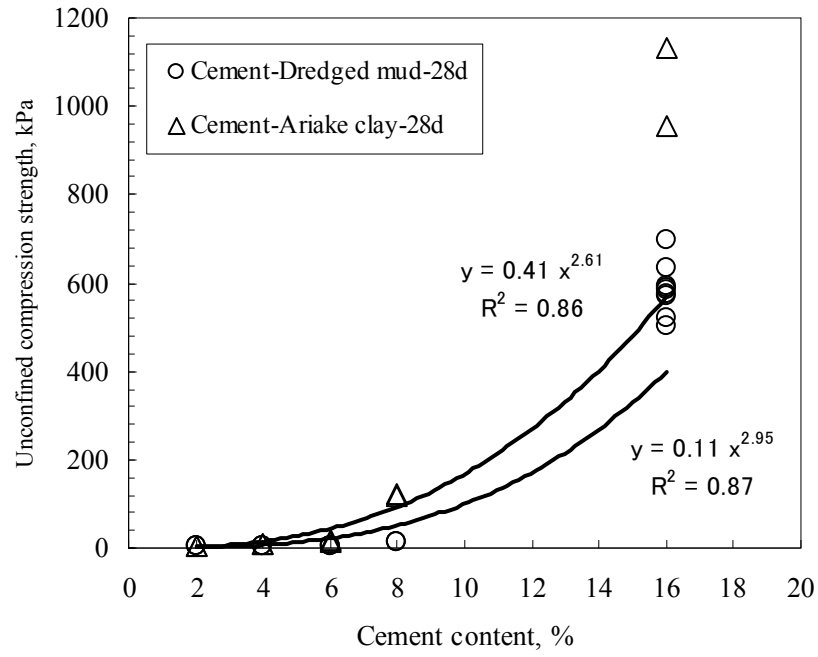


Fig. 6-5 Non-linear relationship between unconfined compression strengths vs. cement content

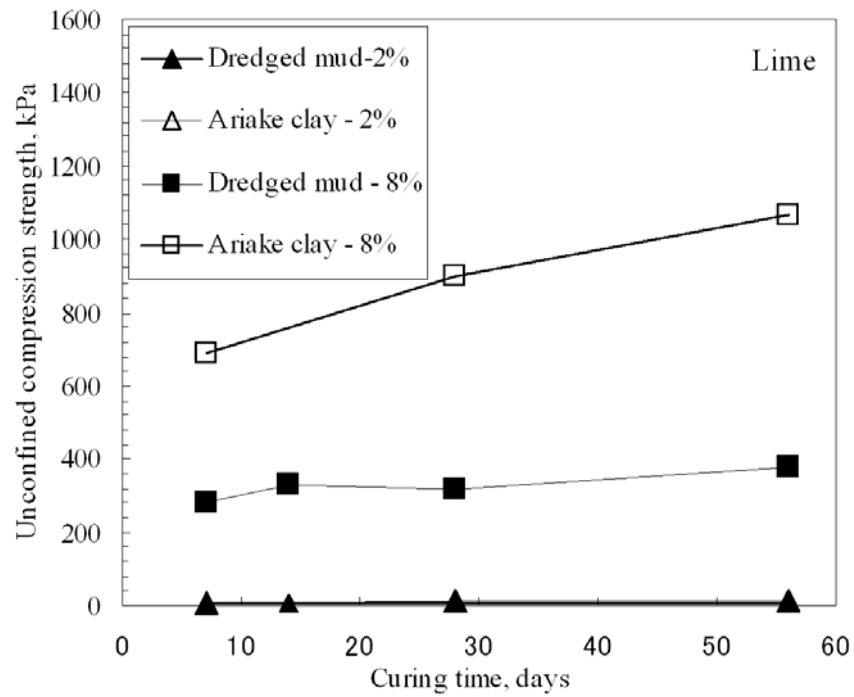


Fig. 6-6 Unconfined compression strengths vs. curing time of lime treated soils

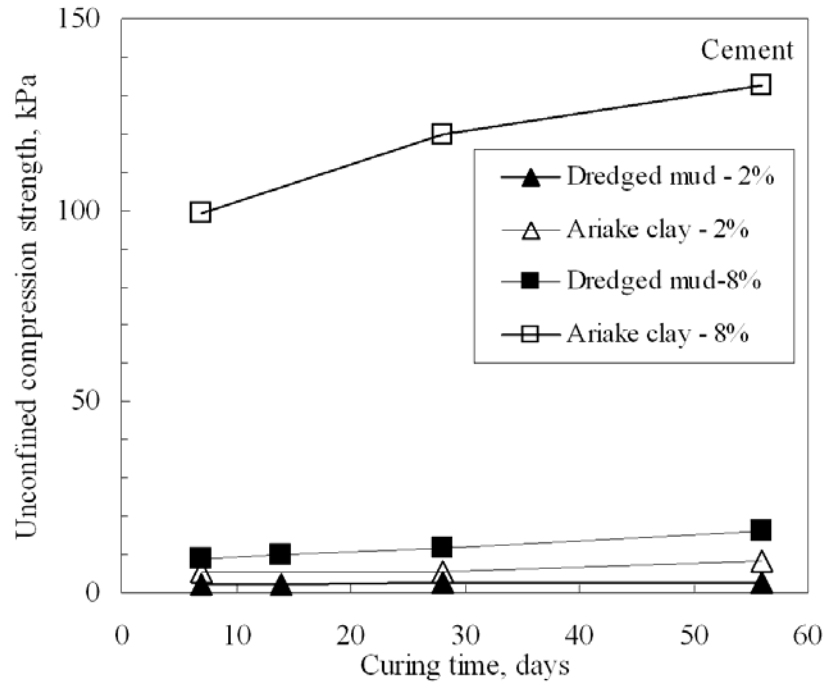


Fig. 6-7 Unconfined compression strengths vs. curing time of cement treated soils

### 6.2.3. Correlation between $q_u$ and admixture water-lime ratio

Figures 6-8 and 6-9 show the correlation between  $q_u$  (28 days) and admixture water - lime ratio ( $wc/c$ ). The relationship of  $q_u$  vs.  $wc/c$  is non-linear.  $wc/c$  is defined as the ratio of the percentage of measured water content of admixture with curing time of 28 days,  $wc(\%)$ , divided by the percentage of cement/lime added,  $c(\%)$ .

Gallavresi (1992) proposed that  $q_u$  may be correlated to admixture water-cement ratio by the relationship:

$$q_u = \frac{q_o}{(wc/c)^n} \quad (6-1)$$

in which  $q_o$  and  $n$  are experimentally fitted values.

In this research, this empirical equation was applied for lime treated clayey soils and the  $q_u$  -  $wc/c$  relationships were also shown in Figs. 6-8, 6-9, 6-10 and 6-11. When applying Eq. (6-1) to the cases tested, the fitted  $q_o$  and  $n$  values are summarized in Table 6-1.

Table 6-1 Summary of fitted values in Eq. 6-1.

Additive		$q_o$ (kPa)	$n$
Dredged mud	Lime	596,892	2.63
	Cement	75.9	0.8
Ariake clay	Lime	7.10 <sup>6</sup>	3.4
	Cement	10531	1.86

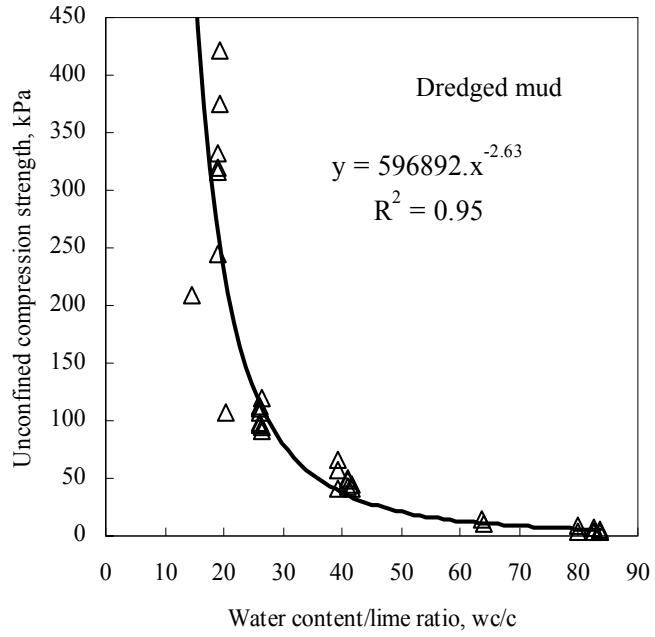


Fig. 6-8  $q_u - w_c/c$  relationship of lime treated dredged mud

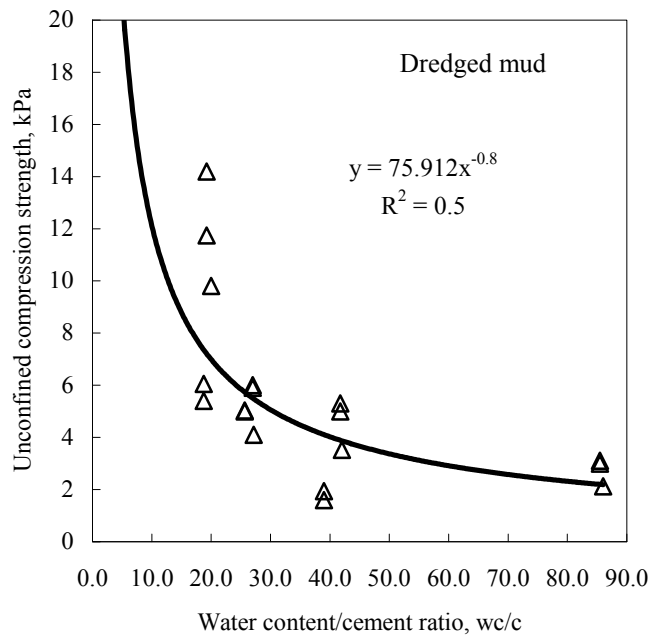


Fig. 6-9  $q_u - w_c/c$  relationship of cement treated dredged mud

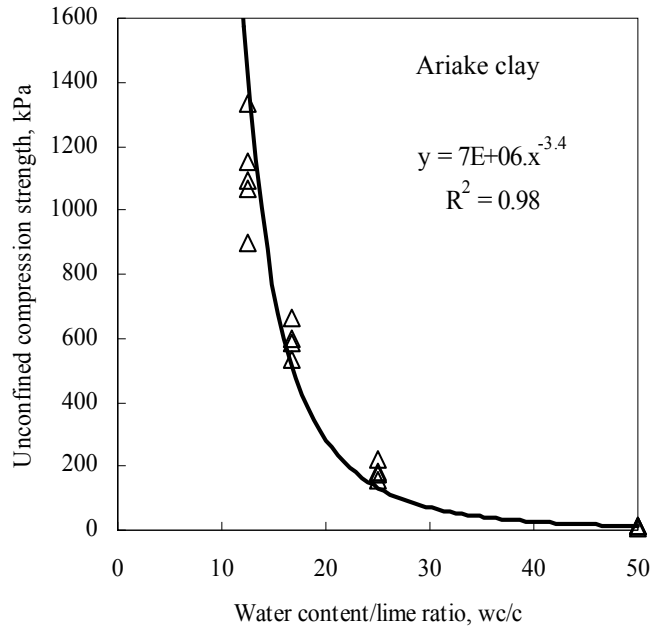


Fig. 6-10  $q_u - w_c/c$  relationship of lime treated Ariake clay

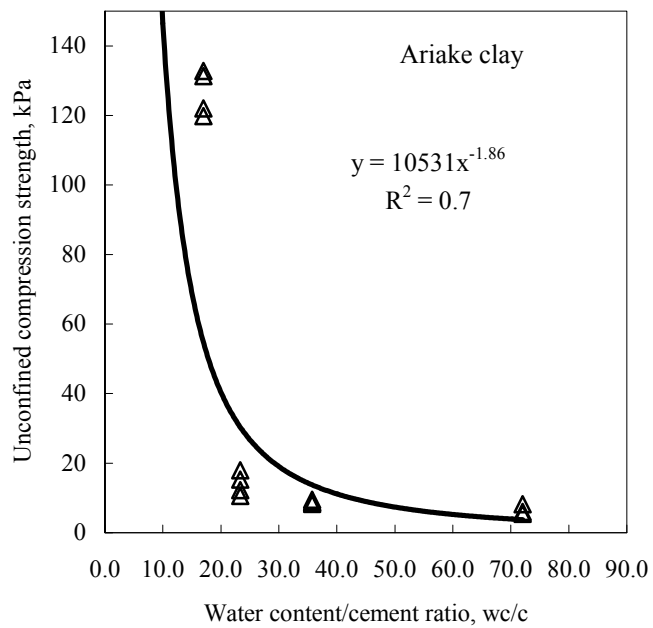


Fig. 6-11  $q_u - w_c/c$  relationship of cement treated Ariake clay

For two clayey soils, based on the unconfined compression test results, undrained shear strength ( $s_u$ ) of lime/cement lightly treated soils (4% cement or 2% lime) is approximately 5kPa. If we assume effective friction angle of about  $30^\circ$ , total unit weight of about  $13\text{kN/m}^3$ . The critical height that the treated soils can self-stand is about 1.3m. We believe  $s_u = 5\text{kPa}$  is strong enough for transportation, and this value is suggested as a criterion.

### 6.3 Predicting undrained shear strength ( $s_u$ )

Considering a scenario of constructing an embankment with saturated clayey fill, a method for predicting  $s_u$  values during and after the embankment construction is explained in the following section.

#### 6.3.1. Method for predicting excess pore pressure ( $u$ )

In case of using strip type geocomposite, as shown in Fig. 6-12, the horizontal and vertical spacing between geocomposite strips may not equal and the influencing area of a strip may be a rectangle. It is proposed to represent the rectangle area by a circle area (unit cell) under the condition of equal area (Chai et. al., 2011) and using Hansbo (1981)'s solution without considering smear effect (all soil is in a remolded state) to calculate average degree of consolidation ( $U$ ):

$$U = 1 - \exp\left(\frac{-8T}{\mu}\right) \quad (6-2)$$

$$T = \frac{c_v t}{D_e^2} \quad (6-3)$$

$$\mu = \ln \frac{D_e}{d_w} - \frac{3}{4} + \pi \frac{2l^2 k}{3q_w} \quad (6-4)$$

where  $c_v$  is the vertical coefficient of consolidation,  $t$  is elapsed time,  $k$  is the hydraulic conductivity of clayey soil,  $l$  is drainage length,  $D_e$  is the diameter of the unit cell,  $d_w$  is the equivalent diameter of a geocomposite strip, and  $q_w$  is the discharge capacity of a geocomposite strip.

In case of continuous geocomposite, the plain strain unit cell consolidation theory (Hird et al., 1992; Chai and Miura, 2002) can be used to calculate  $U$  value; the expressions for  $T$  and  $\mu$  in Eq. (6-2) are as follow:

$$T = \frac{c t}{4B^2} \quad (6-5)$$

$$\mu = \frac{2}{3} + \frac{4kl^2}{3q_{wp}B} \quad (6-6)$$

where  $B$  is the half of the space between two plane strain geocomposite sheets, and  $q_{wp}$  is the discharge capacity of a geocomposite per unit width.

During an embankment construction, backfill is placed layer by layer. To predict the vertical effective stress variation in each soil layer, the following assumptions are made (Chai and Miura, 2002):

a) Approximate the construction process by stepwise loads (Fig. 6-13).

b) For a given soil layer, take the total load at  $i$  step as  $p_i$ , and the degree of consolidation at time  $t_i$  as  $U_i$ . At  $t_i$ , incremental load of  $j$  step  $\Delta p_j$  is applied. Then for a total load  $p_j = p_i + \Delta p_j$ , the degree of consolidation ( $U_{j0}$ ) at  $t_i$  will be:

$$U_{j_0} = \frac{U_i \cdot p_i}{p_i + \Delta p_j} \quad (6-7)$$

Then, an imaginary time corresponding to  $U_{j_0}$  (under load  $p_j$ ) for geocomposite strip case is:

$$t_{j_0} = -\frac{D_e^2}{8 \cdot c_h} \mu \cdot \ln(1 - U_{j_0}) \quad (6-8a)$$

and for continuous geocomposite sheet case is:

$$t_{j_0} = -\frac{B^2}{2 \cdot c_h} \mu \cdot \ln(1 - U_{j_0}) \quad (6-8b)$$

From  $t_i$ , for a time increment of  $\Delta t$ , i.e. at time  $t_i + \Delta t$ , the time for predicting the degree of consolidation using Eqs. (6-2), and (6-3) (or (6-5)) will be  $(t_{j_0} + \Delta t)$ . When the average degree of consolidation at given time ( $t$ ),  $U(t)$ , is known, the average effective vertical stress,  $\sigma'_v(t)$  value can be easily calculated.

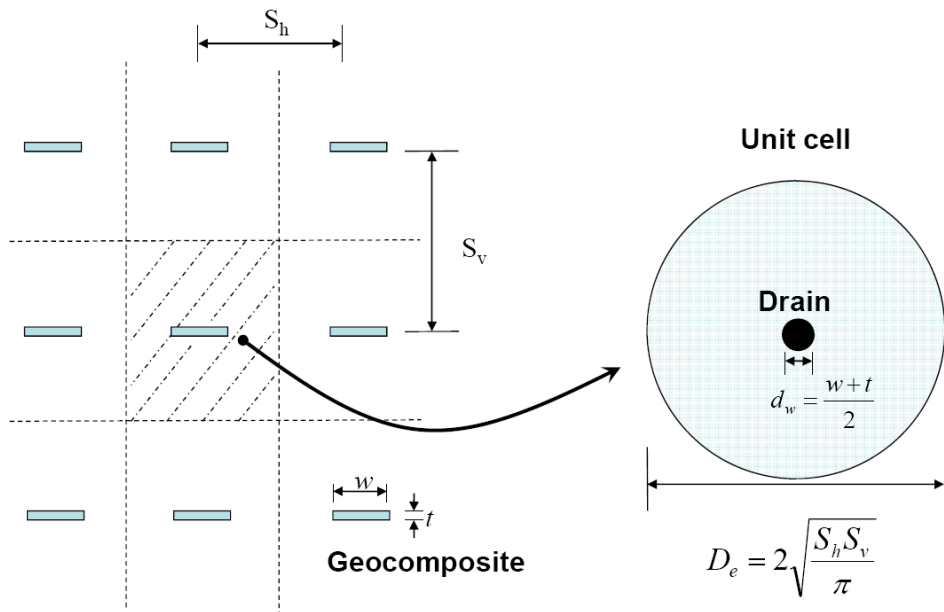


Fig. 6-12 Unit cell model (Chai et. al., 2011)

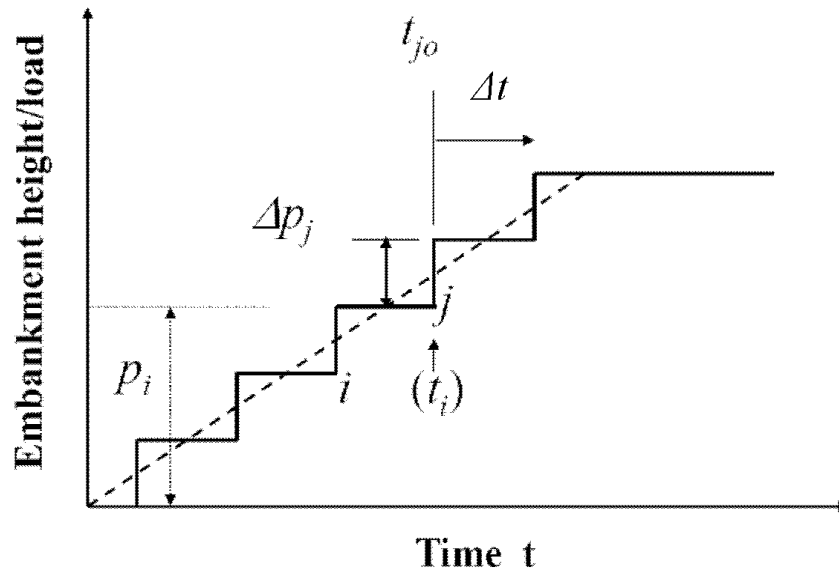


Fig. 6-13 Stepwise loading (Chai and Miura, 2002)

### 6.3.2. Method for predicting $s_u$ value

For simplicity, it is proposed to use Ladd's (1991) equation to predict the undrained shear strength (including the initial value) due to consolidation effect ( $s_{u1}$ ).

$$s_{u1} = S \cdot \sigma'_v \cdot OCR^m \quad (6-9)$$

where  $\sigma'_v$  is vertical effective stress,  $OCR$  is overconsolidation ratio, and  $S$  and  $m$  are constants. Ladd (1991) proposed that range for  $S$  is 0.162 to 0.25 and for  $m$  is 0.75 to 1.0. For embankment construction, using clayey soil without compaction within the embankment,  $OCR \approx 1.0$  can be used. Then if  $\sigma'_v$  is known, the only parameter value needs to be determined is  $S$ .

In case of using cement- or lime-treated soil before the completion of pozzolanic reaction of cement or lime with water/soil, there will be strength increase due to the cement or lime induced cementation effect during the consolidation process. The consolidation and cementation effects will develop together and may influence each other. Generally, consolidation may enhance the cementation effect and the cementation may hinder the deformation caused by consolidation. Nevertheless, for simplicity we assume that for cement or lime lightly treated soils, the consolidation and cementation effects can be evaluated separately. It is proposed that undrained shear strength increase due to the cementation effect ( $s_{u2}$ ) can be evaluated using cement- or lime-treated samples without consolidation but cured for about 4 weeks.  $s_{u2}$  can be measured by unconfined compression test or laboratory vane shear test, whichever is convenient to be used. Based on the results of unconfined compression strength and therefore, empirical equation (6-1),  $s_{u2}$  can be calculated as follow:

$$s_{u2} = \frac{q_u}{2} = \frac{q_o}{2(wc/c)^n} \quad (6-10)$$



Then the total undrained shear strength ( $s_u$ ) will be:

$$s_u = s_{u1} + s_{u2} \quad (6-11)$$

Note as a general tendency, using Eq. (6-11) tends to over-estimate  $s_{u1}$  value (due to consolidation) if the constants  $S$  and  $m$  are calibrated from the untreated soil, and underestimate  $s_{u2}$  value (due to cementation). For the cases investigated, the amount of the cement or lime used was small, and for total undrained shear strength, Eq. (6-11) resulted in an acceptable result. However, with the increase of the amount of cement or lime, Eq. (6-11) has to be used in caution.

### 6.3.3. Application of proposed method on laboratory large scale model test

The values of parameters for predicting the pore water pressure variations of the model tests are summarized in Table 6-2. As seen in Figs. 6-14 and 6.15, the agreement between the measured and calculated  $u$  values of Cases-1 and 4 are good, but for Cases-2, 3 for lime-/cement-treated Ariake clay and Cases-5, 6 for lime-/cement-treated dredged mud, there are differences. Cases-2, 3 and 5, 6 used cement or lime lightly treated clayey soils, the reactions between the soil and the cement or lime influenced the generation and dissipation of the pore water pressures. Pozzolanic effect tends to reduce the generation of positive pore water pressure, and hardening (cementation) effect tends to increase the coefficient of consolidation of the soil and then increase the rate of pore water pressure dissipation. All these effects can not be considered by the calculation method adopted. Being mentioning these factors, we consider that the predictions resulted in acceptable results.

Table 6-2 Geocomposite and soil parameters used for predicting the behavior of the model tests

Parameter	Units	Value					
Geocomposite							
Width of geocomposite, $w$	mm	150					
Thickness of geocomposite, $t_g$	mm	5.5					
Discharge capacity, $q_w$	m <sup>3</sup> /yr/m	25,000					
Length of geocomposite, $l$	m	0.6					
Vertical spacing, $S_v$	m	1.0					
Horizontal spacing, $S_h$	m	0.3					
Soil parameters		Case-1	Case-2	Case-3	Case-4	Case-5	Case-6
Coef. of horizontal consolidation, $c_v$	M <sup>2</sup> /yr	1.6	4.0	5.0	3	6	6
Vertical permeability, $k_v$	m/s	7.3x10 <sup>-10</sup>	9.3x10 <sup>-10</sup>	9.5x10 <sup>-10</sup>	7x10 <sup>-10</sup>	1.1x10 <sup>-9</sup>	1.1x10 <sup>-9</sup>

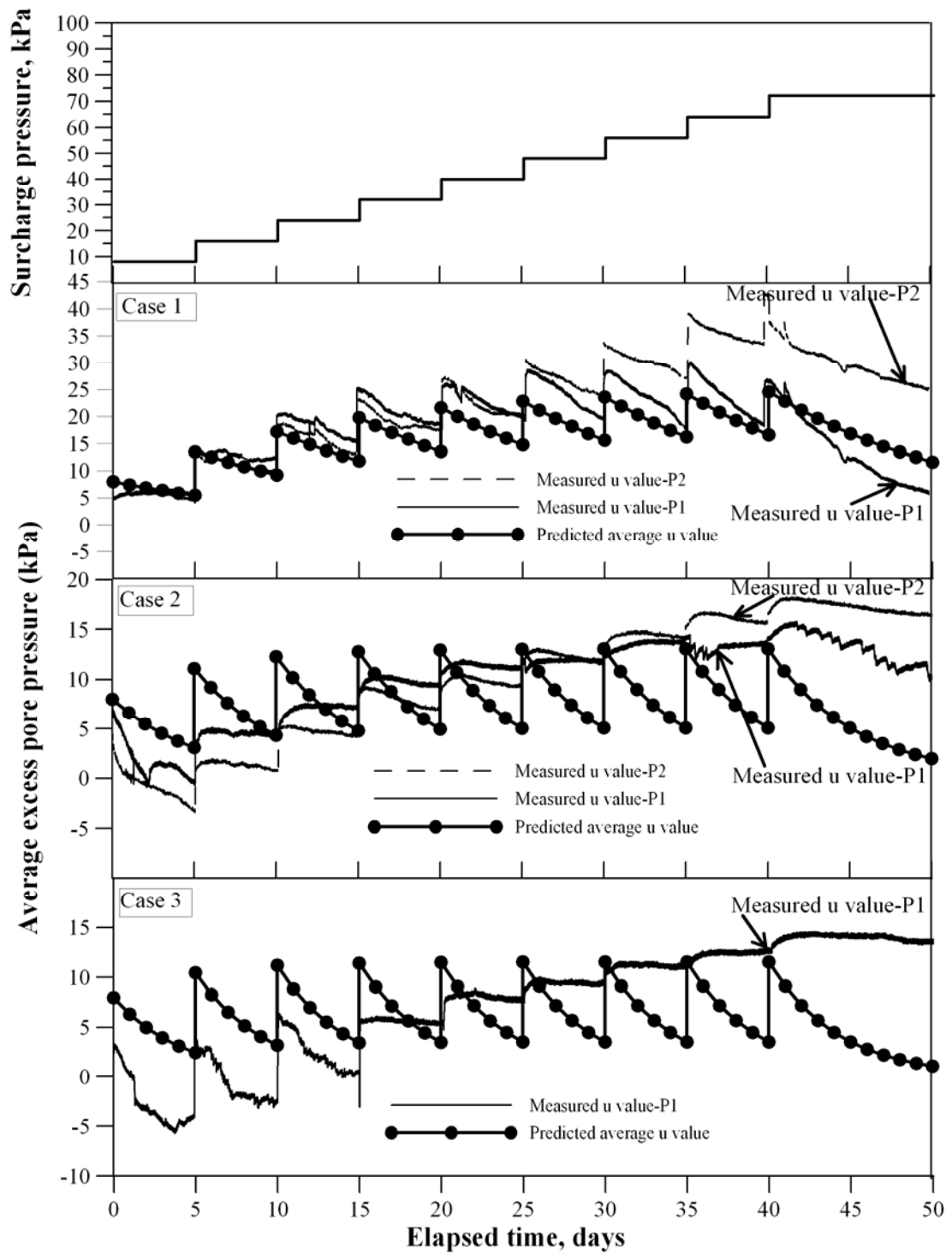


Fig. 6-14 Comparison between measured and predicted excess pore pressure of Cases 1, 2 and 3

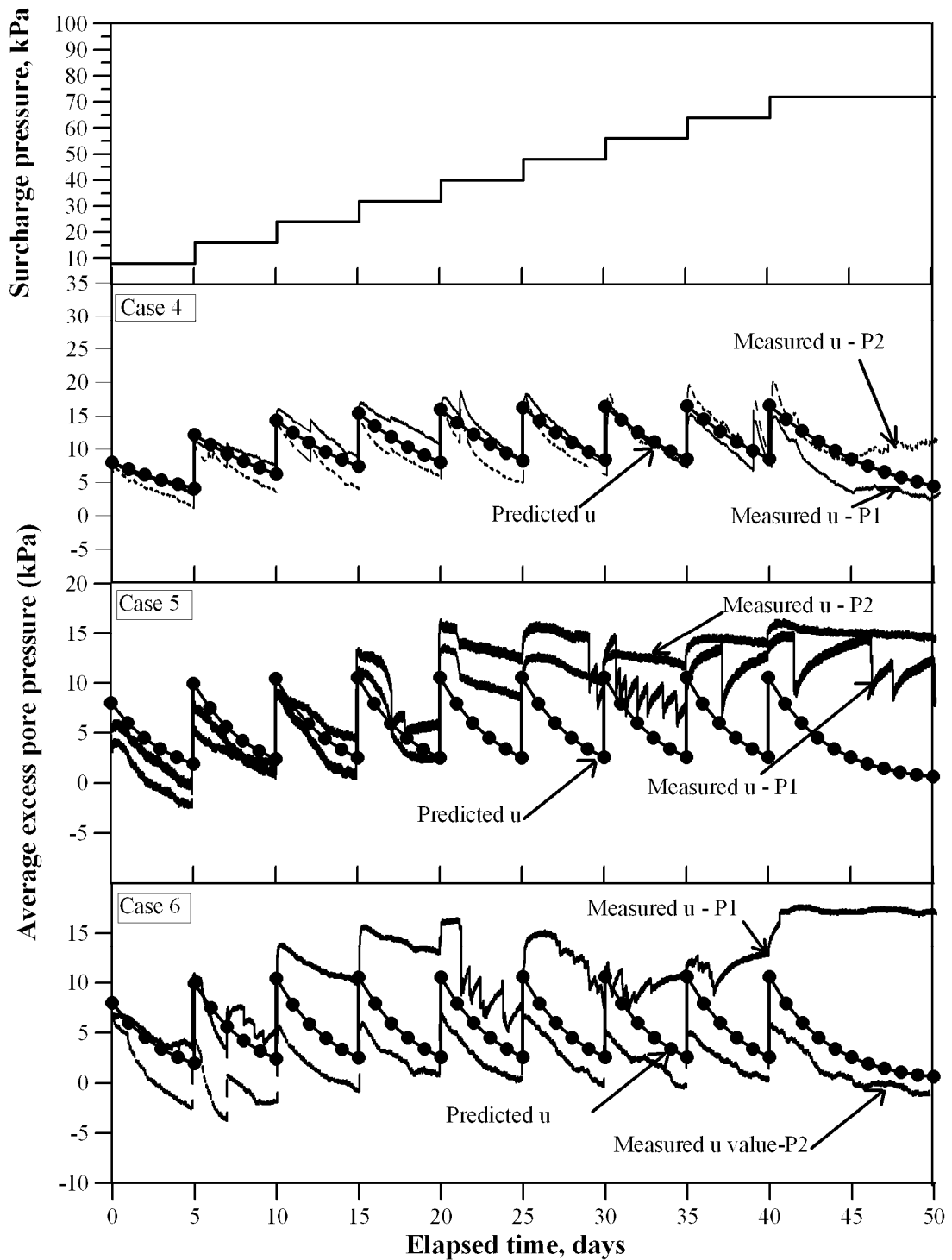


Fig. 6-15 Comparison between measured and predicted excess pore pressure of Cases 4, 5 and 6

With the predicted average  $u$  values, the  $s_u$  values calculated by Eq. (6-9) as well as Eq. (6-11) are plotted in Fig. 6-16 and 6-17. In the calculation, the average degree of consolidation was used, but the effect of the friction on the vertical consolidation pressure was considered by assuming an interface friction angle  $\delta \approx 3^\circ$ , and  $K_o = 0.5$ . The back estimated  $S$  value in Eq. (6-9) is 0.23. For six cases tested, at the end of the tests, the calculated average degree of consolidations is from 70 to 90%. As discussed previously, the drainage boundary condition for the soil layer below the geocomposite is

close to the field case and the comparison is made for this soil layer only. The agreement between the measured and calculated values is fair.

To investigate approximately the relative importance of the cementation effect and the consolidation effect, soil samples for unconfined compression test were prepared using the cement and the lime lightly treated soils with the same conditions as for making the model grounds, and cured for about 8 weeks without consolidation. For Ariake clay, the cement- and lime-treated samples resulted in unconfined compressive strength ( $q_u$ ) of about 9.5 and 12.4 kPa or  $s_u$  value of about 4.8 and 6.2 kPa, respectively. For dredged mud, the  $s_u$  values of cement- and lime-treated samples about 5.0 and 4.0 kPa, respectively. Considering the initial  $s_u$  values of the model grounds of Cases-2, 3 and 5, 6, under the condition that the density of the soil is not changed, the increments on  $s_u$  value due to the cementation effect are about 1.8, 2.7 kPa and 2.0, 1.1 kPa, respectively. Therefore, for Cases-2, 3 and 5, 6, it is considered that the increase of  $s_u$  value is mainly due to the effect of consolidation (more than 75%).

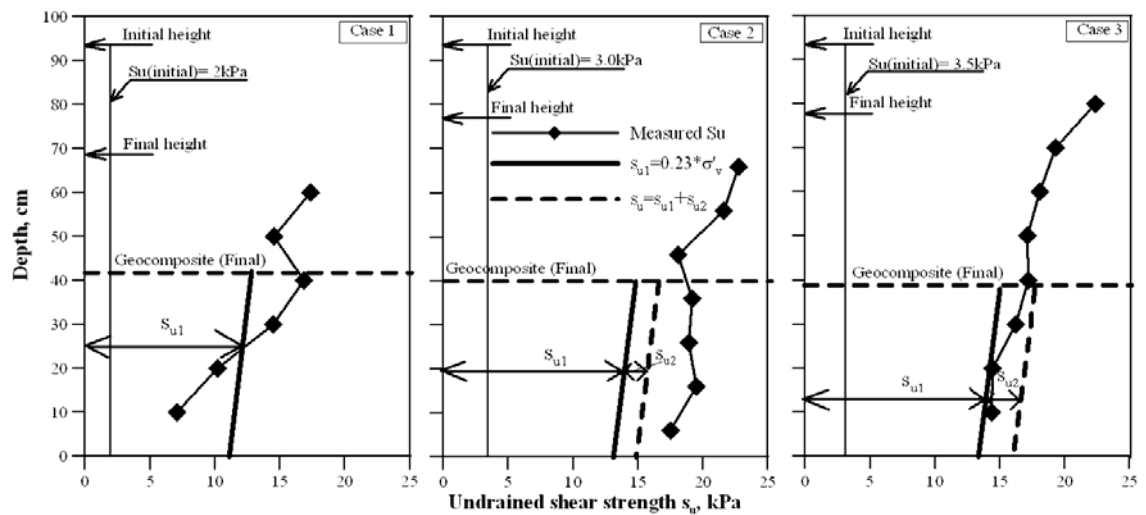


Fig. 6-16 Increase of undrained shear strength ( $s_u$ ) of Cases 1, 2 and 3

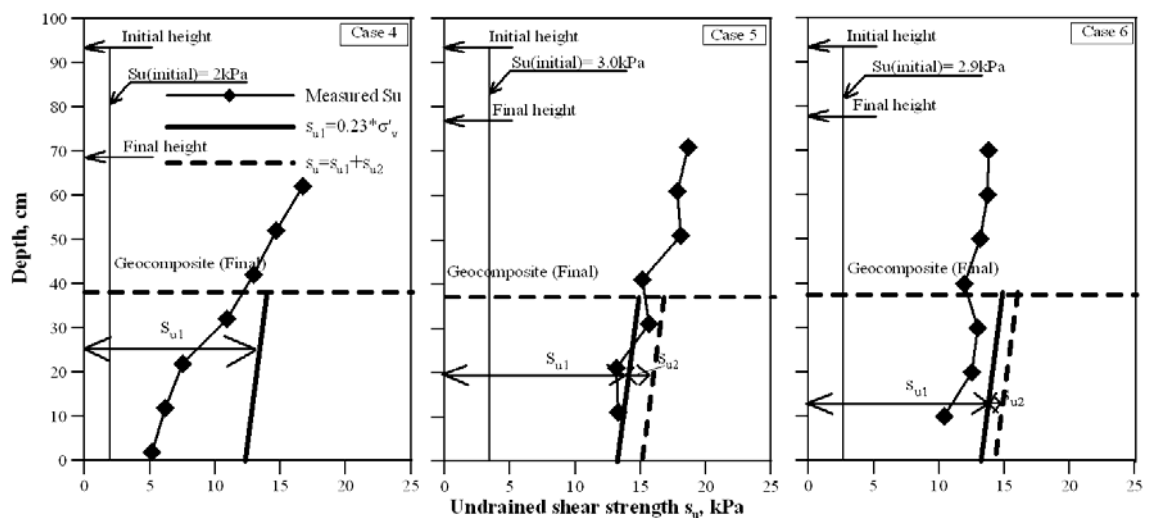


Fig. 6-17 Increase of undrained shear strength ( $s_u$ ) of Cases 4, 5 and 6

## 6.4 Analyzing case histories

### 6.4.1. Brief description of case histories

There are several cases in Japan that embankments were successfully constructed with clayey backfill with geocomposites such as Noto Airport (Nagahara et al., 2000) and Shizuoka airport (Tatta et al., 2003) and a case history reported by Inagaki et al. (2000). First case (Case A) analyzed here is one of the embankments at Noto Airport, Japan. Noto Airport is located at about 10 km from Wajima city, Ishikawa Prefecture, and the site was not flat and for constructing the airport, large amount of earthwork was required, which includes a 35 m height embankment construction. Due to the availability of the local fill material, the clayey sand or sandy clay with high water content was used as fill material. To accelerate the self-weight induced consolidation process of the fill material, drainage/reinforcement geocomposite was used (Nagahara et al., 2000; personal communication with M. Ito at Maeda Kosen Co. Ltd. Japan, 2012). Another case history (Case B) relating to a large-scale embankment construction is carried out at Shizuoka airport. The height of embankment is about 36 m using horizontal geocomposite for drainage for lower part of the embankment and 9 m thick upper embankment without using geocomposite. The embankment also used high water content soil available at the local area as backfill material. The horizontal drainage material was used to accelerate the self-weight induced consolidation and improve the stability of the embankment (Tatta, N. et al., 2003).

The cross section of the embankment of Case A is shown in Fig. 6-18. Totally, 12 layers of geocomposite were installed. For the zones at the right side of *A-A* line (Z-1b and Z-S1 to Z-S6) in Fig. 6-18, the vertical spacing ( $S_v$ ) of the geocomposites was about 2.5 m. Five layers of geocomposites were extended 15 m into the embankment from *A-A* line and had a  $S_v$  value of about 5.0 m. The plan layout of the geocomposites is illustrated in Fig. 6-19. The geocomposite had a width of about 0.3 m, and horizontal spacing  $S_h$  of 2.0 m. For Case B, the cross section of embankment is shown in Fig. 6-20. The arrangement of the geocomposites is described in Fig. 6-21. There are 6 layers of geocomposite were installed. The improved zone was divided into 8 zones, namely Z-T1 to Z-T8. The properties of geocomposite used are similar with that of first Case A. But the  $S_v$  and  $S_h$  values as shown in cross section 2 - 2 in Fig. 6-21 are 5.0 m and 2.0 m, respectively. Using a 0.3 m wide strip sample, the tensile strength was 9.0 kN and failure strain of about 10%. The manufacturer reported discharge capacity ( $q_w$ ) is about 933 m<sup>3</sup>/year under confining pressure up to 200 kPa. It is generally agreed that the field discharge capacity ( $q_w$ ) is lower than laboratory value due to the effects of confining condition, elapsed time and deformation of the drain. However, regarding to how much reduction needs to be applied on a laboratory value for design, there are different reported numbers. Bergado et al. (1996) proposed a factor of about 9, while Chai et al. (2004) reported that the reduction of  $q_w$  value with elapsed time is strongly related to the hydraulic radius ( $R$ ) of the drainage channel. For  $R > 0.5$  mm and for all prefabricated vertical drains (PVDs) and prefabricated horizontal drains (PHDs) tested,  $q_w$  value after 3 months elapsed time is more than 30% of corresponding initial value, e.g. a reduction factor of less than about 3. The confining pressure used in the laboratory test was relatively high and since there is no

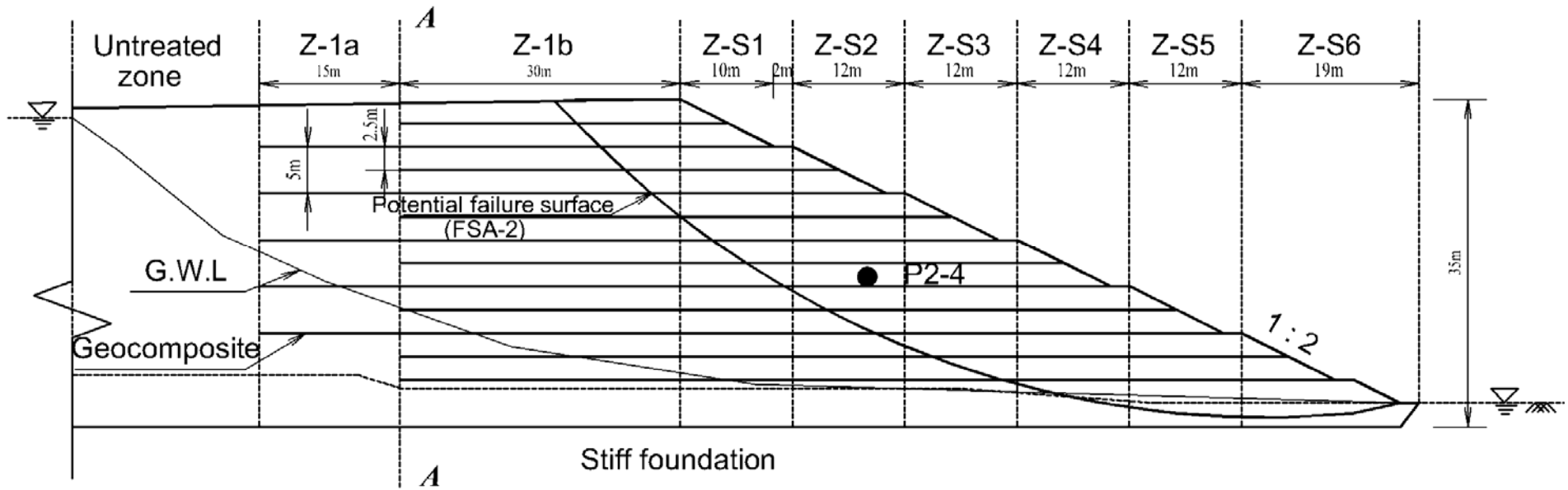


Fig. 6-18 Cross section of embankment of Case A

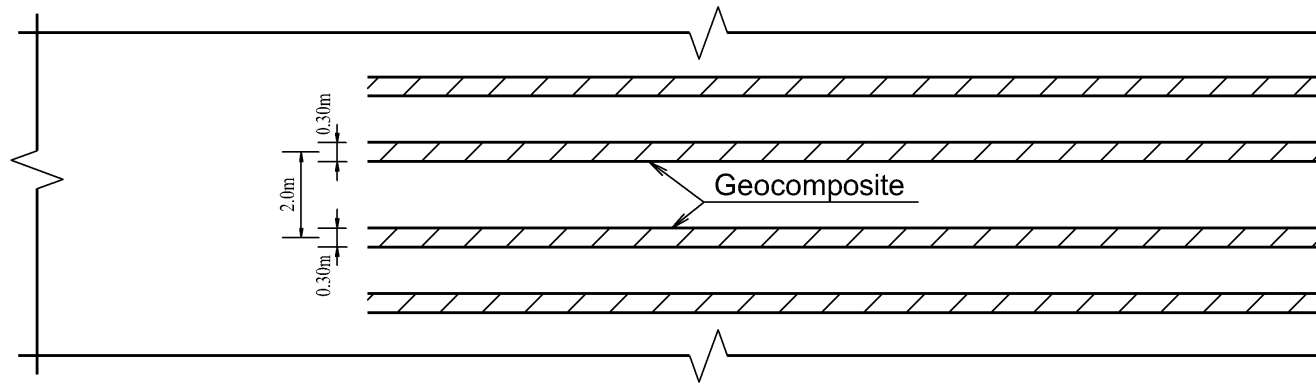


Fig. 6-19 Layout of geocomposite of Case A

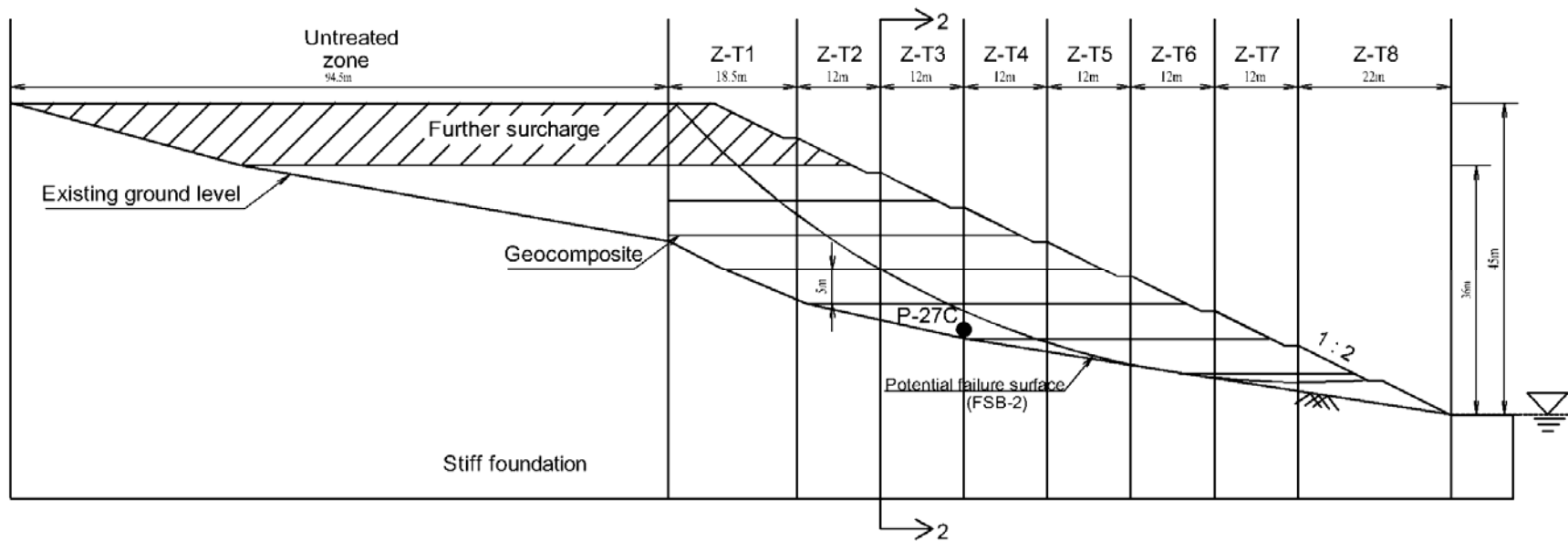


Fig. 6-20 Cross section of embankment of Case B

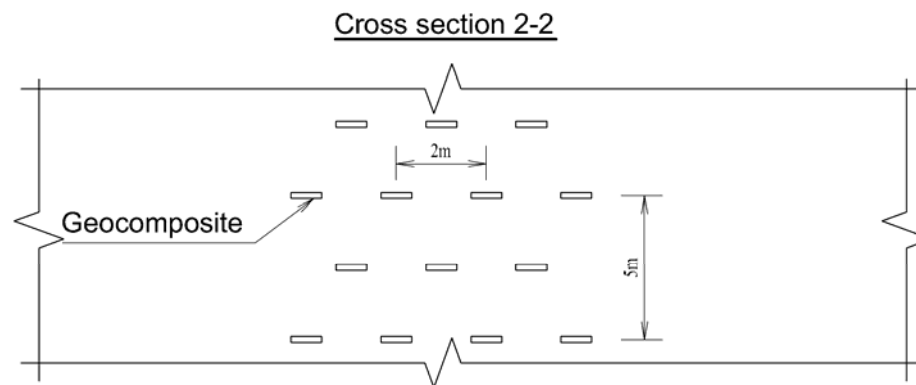


Fig. 6-21 Arrangement of geocomposite of Case B

long-term confined in clay test data available, a reduction factor of 4 was arbitrarily assumed, i.e.  $q_w = 233 \text{ m}^3/\text{year}$  was adopted in the analysis.

The basic properties of the backfill are listed in Table 6-3. In the table, the initial void ratio ( $e_o$ ) was calculated from  $w_n$  and  $\gamma_t$  assuming the specific gravity of the soil particles of 2.7. For Case A, the compacted fill had a unit weight of about  $15.5 \text{ kN/m}^3$  and cone resistance of less than  $600 \text{ kN/m}^2$ . The data in Table 6-3 indicate that the compacted backfill was in an partial saturated state with a degree of saturation of 86 ~ 98%. The average construction rate was about 0.27 m/day. There was a piezometer, P2-4 (see Fig. 6-18 for its location) installed inside the embankment and positive pore water pressures were measured. For Case B, the average construction rate was about 0.3 m/day and the construction duration was about 4 months. The compacted fill had a unit weight of about  $20.4 \text{ kN/m}^3$ . There was also a piezometer, P-27C (see Fig. 6-20) installed in the field, and the measured values are compared with predicted values.

Table 6-3 Basic properties of backfill soil (data from Nagahara et al., 2000 and Tatta, N. et al., 2003)

		Case A	Case B
Natural water content, $w_n$	%	50 - 68	31
Unit weight, $\gamma_t$	$\text{kN/m}^3$	15.5	20.3
Initial void ratio, $e_o$		1.56 - 1.87*	0.83*
Compression index, $C_c$		2.0	0.42
Recompression index, $C_r$		0.36	0.042
Particle size distribution, %	Gravel (100-4.75mm)	31.0	
	Sand (4.75-0.075mm)	33.0	
	Silt (0.075-0.005mm)	21.7	
	Clay (<0.005m)	14.3	

\*Calculated from  $w_n$  and  $\gamma_t$  values assuming the specific gravity ( $G_s$ ) of the soil particles of 2.7.

#### 6.4.2. Prediction of undrained shear strength increment ( $\Delta s_u$ )

The values of the parameters used for predicting the excess pore water pressure ( $u$ ) in the embankment are listed in Table 6-4. Firstly, the  $u$  value variations at P2-4 location for Case A and P-27C for Case B were calculated and compared with the measured values in Fig. 6-22 and 6-23. The coefficient of consolidation in the horizontal direction has been back-evaluated. For Case A, although both the measured and calculated maximum values are close, there are considerable differences in term of  $u$  variation. For Case B, during the construction process, the predicted values are higher than the measured ones. The calculation indicates rising and dissipating cycles induced by stepwise loading, but the measurement does not show this kind of phenomenon. The reason considered is that the construction process might not be an idealized stepwise pattern and that the calculation is carried out under the assumption that the fill material was full saturated, but in the field, this condition was not strictly satisfied. Nevertheless, we consider that the method and the parameters adopted are able to investigate the self-weight induced consolidation process during the embankment construction.



Using the method described in the previous section, the variation of  $u$  values within the embankment corresponding to the end of the embankment construction was calculated first. Then it is assumed that the increase of undrained shear strength,  $\Delta s_u$ , due to self-weight induced consolidation can be evaluated by Eq. (6-9) using a constant of  $S = 0.25$  and  $OCR = 1$ , and the results are plotted in Fig. 6-24 and 6-25 with different zones for Case A and Case B, respectively. During the calculations, the drainage length ( $l$ ) of geocomposite was varied according to the actual length at different elevation. It is noticed that Eq. (6-9) is for consolidated clayey soil. Unfortunately, there are no field measured  $s_u$  values from these case histories to confirm or check the applicability of Eq. (6-9) for compacted soil. Further study is needed for this issue. Conceptually, if the compaction resulted in an apparent overconsolidated soil layer, using Eq. (6-9) and assuming  $OCR = 1$  may overestimate the increment on  $s_u$  value ( $\Delta s_u$ ), while if the compaction induced excess pore pressure is not dissipated before placing an overlaying soil layer, it may under-estimate the value of  $\Delta s_u$ .

Table 6-4 Parameters for predicting  $\Delta s_u$  values of the case histories

Parameters	Case A	Case B
Length of geocomposite, m	5 ~ 115	25 ~ 55
Discharge capacity of geocomposite, $q_w$ (m <sup>3</sup> /yr)	233	233
Vertical spacing of geocomposite, $S_v$ (m)	2.5 ~ 5.0	5.0
Horizontal spacing of geocomposite, $S_h$ (m)	2.0	2.0
Speed of construction, $V$ (m/day)	0.27	0.3
Hydraulic conductivity of backfill, $k$ (m/s)	$4.6 \times 10^{-8}$	$4.77 \times 10^{-8}$
Total unit weight of backfill, $\gamma_t$ (kN/m <sup>3</sup> )	15.5	20.4
Back Analysis		
Coefficient of consolidation of backfill, $c_v$ (m <sup>2</sup> /day)	10	7

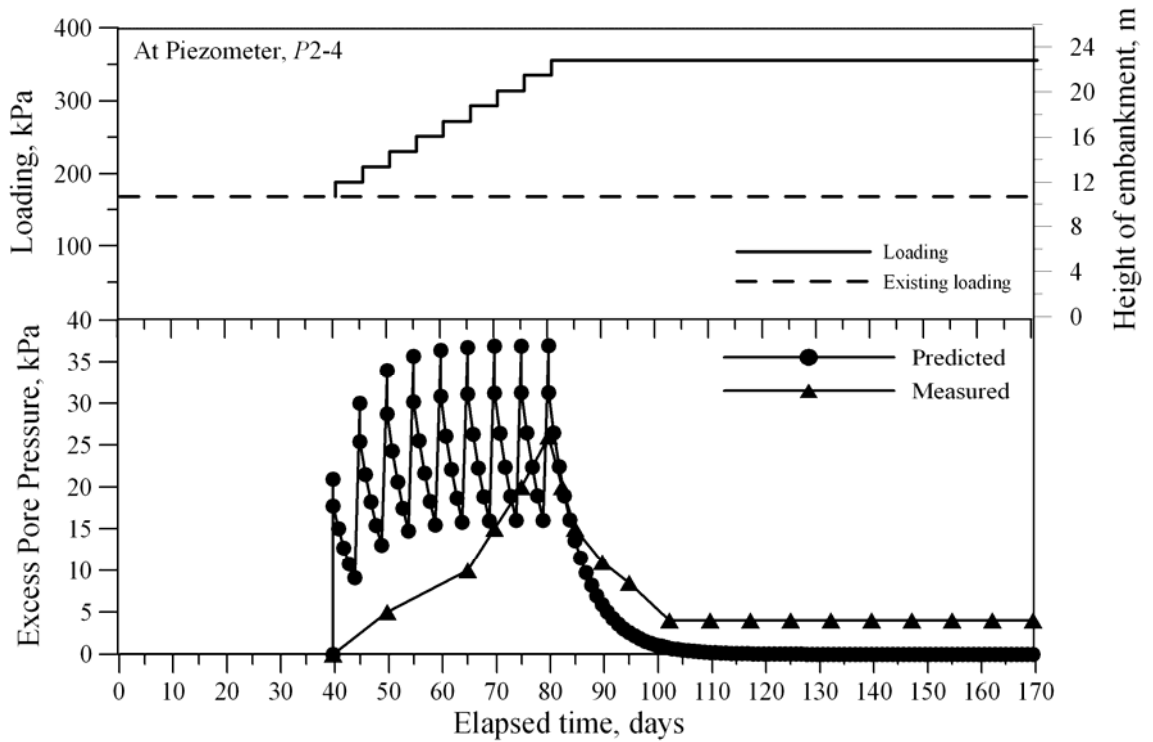


Fig. 6-22 Comparison between measured and predicted average excess pore water pressure of Case A

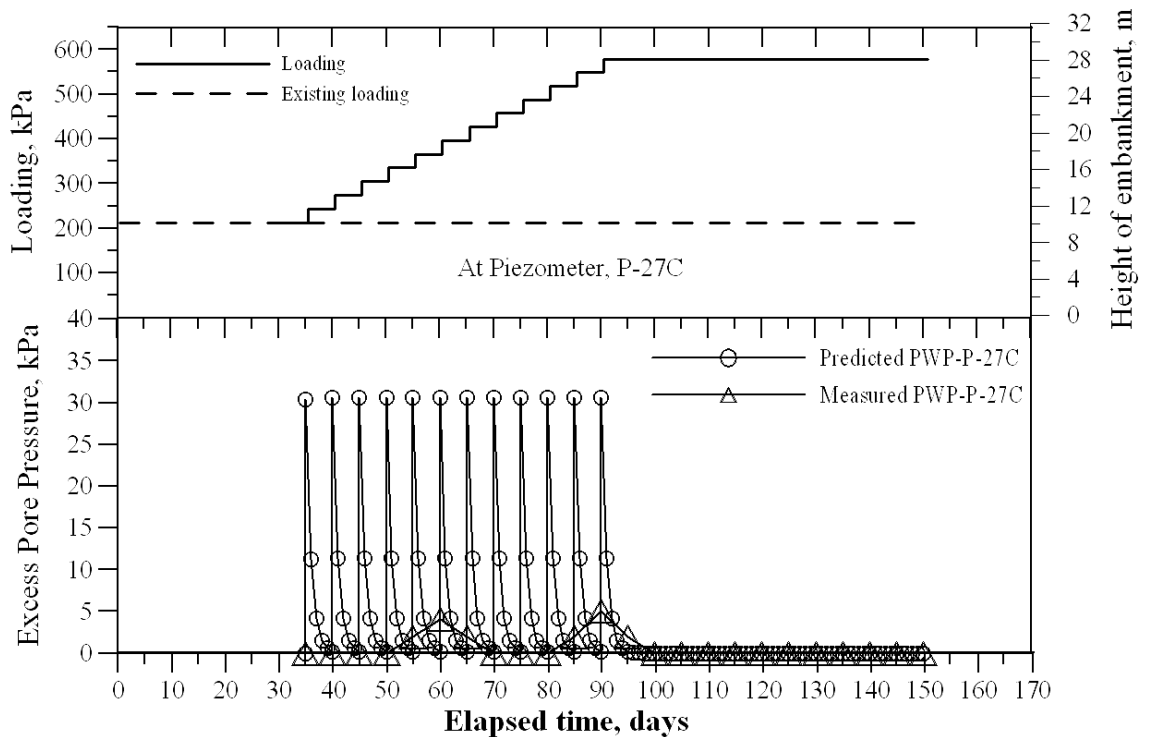


Fig. 6-23 Comparison between measured and predicted average excess pore water pressure of Case B

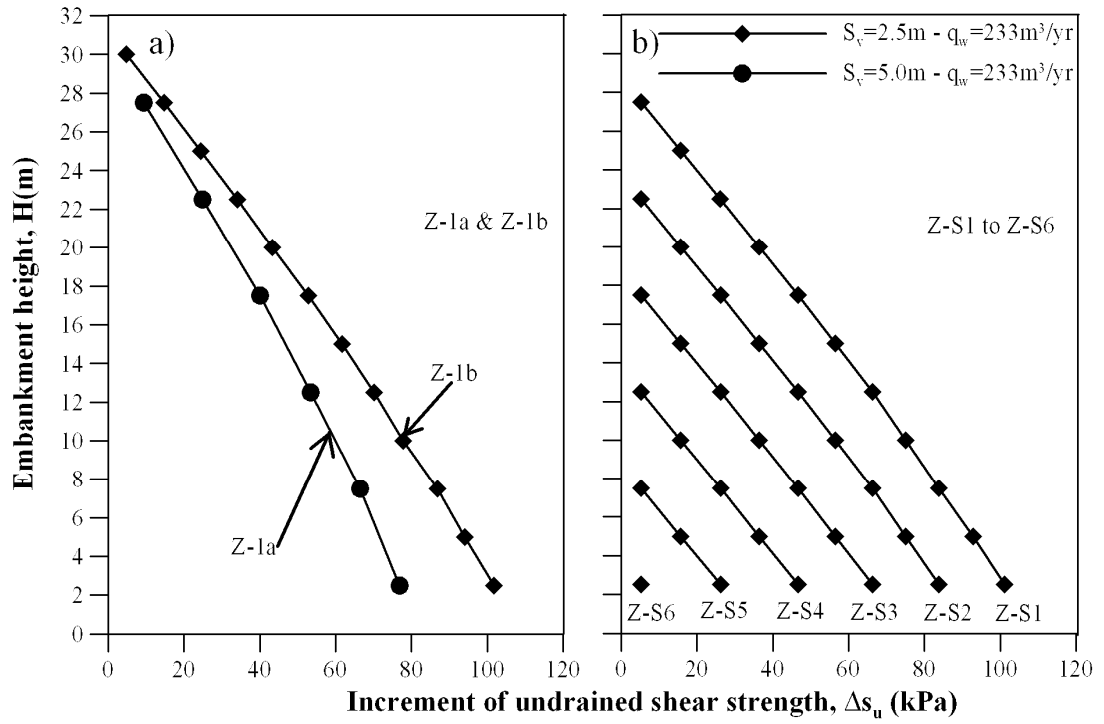


Fig. 6-24 Prediction of  $\Delta s_u$  values of Case A

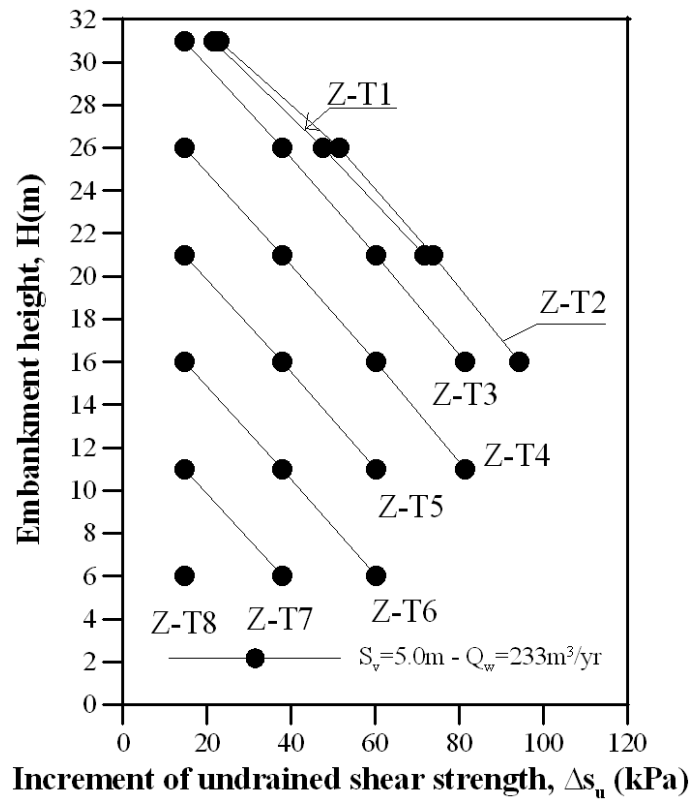


Fig. 6-25 Prediction of  $\Delta s_u$  values of Case B

### 6.4.3. Evaluation of factor safety (FS)

For Case A, Inagaki et al., (2000) reported that the compacted embankment backfill material had an initial undrained shear strength,  $s_{uo}$ , of about 30 kPa. This value is assumed for Case B also since there are no measured value reported. The  $s_u$  values in the embankment at the end of construction are the sum of  $s_{uo}$  and the increment due to consolidation ( $\Delta s_u$ ) in Fig. 6-24 and 6-25. FS values were computed using Bishop's Simplified Method by Slope/W 2004 software (Geo-slope International LTD., Alberta, Canada). Six calculations (3 cases for each case history) were conducted and the parameters and FS values are listed in Table 6-5. For Case A, the potential failure surface for FSA-2 is illustrated in Fig. 6-18 and for Case B, the potential failure surface for FSB-2 is illustrated in Fig. 6-20. For considering the reinforcement effect cases FSA-3 and FSB-3, both rupture and pullout failure mechanisms for the geocomposite are considered. In case of pullout failure, the interface shear strength between the geocomposite and the backfill soil was assumed as 0.8 time of the corresponding shear strength of the backfill soil.

Table 6-5 Parameters for stability analysis

Case	$s_{uo}$ kPa	$\Delta s_u$ kPa	Allowable tensile force ( $T_a$ ) kN/m	$q_w$ m <sup>3</sup> /yr	FS
FSA-1	30	0	0	233	0.50
FSA-2	30	$0.25\sigma'_v$	0	233	1.26
FSA-3	30	$0.25\sigma'_v$	4.5	233	1.27
FSB-1	30	0	0	233	0.41
FSB-2	30	$0.25\sigma'_v$	0	233	1.18
FSB-3	30	$0.25\sigma'_v$	4.5	233	1.19

FS values are shown in Fig. 6-26 and 6-27. It can be seen that assuming the embankment is constructed in an undrained condition, i.e., the whole fill material has a  $s_u$  value of 30 kPa, the embankment could not be constructed. Of course, actually, there would be certain partial consolidation during the embankment construction even without the geocomposite. Comparing the FS values of with and without using reinforced function of geocomposite (FSA-2 and FSA-3 for Case A, and FSB-2 and FSB-3 for Case B) shows that for the material used, the reinforcement effect on FS value is very small (as seen in FSA-3 and FSB-3).

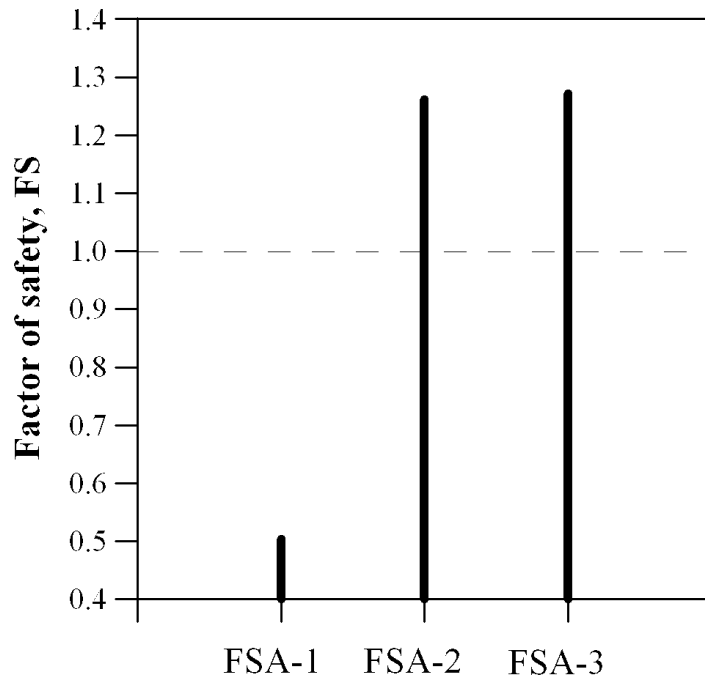


Fig. 6-26 Effect of  $s_u$  increment and  $T_a$  on  $FS$  of embankment in Case A

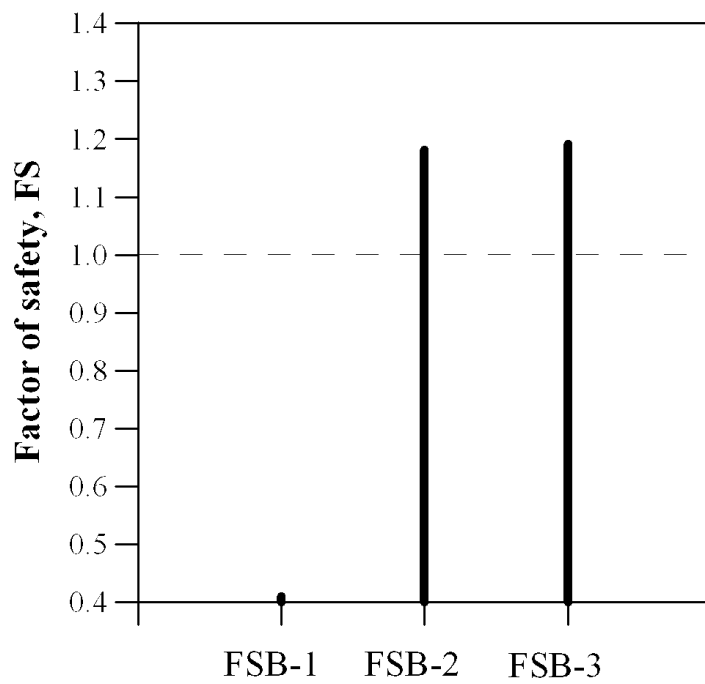


Fig. 6-27 Effect of  $s_u$  increment and  $T_a$  on  $FS$  of embankment in Case B

## 6.5 Summaries

Shear strength of lime and cement treated clayey soils were investigated by unconfined compression and laboratory vane shear tests. After that, the methods for predicting excess pore water pressure ( $u$ ) and undrained shear strength ( $s_u$ ) were discussed in detail. Finally, applying the proposed

method to analyze two case histories of embankments with clayey backfills are described. Based on the results of the tests and the analyses, the following conclusions can be drawn.

1) *Non-linear relationship between  $q_u$  and the amount of the lime or the cement additive.* Adding 2% of the lime or the cement into the soils, there was almost no effect on their strength. It is believed due to the existence of humic acid, a type of organic material in the soils, the small amount of cement/lime added just reacted with the acid and did not forming bond between clay particles. For 2 - 16% of the lime or the cement added, the relationship between  $q_u$  and the amount of additive is non-linear.

2) *Effectiveness of lime and cement treatment.* For both the soils tested, adding the same amount of lime or cement, the unconfined compression strength ( $q_u$ ) of the lime-treated soils was much higher than that of the cement-treated soils.

3) For two clayey soils tested, the undrained shear strength ( $s_u$ ) of 5kPa was experienced that it is strong enough for transportation and was suggested as a criterion.

4) *Method for predicting the undrained shear strength ( $s_u$ ).* A semi-theoretical method for calculating  $s_u$  value is described. Comparing the measured and calculated  $s_u$  values of the model tests confirms the validity of the method.

5) *Analysis of case histories.* Two case histories of constructing 35 m and 36 m height embankments with clayey backfill was analyzed by the proposed method. The results indicate that the drainage effect of the geocomposite increased the  $s_u$  value of the clayey backfill and therefore the factor of safety ( $FS$ ) against the slip circular failure substantially. It is considered that results presented in this paper can form a base for developing a design method of embankment construction using saturated or close to saturated clayey backfill.

## CHAPTER 7 CONCLUSIONS AND RECOMMENDATIONS

### 7.1 Conclusions

This study has mainly investigated the physico-chemical and mechanical behavior of lime/cement lightly treated clayey soils. Physico-chemical properties investigated are: Atterberg's limit, particle size distribution, ion concentration, pH value and electrical conductivities of the pore water, and microstructure analysis using scanning electron microscope (SEM) image and mercury intrusion porosimetry (MIP) test results. The mechanical properties considered are: permeability, coefficient of consolidation and undrained shear strength. A newly developed flexible-wall permeameter was used to investigate permeability behavior of lime-/cement-treated clayey soils. Further, large scale model tests were conducted to investigate the suitability of constructing embankment with clayey soils using light lime/cement treatment and dual function (drainage and reinforcement) geocomposite. Based on the model test results, a method for predicting undrained shear strength ( $s_u$ ) of clayey soils induced by horizontal geocomposite under stepwise loading as well as cementation effect has been proposed. The main findings can be revealed as follow:

#### (1) *Physico-chemical properties*

(a) When the cement additive is less than 4% or 2% for the lime, there were obvious changes in particle size distribution but the strength does not increase significantly.

(b) The plastic limit increases with an increase of cement/lime content, and the rate of increase is higher at lower cement/lime content. The reason is: due to the effect of small amount of cement or lime, clusters of clay particles are formed with larger inner voids, which can hold more water when the soil reaches its liquid limit than that of a soil without treatment.

(c) The pH values increase rapidly at less than 4% of cement content and 2% of lime content but the rate of increase is insignificant at higher cement/lime content.

#### (2) *Unconfined compression strength ( $q_u$ )*

For two clayey soils tested, with 2-16% additive, there is non-linear relationship between unconfined compression strength ( $q_u$ ) and the amount of the lime or the cement. Lime treatment is more effective than cement. For soils tested, adding the same amount of lime or cement, the  $q_u$  value of the lime-treated soils was much higher than that of the cement-treated soils.

### **(3) Compression index ( $C_c$ ) and coefficient of consolidation ( $c_v$ )**

(a) With the increase of the amount of the lime or the cement additive,  $C_c$  values were increased, and the lime treated soils had more increase than that of the cement treated soils.

(b) The coefficient of consolidation ( $c_v$ ), in the overconsolidated range, is scattered, but in the virgin consolidation range there is a clear trend increasing in  $c_v$  with the increase of lime/cement content for both treated soils.

### **(4) Permeability**

(a) The pore size distribution of the soil is the main factor influencing the  $k$  value. Under identical void ratio ( $e$ ) conditions, when the amount of cement or lime added is large enough that the cementation products formed during the pozzolanic reactions begin to fill the inter-aggregate pores, the  $k$  value begins to decrease. For the conditions tested, the threshold values are 8% the cement and 4% the lime by dry weight.

(b) The chemical properties of the pore water also affect the  $k$  value through their influence on the thickness of the diffuse double layer (DDL). Cement-treated soils tend to have a thinner DDLs and higher  $k$  values than the lime-treated soils with similar microstructures.

(c) The  $e$ - $\log(k)$  relationship is nearly linear, which implies that Taylor's (1948)  $e$ - $\log(k)$  relationship can be applied to the cement- and lime-treated soils.

(d) The directly measured  $k$  values are similar and comparable to those calculated from the results of the oedometer tests. However, the results from the oedometer test appear more scattered than those from the direct measurements.

### **(5) Combination of lime/cement treatment with geocomposites**

(a) Geocomposite has a high confined in clay discharge capacity can be a sufficient drainage path for accelerating the consolidation rate of clayey soil. For the conditions adopted: loading rate of 1.6 kPa/day and geocomposite vertical spacing of about 1.0 m, at the end of loading, the average degree of consolidations were from 70 to 90%.

(b) Combination of cementation and consolidation effects due to geocomposite result in a denser and stronger embankment with clayey fill material comparing with cases of cement/lime treatment alone.

### **(6) Method for predicting undrained shear strength ( $s_u$ )**



(a) A semi-theoretical method for calculating  $s_u$  value is proposed for the situation of constructing an embankment with clayey backfill and using geocomposite (drainage and reinforcement). Comparing the measured and calculated  $s_u$  values of the model tests confirms the validity of the method.

(b) Two case histories of constructing 35 m and 36 m height embankments with clayey backfill was analyzed by the proposed method. The results indicate that the drainage effect of the geocomposite increased  $s_u$  values of the clayey backfill and therefore the factor of safety ( $FS$ ) against the slip circular failure substantially.

## 7.2 Recommendations

Regarding the physico-chemical behaviors of cement/lime lightly treated clayey soils, there are still unclear points need to be investigated. Followings are two important issues warrant further study

(a) Very big differences existed on the effect of cement and lime additives for the two clayey soils studied. Detailed studies on the influence factors, such as the compositions of the soils, types of organic content (humic acid and fulvic acid, etc), oxidation of sulfide minerals and salinity on the strength of the lime-/cement-treated soils are needed.

(b) Method for predicting the geocomposite induced degree of consolidation of lime-/cement- treated clayey soil needs to be refined. For natural clayey soils, the agreement between the measured and calculated  $u$  values are good, but for lime-/cement-treated soils, there are discrepancies. Pozzolanic effect tends to reduce the generation of positive pore water pressure, and hardening (cementation) effect tends to increase the coefficient of consolidation of the soil and then increase the rate of pore water pressure dissipation. All these effects can not be considered by the current calculation method. Therefore, how to predict the negative pore pressure increment due to cementation effect is still an issue to be resolved in the future research.

## REFERENCES

1. Anandarajah, A., 2003. Mechanism controlling permeability change in clays due to changes in pore fluid. *Journal of Geotechnical and Geoenvironmental Engineering*, Vol. 129, No. 2, 163–172.
2. Ahnberg, H., Johansson, S.E, Phil H. and Carlsson T. 2003. Stabilising effects of different binders in some Swedish soils. *Ground improvement*, No. 1, pp. 9-23.
3. Al-Mukhtar, M., Khattab, S. and Alcover, J. F. 2012. Microstructure and geotechnical properties of lime-treated expansive clayey soil. *Engineering Geology*, Vol. 139-140, p.p. 17-27.
4. Bjerrum, L. 1973. Problems of Soil Mechanics and Construction on Soft Clays. In: *Proceedings of the 8<sup>th</sup> International Conference on Soil Mechanics and Foundation Engineering*, Vol. 3, p.p. 111-159.
5. Broms, B. B., and Boman, P. O. 1979. Lime column a new foundation method. *Journal of Geotechnical Engineering Division, ASCE*, 105, No. GT4, p.p. 539-556.
6. Bergado, D.T., Manivannan, R., Balasubramaniam, A.S., 1996. Proposed criteria for discharge capacity of prefabricated vertical drains. *Geotextiles and Geomembranes* Vol. 14, p.p. 481–505.
7. Carli, F., and Motta, A. 1985. Particle size distribution of reference materials by microcomputerized mercury porosimetry. *Manual of Porosimeter, 2000 Series*, Carlo Erba Instruments, p.p. 7.2–7.8.
8. Choquette, M., Bérubé, M. A. and Locat, J. 1987. Minerological and microtextural changes associated with lime stabilization of marine clays from Eastern Canada. *Applied Clay Science*, Vol. 2, p.p. 215-232.
9. Chai, J. C. and Miura, N. 2002. Long-term transmissivity of geotextile confined in clay. In: *Proceeding 7<sup>th</sup> International Conference on Geosynthetics*, Nice, France, Balkema Publishers, Vol. 1, p.p. 155-158.
10. Chai, J. C., Miura, N. and Nomura, T. 2004. Effect of hydraulic radius on long-term drainage capacity of geosynthetics drains. *Geotextiles and Geomembranes* Vol. 22, p.p. 3-16.
11. Chai, J.C. and Miura, N. 2005. Cement/lime mixing ground improvement for road construction on soft ground. *Ground Improvement - Case Histories*, Ed. B. Indraratna, and J. Chu, Elsevier, p.p. 279-304.
12. Chai, J.C., Hino, T., Igaya, Y. and Yamauchi, Y. 2011. Embankment construction with saturated clayey fill material using geocomposites. *Geotechnical Engineering Journal of the SEAGS & AGSSEA* Vol. 42 (1), p.p. 35-41.
13. Chai, J. C. and Quang, D. N. 2013. Geocomposite induced consolidation of clayey soils under stepwise loading. *Geotextiles and Geomembranes* Vol. 37, p.p. 99-108.
14. Chew, S.H., Kamruzzaman, A.H.M. and Lee, F.H. 2004. Physicochemical and Engineering behavior of cement treated clays. *Journal of Geotechnical and Geoenvironmental*

Engineering, ASCE Vol. 130 (7), p.p. 696-706.

15. Diamond, S. 1970. Pore size distributions in clays. *Clays and Clay Minerals*, Vol. 18, p.p. 7-23.
16. Delage, P. and Lefebvre, G. 1984. Study of the structure of a sensitive Champlain clay and of its evolution during consolidation. *Canadian Geotechnical Journal*, Vol. 21, p.p. 21-25.
17. Das, M. Braja 2007. *Advanced soil mechanics*, Taylor and Francis, New York, USA.
18. Gallavresi, F. 1992. Grouting improvement of foundation soils. In: *Proceeding of the 1992 ASCE specialty conference on Grouting, soil improvement and geosynthetics*, ASCE, New York, Vol.1, p.p. 1-38.
19. GEO-SLOPE User's guide, 2004. *Stability modeling with Slope/W 2004 version*, GEO-SLOPE International Ltd.
20. Hansbo, S. 1981. Consolidation of fine-grained soils by prefabricated drains. In: *Proceeding 10th International Conference Soil Mechanic and Foundation Engineering*, Stockholm, Vol. 3, p.p. 677-682.
21. Horpibulsuk, S., Miura, N. and Bergado, D.T. 2004. Undrained shear behavior of cement admixed clay at high water content. *Journal of Geotechnical and Geoenvironmental Engineering*, ASCE, Vol. 130, No. 10.
22. Horpibulsuk, S., Rachan, R., Chinkulkijniwat, A., Raksachon, Y., Suddeepong, A. 2010. Analysis of strength development in cement-stabilized silty clay from microstructural considerations. *Construction and Building Materials*, Vol. 24, p.p. 2011-2021.
23. Hird, C.C., Pyrah, I.C., and Russell, D. 1992. Finite element modeling of vertical drains beneath embankments on soft ground. *Geotechnique* Vol. 42, 499-511.
24. Hino, T., Taguchi, T., Chai, J.C., and Shen, S.L. 2008. The Ariake sea coastal road project in the Saga lowlands: Properties of soft foundations and use of dredged clayey soil as an embankment material. In: *Proceeding of the International Symposium on Lowland Technology*, ISLT, IALT, Busan, Korea, p.p. 467-472.
25. Inagaki, M., Morikage, A., Kumagai, Y., Yokota, Y., Itou, S., and Kawamura, K. 2000. Effect of belt drainage materials in the high embankment construction using high water content clay. *Geosynthetic Engineering Journal*, Japan Chapter International Geosynthetic Society Vol. 15, 50-57 (in Japanese with English abstract).
26. Jamiolkowski, M., Ladd, C. C., Germaine, J. T., and Lancellotta, R. 1985. New Developments in Field and Laboratory Testing of Soils. In: *Proceedings of the 11<sup>th</sup> International Conference on Soil Mechanics and Foundation Engineering*, Vol. 1, p.p. 57-153.
27. Kawasaki, T., Niina, A., Saitoh, S., Suzuki, Y. and Honjo, Y. 1981. Deep mixing method using cement hardening agent. In: *Proceedings of 10th International Conference on Soil Mechanics and Foundation Engineering*, Stockholm, p.p. 721-724.
28. Kang M. S., Watabe Y. and Tsuchida, T. 2003. Effect of Drying Process on the Evaluation of Microstructure of Clays using Scanning Electron Microscope (SEM) and Mercury Intrusion Porosimetry (MIP). In: *Proceedings of The Thirteenth (2003) International Offshore and Polar Engineering Conference*, USA, p.p. 385-392.

29. Ladd, C. C. and Foott, R. 1974. In: Proceedings of the ASCE, Geotechnical Division, Vol. 100, p.p. 763-786.
30. Locat, J., Bérubé, M.A. and Choquette, M. 1990. Laboratory investigations on the lime stabilization of sensitive clays: Shear strength development. Canadian Geotechnical Journal Vol. 27, 294-304.
31. Lapierre, C., Leroueil, S. and Locat, J. 1990. Mercury intrusion and permeability of Louiseville clay. Canadian Geotechnical Journal Vol. 27, 761-773.
32. Ladd, C. C. 1991. Stability evaluation during staged construction. Journal of Geotechnical Engineering Division, ASCE 117 Vol. 4, 540-615.
33. Locat, J., Tremblay, H. and Leroueil, S. 1996. Mechanical and hydraulic behavior of a soft inorganic clay treated with lime. Canadian Geotechnical Journal Vol. 33, 654-669.
34. Lorenzo, G. A. and Bergado, D. T. 2003. New consolidation equation for soil-cement pile improved ground. Canadian Geotechnical Journal, Vol. 40, p.p. 265-275.
35. Mesri, G. 1975. In: Proceedings of the ASCE, Vol. 101, Geotechnical Division, p.p. 409-412.
36. McCallister, L.D., and Petry, T.M. 1992. Leach tests on lime treated clays. Geotechnical Testing Journal, Vol. 15, 106-114.
37. Mitchell, J.K. 1993. Fundamentals of soil behavior, John Wiley & Sons, Inc, New York.
38. Miki, H., Iwabuchi, J. and Chida, S. 2005. New soil treatment methods in Japan.
39. Mahanta, K. K., Mishra, G. C., Kansal, M. L. 2012. Estimation of electric double layer thickness from linearized and nonlinear solutions of Poisson-Boltzman equation for single type of ions. Applied Clay Science, Vol. 59-60, p.p. 1-7.
40. Nagahara, H., Tsuruyama, N., Imai, T., Ishiguro, T., Fujiyama, T. and Ohta, H. 2000. An analysis of airport fill with geotextile horizontal drain. Geosynthetic Engineering Journal, Japan Chapter International Geosynthetic Society Vol. 15, 58-67 (in Japanese with English abstract).
41. Okumura, T. and Terashi, M. 1975. Deep lime-mixing method of stabilization for marine clays. In: Proceeding of the 5<sup>th</sup> Asian Region Conference on Soil Mechanic and Foundation Engineering, Bangalore, Vol. 1, p.p. 69-75.
42. Quang, D. N., Chai, J. C., Hino, T. and Negami, T. 2011. Mechanical properties of soft clays lightly treated by cement/lime. In: Proceeding International Symposium on Sustainable Geosynthetics and Green Technology for Climate Change (SGCC2011).
43. Quang, D. N. and Chai, J. C. 2012. Physico-chemical and mechanical properties of cement/lime lightly treated clayey soils. In: Proceeding 5th China Japan Geotechnical Symposium.
44. Raisinghani, D.V. and Viswanadham, B.V.S 2010. Evaluation of permeability characteristics of a geosynthetic-reinforced soil through laboratory tests. Geotextiles and Geomembranes Vol. 28, 579-588.
45. Raisinghani, D.V. and Viswanadham, B.V.S 2011. Centrifuge model study on low permeable slope reinforced by hybrid geosynthetics. Geotextiles and Geomembranes Vol. 29, p.p. 567-580.

46. Skempton, A.W. 1957. In: Proceedings of the Institute of Civil Engineers, Vol. 7, p.p. 409-412.
47. Suzuki, Y. 1982. Deep chemical mixing methods using cement as hardening agent. In: Symposium of Soil and Rock Improvement Technology Including Geotextile, Reinforced Earth and Modern Piling Methods Asian Institute of Technology, Bangkok, p.p. B-1-1-B-1-24.
48. Schmitz, Robrecht M., 2006. Can the diffuse double layer theory describe changes in hydraulic conductivity of compacted clays ?. Geotechnical and Geological Engineering 24, 1835-1844.
49. Terashi, M., Tanaka, H. and Okumura, T. 1979. Engineering properties of lime treated marine soils and DMM. In: Proceedings of 6th Asian Regional Conference on Soil Mechanics and Foundation Engineering, Vol.1, p.p. 191-194.
50. Terashi, M. 1983. Practice and problems of the deep mixing method of soil stabilization. Soils and Foundations Vol. 31-8, p.p. 75-83.
51. Tatsuoka, F. and Yamauchi, H. 1986. A reinforcing method for steep clay slopes using a non-woven geotextile. Geotextiles and Geomembranes, Vol. 4, p.p. 241-268.
52. Tatsuoka, F., Kohata, Y., Uchida, K. and Imai, K. 1996. Deformation and strength characteristics of cement treated soils in Trans-Tokyo Bay Highway project. In: Proceedings of the 2<sup>nd</sup> International Conference On Ground Improvement Geosystems Vol. 1, p.p. 453-459.
53. Tang, Y. X. Miyazaki, Y. and Tsuchida, T. 2001. Practices of reused dredging by cement treatment. Soils and Foundations, Vol. 41(5), 129-143.
54. Taechakumthorn, C. and Rowe, R. K. 2012. Performance of a reinforced embankment on a sensitive Champlain clay deposit. Canadian Geotechnical Journal Vol. 49, p.p. 917-927.
55. Tatta, N., Kawauchi, M., Matsumura, T., Nakamura, Y. and Ito, S. 2003. Behavior of high airport embankment with horizontal drain. Geosynthetic Engineering Journal, Japan Chapter International Geosynthetic Society Vol. 18, p.p. 311-316 (in Japanese with English abstract).
56. Tanaka, H., Shiwakoti, R. D., Omukai, N., Rito, F., Locat, J. and Tanaka, M. 2003. Pore size distribution of clayey soils measured by mercury intrusion porosimetry and its relation to hydraulic conductivity. Soils and Foundations, Vol. 43, No. 6, p.p. 63 – 73.
57. Uddin, K., Balasubramaniam, A.S and Bergado, D.T. 1997. Engineering behavior of cement treated Bangkok soft clay. Geotechnical Engineering Journal, Vol. 28, p.p. 89-119.
58. Washburn, E. W. 1921. Note on a method of determining the distribution of pores sizes in a porous material. In: Proc. Nat. Acad. Sci. U.S. 7, p.p. 115 – 116.
59. Yamanouchi, T. and Miura, N. 1967. Multiple – sandwich method of soft clay banking using cardboard wicks and quicklime. In: Proc. 3<sup>rd</sup> Asian Reg. Conf. SMFE. Haifa, Israel, Vol. 1, p.p. 256-260.
60. Yamanouchi, T., Horikawa, M. and Miura, N. 1971. In-situ experiments on soft clay banking by means of multiple-sandwich method using cardboard wicks and quicklime. In: Proc. 4<sup>th</sup> Asian Reg. Conf. SMFE. Bangkok, Thailand, Vol. 1, p.p. 342-345.

61. Yamanouchi, T., Miura, N., Matshubayashi, N. and Fukuda, N. 1982. Soil improvement with quicklime and filter fabric. *J. Geotech. Eng. Division, ASCE*, Vol. 108 (GT7), p.p. 953-965.
62. Yamadera, A. 1999. Microstructural study of geotechnical characteristics of marine clays. Ph.D Dissertation, Saga University, Japan.
63. Yasuhara, K. 2002. Sandwiched and hybrid reinforcement of earth structures and foundations using geosynthetics. In: *Proceedings of the International Symposium on Lowland Technology*, Saga University, p.p. 27-39.
64. Yasuhara, K., Tanabashi, Y., Miyata, Y., Hirai, T., and Ghosh, C. 2003. Hybrid-sandwiched reinforcement using geosynthetics. *Geosynthetics Engineering Journal*, Japan Chapter, International Geosynthetic Society Vol. 18, p.p. 275-282 (in Japanese with English abstract).
65. Zheng, J. J., Chen, B. G., Lu, Y. E., Abusharar, S. W., Yin, J. H. 2009. The performance of an embankment on soft ground reinforced with geosynthetics and pile walls. *Geosynthetics International* Vol. 16 (3), p.p. 173-182.